EXPERIMENTAL AND NUMERICAL CHARACTERIZATION OF SOFTBALLS

By

JOSEPH GERALD DURIS

A thesis submitted in partial fulfillment of
the requirements for the degree of

MASTER OF SCIENCE IN MECHANICAL ENGINEERING

WASHINGTON STATE UNIVERSITY
Department of Mechanical and Materials Engineering

December 2004

To the Faculty of Washington State University:

The members of the Committee appointed to examine the thesis of Joseph Gerald Duris find it satisfactory and recommend that it be accepted.

_____
Chair

_____

_____

ACKNOWLEGEMENT

I would like to thank Dr. Lloyd V. Smith for his careful guidance, instruction, and patience throughout the course of my studies. His time and friendship are greatly appreciated. I would also like to thank the other members of my committee Dr. Hutton and Dr. Cofer for their support and time. The Amateur Softball Association (ASA) funded this research and without their desire to study the game of softball from a scientific viewpoint, this research would not have been possible.

A special thanks to Charlena Grimes for her support and guidance when I was an undergraduate. It is people like Char who make WSU a great place. Also, a big thanks to Kurt Hutchinson, Henry Ruff, Jon Grimes, and Norm Martel for all their help over the years on various projects. The engineering shops did a great job designing and building the cannon that was used for the experimental research. The office staff including Gayle, Jan, Annette, Mary, Diane, and Jaime have all been tremendous and have made life very simple. Tom Mase at Michigan State University performed the DMA and did a great job.

Aaron, Brian, Curtis, Dale, Jared, Phil, Steve, Travis, and others have all helped keep me sane and have given me some valuable lessons in fluid dynamics. Team Circumventors made a good run at the IM championships, but unexpected injuries and some poor officiating ending our season early.

Last, but definitely not least, I would also like to thank my family including my mom, dad, Debbie and my sisters Susie and Jenny and their husbands Rick and Matt and my grandparents. I love all you guys, thanks for being such a great family. Kelly, thank you so much for taking care of me and being so patient and understanding while I was busy writing this thesis. I feel so lucky to have such an amazing, beautiful girl in my life!

EXPERIMENTAL AND NUMERICAL

CHARACTERIZATION OF SOFTBALLS

Abstract

by Joseph Gerald Duris, M.S.
Washington State University
December 2004

Chair: Lloyd V. Smith

The performance of baseball and softball bats can depend strongly on the properties of the ball. Ball hardness is measured in a quasi-static compression test and the coefficient of restitution (COR) is measured by impacting the ball at 60 mph against a rigid flat plate. There is concern that these current methods of measuring softball performance are not adequate.

The ball COR and dynamic compression were measured as a function of speed, geometry, degradation, and environmental conditions. A dynamic compression test, where the ball impacts a rigidly mounted load cell, was used to compare static and dynamic compression. A cylindrical impact surface was observed to decrease the COR and dynamic compression, but increase the contact time. The frequency of ball testing was observed to affect the ball's measured response. Humidity was observed to have a negligible effect on a ball's COR and dynamic hardness, but a measurable effect on its static hardness. Removing the cover of the softball increased the COR and decreased the dynamic compression.

The validity of normalizing bat performance to account for differences in the softball was investigated. It was found that the current method of normalizing for the COR may not be valid, while normalizing for ball mass appeared to work very well. Increasing ball hardness was

observed to increase bat performance, especially for high performing bats whose barrel stiffness is low.

Two viscoelastic material models of the softball were investigated using the dynamic finite element code LS-Dyna. A three parameter Power law model was found to be in good agreement with experimental results. A parameter study was undertaken to determine how the parameters of the Power Law model affected the COR dynamic compression. The relaxation curve of the polyurethane foam core of the softball was experimentally determined using dynamic mechanical analysis (DMA). A Prony series model was used to fit the relaxation curve, but the numerical results were in poor agreement with experimental data.

Dedication

This thesis is dedicated to my family.

TABLE OF CONTENTS

LIST OF TABLES

LIST OF FIGURES

CHAPTER ONE

LITERATURE REVIEW

1.1 Introduction

Advances in the design and manufacture of baseball and softball bats have improved their hitting performance significantly. Regulating agencies have placed limits on the hitting performance of bats in an effort to maintain a balance between the offensive and defensive aspects of the game. Bat performance may be measured and quantified in a number of different ways. All methods of determining bat performance are subject to experimental error and manufacturing deviations. Since performance is given as a limit, small changes in performance can have a large competitive and regulative effect. There is interest on the part of regulating agencies and manufacturers, therefore, to improve the accuracy and repeatability of methods to determine bat performance. The current study considers the effects of softballs in measuring bat performance.

Little experimental research has been published regarding the properties of softballs. Modern day softballs are primarily made of a solid polyurethane core with a leather or synthetic cover. Current methods of ball testing may not adequately describe the rate effects of the viscoelastic softball. For example, the current method of measuring ball hardness displaces the ball 10,000 times slower than speeds seen in play. The COR test is done against a flat plate at speeds below game conditions. It is unknown how the properties of the softball change over time, with repeated use, and with temperature or humidity.

Softball bats have evolved from the solid wood design of the past to the multi wall aluminum and composite bats of today. Modern bats have a much lower barrel stiffness than the bats that they replaced. The reduction in barrel stiffness causes the bat to absorb some of the

impact energy, therefore reducing the ball deformation upon contact. When the bat absorbs this energy, more energy is returned to the ball after the impact. This outcome has become known as the trampoline effect. While many factors contribute to increased bat performance, the trampoline effect is the most dominant.

The relative speeds of the bat and ball, along with ball hardness and mass, determine the impact force in the bat-ball collision. A higher impact force increases barrel deformation, which increases performance. The increased barrel deformation causes the ball to deform less, giving less energy loss. Therefore, the properties of the softball can have a large effect on the performance of softball bats. Until plastic damage occurs in the ball or bat, performance will continue to increase with increasing impact forces. There is concern that current methods of measuring ball hardness do not predict actual impact forces seen in play. An improved method of measuring ball hardness will be investigated in this study.

There is demand from a research and development standpoint to be able to predict bat performance using finite element analysis. An accurate model of the bat-ball collision would provide an opportunity to evaluate bat designs without the time and expense of manufacturing a prototype. However, current ball models do not accurately describe the rate effects of the softball. This may be a consequence of the scarcity of experimental softball data currently available. Analytical and empirical models have not been examined carefully to determine if the rate dependence of the viscoelastic softball can be reproduced.

In the following, the history, modeling, and experimental results of the COR are discussed. The static and dynamic compression are defined and the correlation between the two measures of hardness is investigated. The bat performance metrics are derived so that one can understand the interaction of the ball and bat during collision. The derivation also gives insight

into the bat performance normalizing procedures used to account for differences in ball properties. The current methods and shortcomings of ball modeling are also examined.

1.2 Coefficient of Restitution

1.2.1 Definition and History

The coefficient of restitution (COR) or e, which is a measure of the elasticity of an impact, is defined as the ratio of the relative normal velocity of two objects (1 and 2) after impact to that before impact [1.1], as

$$e = -\left(\frac{v_1 - v_2}{V_1 - V_2}\right), \tag{1 .1}$$

where v_1 and v_2 are the post impact rebound speeds and V_1 and V_2 are the incident speeds. The coordinate system chosen is such that the value V_1 is negative. A collision that is perfectly elastic would have e = 1, while a perfectly inelastic collision would have e = 0 [1.2]. For a collision in which one of the objects is rigid, eq. (1.1) reduces to the ratio of the rebound to the incident speed of the moving object

$$e = \frac{-v_1}{V_1}. \tag{1.2}$$

ASTM F 1887-02 defines the COR for a baseball and softball as "a numerical value determined by the exit speed of the ball after contact divided by the incoming speed (60 mph) of the ball before contact with a massive, rigid, flat wall of either wood or metal [1.3]." The requirement of a ball impacting a rigid wall implies eq. (1.2) is used for the calculation of ball COR. Throughout this paper, the ball COR e will be computed via eq. (1.2) according to ASTM F 1887-02, unless otherwise stated.

Several people have investigated the behavior of the COR for a variety of sporting balls and other spherical objects. Isaac Newton's work led the concept of the COR and researchers as

early as Hodgkinson (1835) realized that the COR was dependent on the relative velocity of the colliding objects as well as the stiffness of the colliding objects [1.4]. More recent experimental research has shown that the COR decreases linearly with increasing incident speed for softballs, baseballs, tennis balls, and golf balls [1.5-1.10]. Heald [1.8] saw a 30% decrease in ball COR over a range of 40-90 mph. Chauvin [1.6] noted that while ball standards in the United states only require the ball COR to be measured at one speed (60 mph), Japanese regulations require the COR to be tested at several speeds. The current US standard allows more design control over how the COR will change with increasing speed. Lu [1.11] states that the COR may not decrease linearly with increasing pitch speeds. This was not experimentally determined by Lu, and over the range of inbound speeds of interest to the testing of softballs, this trend has not been experimentally verified. The decrease in the COR with increasing speed can be attributed to a combination of three energy loss mechanisms [1.12]:

1) Increased excitation of internal waves or vibration modes in the rigid wall and the ball
2) Increased plastic deformation of the ball or rigid wall
3) Viscoelastic behavior of the ball or rigid wall

For a sphere impacting a rigid wall, Li [1.13] stated that less than 4% of the total energy could be attributed to the propagation of elastic waves. This leaves the latter two methods as the primary sources of energy dissipation. It is common knowledge that a typical bat-ball impact does not result in noticeable damage to the ball. Therefore, a 60 mph rigid wall impact, which is slower than game conditions, will also have no noticeable plastic deformation. Energy losses due to plastic deformation of the ball can therefore be neglected. This leaves the primary method of energy dissipation of the softball to be viscoelastic. It is apparent that with increasing speed, each mechanism of energy loss would be increased, thereby reducing the COR. Chauvin [1.6]

explains that energy is expended in the process of deforming the ball during impact, and with increasing speed, more deformation occurs. The additional deformation results in less kinetic energy after the impact.

1.2.2 COR Models

As mentioned above, the COR depends on the stiffness of the two colliding bodies. Hodgkinson [1.14] found that when materials of different stiffness collide, they contribute to the overall COR proportionally to each object's relative compliance. The total energy dissipated is the sum of energies dissipated in each of the colliding bodies [1.14]. The relationship found by Hodgkinson was

$$e_* = \frac{k_2 e_1 + k_1 e_2}{k_1 + k_2}, \tag{1.3}$$

where e_* is the composite COR of the two materially dissimilar bodies colliding and e_1 and e_2 are the COR's for each material in a self similar collision (collision between two objects of the same material) [1.14]. The k_i are the stiffness of each material, and a value proportional to Young's modulus $k_i \sim E_i$ or yield strength $k_i \sim Y_i$ is suggested. Results from Coaplen [1.14] suggest that yield strength gives a better fit to experimental data.

If the COR is known for each material at the speed of the composite impact, and the stiffness of each material is known, a composite COR can be predicted. Coaplin [1.14] improved eq. 1.3 by making the expression "energetically consistent". According to Coaplin, the energetic COR is defined as "the square root of the ratio of work done by the normal contact force during restitution, W_r, to the work done by the normal contact force during compression, W_c [9.3]." In other words, the collision consists of two stages of contact, one in which the colliding materials are approaching each other (W_c), and the other in which the two bodies are moving away from

each other (W_r) but are still in contact. Following a derivation using the definition of work, Coaplin arrived at the expression

$$e_*^2 = \frac{k_2 e_1^2 + k_1 e_2^2}{k_1 + k_2}, \tag{1.4}$$

which only varies from eq. 1.3 by the squared terms in the numerator. The terms in eq. (1.4) are defined in the same way as Eq. 1.3.

Cross [1.2] derived a similar expression to eq. (1.4), but used the idea that most of the energy dissipation occurs in only one of the objects for many impacts of interest due to the fact that one object is much stiffer than the other. For example, when a softball impacts a rigid steel wall, the ball deforms significantly while the wall remains flat. With this modification, Cross found the composite COR to be

$$e_*^2 = \frac{k_2 e_1^2 + k_1}{k_1 + k_2}. \tag{1.5}$$

Equation 1.5 is very similar to eq. (1.4), but assumes that $e_2^2 \to 1$, implying that no energy is lost in the stiffer (k_2) object. It is assumed that energy losses due to vibration in the stiffer object can be neglected. Li [1.13] stated that less than 4% of the total energy could be attributed to the propagation of elastic waves, which supports Cross' assumption.

Johnson [1.16] derived an expression for the COR of a Maxwell material. The Maxwell viscoelastic material model is a spring in series with a dashpot with a spring constant k and a damping coefficient η. The analytical expression for the COR of a Maxwell material was shown to be

$$e = 1 - (4/9)(T_C / T), \tag{1.6}$$

where T_C is the contact time and T is the relaxation time of the material which is equal to the spring constant divided by the damping constant. This equation is valid for impacts where the contact time is much shorter than the relaxation time.

Thornton [1.17] developed expressions for the COR that attempted to account for the transition from elastic to plastic deformation. For a sphere impacting a rigid wall under the assumption that $V_1 >> V_y$, where V_y is the speed that is just large enough to initiate yield in the sphere of density ρ, Thornton's expression reduces to

$$e_*^2 = 1.324\left(\frac{P_y^5}{E_*^4\rho}\right)^{1/8}(V_1)^{-1/4}, \tag{1.7}$$

where $P_y \approx 2.8\sigma_y$ and σ_y is the yield strength of the material. E_* is the composite Young's modulus of the two impacting bodies and is defined in relation to the Poisson's ratio υ_i and Young's moduli E_i of the two materials (1 and 2) as

$$\frac{1}{E_*} = \frac{1-\upsilon_1^2}{E_1} + \frac{1-\upsilon_2^2}{E_2}. \tag{1.8}$$

An alternative prediction of the COR was made by Stronge [1.18] which only varies from eq. (6) by the prefactor

$$e_*^2 = 1.33\left(\frac{P_y^5}{E_*^4\rho}\right)^{1/8}(V_1)^{-1/4}. \tag{1.9}$$

Several other expressions similar to eqs. (1.8, 1.9) have been found and vary only by the prefactor [1.13]. The difference between each expression can be attributed to a variety of assumptions made in each model.

The consequence of the dependence of COR on the stiffness of the impact structure becomes apparent when one considers a ball impacting a bat. The ball COR is measured against

a much more rigid and stiff surface than a bat, but at speeds much lower than game conditions [1.6]. Further, all bat standards assume that the ball COR is a constant for the ball when impacting a bat, but each bat that the ball is tested upon will have a different stiffness.

1.2.3 Conditioning

Another factor that influences the COR of a softball is the environment in which the ball is conditioned and tested. ASTM F 1887-02 [1.3] requires that softballs and baseballs be conditioned at 50% (±10%) relative humidity (RH) at $72^0 F$ ($\pm 4^0 F$) for a minimum of 24 hours. Softballs, typically made of a polyurethane foam core, and baseballs, which use a multi layered ball of varying construction, require much longer time periods to reach moisture content equilibrium than ASTM F 1887-02 allows.

It has been reported [1.19, 1.20] that the Colorado Rockies, a professional baseball team, have recently begun to conditioning their baseballs at 40% RH at $90^\circ F$ due to the very dry climate of Denver, Co. A paper by Kagan [1.19] investigated the effects of humidity on several baseballs and found that the COR decreased linearly with increasing humidity. In this study, Kagan conditioned the baseballs for 47 days at various levels of humidity ranging from 0.0% to 100% RH. The average change in mass over this range of humidity was found to be 13.9 grams, for a 10.38% difference. Using expressions borrowed from Adair [1.21], Kagan calculated the variation in distance from the two extreme cases of humidity to be 28 ft. This implies that a completely dry ball will travel 28 ft farther than a completely wet ball. From a more realistic standpoint, the variation in distance of a ball at 33% to that of a ball a 75% RH would be about 12 ft. Drane [1.21] investigated the effects of temperature on baseball COR. Baseballs were conditioned to four different temperatures, specifically 25, 40, 70, and $120^0 F$. For 60 mph impacts, the baseball COR increased with statistical significance logarithmically with increasing

temperature. For 100 mph impacts, possibly more representative of game conditions, the baseball COR was not affected at and above $40^{\circ}F$. However, the subfreezing temperature of $25^{0}F$ did significantly reduce the ball COR.

While the games of baseball and softball are similar, the materials used in the ball construction for each game are very different. Therefore, research pertaining to baseball conditioning may not be relevant to softballs. Moreland [1.23] concluded that temperature has a greater effect than humidity on the relaxation and creep behavior of polyurethane foams. No data could be found relating specifically to softball temperature or humidity conditioning.

Other research has focused on alternative methods of measuring the COR. Giacobbe [1.24] found that the COR could be determined solely on the damping coefficient. For a simple, one degree of freedom spring-mass-damper model, the COR was found to be

$$COR = e^{-\pi\zeta\sqrt{1-\zeta^2}}, \tag{1.10}$$

where ς is the damping coefficient. This model fails to account for the velocity rate dependence of the COR and the stiffness of the object being impacted and, therefore, may only be appropriate for self similar collisions. Giacobbe [1.24] also expanded this expression for a two degree of freedom mass-spring-damper system, but the expression for the COR was not published. It was found, however, that the two degree of freedom model agreed with experimental data slightly better than the one degree of freedom model. Stensgaard [1.12] and Aguair [1.25] showed that the COR could be measured by recording the sound of the impacts when a ball is dropped from a known height onto a rigid, flat surface. The recording gives a measure of the time between each cycle of the ball bouncing. A personal computer was used to record the sound of the impact and subsequent data reduction gave the COR for each impact. Their results show that the COR decreases with increasing impact speed, which agrees with the

experimental results of others who measured the COR using more traditional techniques. Although this method does not suit itself well to the testing of most sporting equipment due to the low impact velocities, it is a novel way to simply and cheaply obtain the COR for low speed impacts. Aguiar [1.25] also pointed out that the gravitational acceleration constant could be measured using this technique, and found that his results agree closely with tabulated values.

1.3 Static and Dynamic Ball Hardness

The two parameters typically used to characterize a softball are the COR and the static compression. Static compression values are obtained via a quasi-static compression test. ASTM F 1888-02, the standard test method for measuring the static compression of a softball or baseball, requires that the ball be compressed ¼" over a 15 second time period between two flat, parallel plates [1.26]. The peak force required to compress the ball over this range is recorded. The ball is rotated 90° and the procedure is repeated. The static compression is the average of the two measured forces required to compress the ball ¼". Heald [1.8] investigated static ball hardness for a variety of softballs and found that the "safety" balls had a significantly lower hardness compared to traditional balls. Since static compression is a simple, cost effective method of determining ball hardness, it has been hoped that static measurements can predict dynamic impact forces. This is important because an increase in ball hardness results in a higher bat-ball collision force, which increases barrel deformation and gives rise to an increase in the trampoline effect.

The effect of ball hardness can be viewed from the perspective of impact force. This has been achieved by firing balls toward a rigidly mounted load cell [1.6, 1.9, 1.24, 1.27]. Using this method, the force vs. time data is acquired. The focus of past work has been toward human safety, and developing numerical models. Conflicting results have been obtained regarding the

correlation between static and dynamic compression. Hendee [1.9] concluded that static and dynamic compression had a linear correlation. In this study, Hendee [1.9] measured the static compression of several types of baseballs by compressing the ball 1 cm (0.394 in) over a 10 second period. The dynamic compression was measured at 30, 60, and 90 mph. A linear correlation was observed between static and dynamic compression for all three impact velocities. Chauvin [1.6] however, found that static compression may not correlate with dynamic compression for a variety of baseballs and softballs. Chauvin [1.6] measured the static compression using a Rockwell hardness tester with a 15 kg load applied with a 0.50 inch diameter steel probe. Dynamic compression was measured by firing a ball at a rigid wall that had a pressure sensitive film attached to it, then subsequently examining the resulting impact pressure distribution. Chauvin's results show that there is virtually no correlation between static and dynamic compression. Heald [1.8], using a similar test setup to Chauvin, found that the size of the impact area decreased with increasing softball hardness while the impact pressure increased with ball hardness. The static vs. dynamic compression data of Heald appear to agree closely with the data of Chauvin. While the methods used to characterize the balls by Chauvin and Heald were not as accurate as those of Hendee, the question is raised ubout the validity of trying to use a static test to predict dynamic behavior. Research by Cross [1.28] supports the results of Chauvin and Heald. Cross noted that the ball compression versus applied load is nonlinear and frequency dependent. Therefore, it may not be appropriate to extrapolate low frequency quasi static compression test data to high frequency dynamic compression data [1.28].

Vinger [1.29], in an effort to simulate impacts with the human eye, used an air cannon to fire baseballs at an artificial orbit attached to a load cell. Several different baseballs were fired at a range of speeds from 35-75 mph. A linear correlation was seen between peak impact force and

velocity. ASTM F 1888 was used to measure the static compression, and it was seen that there was a general trend of increasing impact force with increasing static compression. Results of Vinger suggest that significant ball deflection occurs upon impact and ball deformation increases with decreasing static compression. Due to the irregular shape of the impact surface (a hole in the impact plate to simulate a human orbit), it is difficult to compare force and deflection data.

Gobush [1.30] measured the impact force of golf balls using a dynamic load cell. It was noticed that golf balls with a high void content had a significantly less smooth force time history compared to other golf balls. Gobush found that the golf ball deformation was extremely sensitive to the strain rate.

An alternative method of measuring dynamic hardness was proposed by Giacobbe and Scarton [1.24]. A variety of sports balls were dropped from a known height and a force transducer was used to obtain the force-time histories of the impact. A dynamic signal analyzer was used to calculate the power spectrum of the impulse. The Scarton Dynamic Hardness (SDH) was defined as the "frequency in cycles per second (Hz) where the power spectrum level drops to -6 dB. [1.24]". The derivative of the power spectrum at the SDH point is called the Derivative Scarton Dynamic Hardness (DSDH). Scarton found that the DSDH was inversely proportional to the SDH

$$DSDH = \frac{-\gamma}{SDH} \quad \text{or} \quad \gamma = -(SDH)(DSDH). \tag{1.11}$$

It was observed that the constant γ was a function of only the damping coefficient ς. The damping coefficient, given by

$$\zeta = \frac{1}{\sqrt{1+\left(\frac{\pi}{\ln(COR)}\right)^2}}, \tag{1.12}$$

can be found by solving eq. 10 for a known COR value. The results of Scarton's work suggest that the SDH can be used to predict relative static and dynamic ball hardness for a variety of sports balls including softballs, baseballs, and golf balls. Higher speed impacts and more data are required to determine if the SDH could be used to accurately predict dynamic ball hardness.

1.4 Performance Measures

The properties of a softball can have a large effect on the performance of softball bats. It is important, therefore, to have a thorough understanding of the science behind the bat performance measures. Regulating agencies have created bat performance standards in both softball and baseball in an attempt to keep the games safe and offensively balanced. Bat manufacturers must follow the standards in order to have their bat approved for play by the regulating agencies. For softball, there are two major standards that regulating agencies use to certify bats. The Amateur Softball Association (ASA) uses the procedure outlined in ASTM F 2219-02 [1.31] to compute a Batted Ball Speed (BBS) while the International Softball Federation (ISF) and the United States Slo-pitch Softball Association (USSSA) use ASTM F 1890-02 [1.32] to compute the Bat Performance Factor (BPF). High school and collegiate baseball bats must adhere to the NCAA standard which uses the Ball Exit Speed Ratio (BESR) as a performance measure. The ASTM and NCAA standards have specifications on the way each performance criterion is measured and calculated. However, since each criterion is based on the same dynamics principles, each can be calculated in a number of ways. In the following, all the performance measures will be calculated according to ASTM F 2219-02 which means the ball inbound and rebound speed will be measured while the bat recoil speed will be calculated using momentum. ASTM F 2219-02 also requires that the bat is initially at rest (ω_i=0). The BBS,

BPF, and BESR have similar derivations that begin with a momentum balance of the bat-ball collision, which has the form

$$(mv_i Q) + I_p \omega_i = -mv_r Q + I_p \omega_r . \tag{1.13}$$

In eq. 1.13, m is the measured ball mass (oz), v_i is the inbound ball speed (in/s), v_r is the ball rebound speed (in/s), and Q is the impact point on the barrel measured from the pivot point (in). The pivot point is 6.0 inches from the knob end of the bat in all standards. Therefore, a ball that impacts the barrel 27.0 inches from the knob end of the bat would have $Q = 21.0$ inches. Also, ω_i is the initial bat rotational speed (rad/s), ω_r is the post impact rotational speed (rad/s), and I_p is the bat moment of inertia ($oz \cdot in^2$). The bat moment of inertia (MOI) is measured from the pivot point and is calculated from the equation

$$I_p = \left(\frac{(\eta)^2 g W_t a}{4\pi^2} \right), \tag{1.14}$$

where g is the gravitational acceleration (in/s/s), W_t is the total weight of the bat (oz), and a (in) is the distance from the balance point (BP) to the pivot point, given by

$$a = BP - 6.0 . \tag{1.15}$$

The balance point is defined as the ratio of the weight at six (W_6) and twenty-four (W_{24}) inches to the total weight of the bat. To measure the BP, a bat is placed on a balance point stand, as shown in figure 1.1, and the weight at the 6.0 inch location and the 24.0 inch location are recorded. The balance point is then calculated by the equation

$$BP = \left(\frac{6W_6 + 24W_{24}}{W_t} \right). \tag{1.16}$$

The period η is calculated by measuring the oscillation time for a bat to swing through ten cycles in a pendulum, as shown in figure 1.2. The pivot point of the pendulum is 6.0 inches from the knob end of the bat. The average period is taken as the average of three period tests

$$\eta = \frac{\left(\frac{time_1}{10} + \frac{time_2}{10} + \frac{time_3}{10} \right)}{3}. \tag{1.17}$$

Assuming the inbound speed of the ball and bat are known, inspection of eq. 1.13 reveals that either the ball rebound or bat rebound speed must be measured. The BBS, BPF, and BESR can all be calculated using either measured ball or bat rebound speeds. Since it is often easier and more accurate in the laboratory to measure the ball rebound speed instead of bat recoil speed, the momentum balance is solved below for the bat rebound speed ω_r. The ASA (BBS) and NCAA (BESR) measure performance based on measuring the ball rebound speed while the USSSA and ISF (BPF) measure the bat recoil speed. For the BESR certification test, the NCAA requires the initial bat swing speed to be non zero, and therefore ω_i must be accounted for. Solving eq. 1.13 for bat rebound speed yields

$$\omega_r = \frac{(v_i + v_r)mQ}{I_p} + \omega_i. \tag{1.18}$$

The Bat-Ball Coefficient of Restitution (BBCOR), or e_{BB}, is defined as the ratio of the outgoing to incoming relative speeds of the bat and ball

$$e_{BB} = \frac{v_r + \omega_r Q}{v_i + \omega_i Q}. \tag{1.19}$$

Combining equations 1.18 and 1.19, and assuming an initially stationary bat yields

$$e_{BB} = \frac{v_r}{v_i} + \frac{mQ^2}{v_i I_p}(v_i + v_r). \tag{1.20}$$

The BPF is defined as a ratio of the BBCOR e_{BB} to the measured ball COR e and is given by

$$BPF = \frac{e_{BB}}{e}. \tag{1.21}$$

The ball COR e is the ratio of the rebound to inbound speed of a ball impacting a rigid wall at 60 mph and is tested according to ASTM F 1887-02 [1.3]. The ball COR is calculated from the equation

$$e = \frac{v_r}{v_i}. \tag{1.22}$$

It is convenient to introduce two dimensionless parameters, the bat recoil factor (r) and the collision efficiency (e_a). The bat recoil factor depends only on the inertial properties of the bat and ball [1.43] and is given by

$$r = \frac{m_n Q^2}{I_p}, \tag{1.23}$$

where m_n is the nominal bal weight (oz). The ASA uses a nominal ball weight m_n=6.75 oz. The collision efficiency is a model-independent relationship that can be derived using conservation laws [1.43], and is defined as

$$e_a = \left(\frac{e_{BB} - r}{1 + r} \right). \tag{1.24}$$

Equation 1.24 is a maximum when the bat recoil factor is a minimum. From an energy standpoint, when eq. 1.23 is small, less energy is transferred to the bat and more is transferred to the ball. As the bat weight increases, $r \to 0$ and $e_a \to e_{BB}$ [1.25].

The batted ball speed formula accounts for the pitch and the swing

$$BBS = (ve_a) + V(1 + e_a), \tag{1.25}$$

where v is the pitch speed and V is the bat swing speed at the impact location. The ASA assumes a pitch speed of $v = 25\,\text{mph}$ and uses a formula for the swing speed that accounts for the impact location and the moment of inertia or I_p. The ASA swing speed formula is

$$V = 85\left(\frac{Q + 8.5}{30.5}\right)\left(\frac{9000}{I_p}\right)^{\frac{1}{4}}. \tag{1.26}$$

Collegiate and high school baseball bats must pass the BESR certification test. The BESR is equal to the collision efficiency plus one half. In equation form, this is simply written as

$$BESR = e_a + \frac{1}{2}. \tag{1.27}$$

1.5 Normalizing

The results of bat performance can depend strongly on the properties of the ball. Ball mass, COR, and compression all have an effect on bat performance. To have a reproducible test in the laboratory, it is required that balls with constant properties be used, or a correction be applied to the raw data to account for differences in ball properties. A test ball that does not change over time and has perfect properties does not exist. In fact, it is very difficult to find balls suitable for testing that even come close to the required tolerances. A correction method is therefore needed. The correction to the data will herein be referred to as normalizing. The ball compression can have a large effect on bat performance, but cannot be normalized because the performance change is bat dependent. For example, a wood bat should show very little to no performance increase with increasing hardness while a hollow aluminum or composite bat will improve drastically with increasing ball hardness. Since normalizing cannot be achieved, compression tolerances are kept very tight.

The two properties of the ball that have been normalized in the past are the COR and ball mass. Two methods currently exist to normalize the COR. The BPF equation (eq. 1.21) was the first attempt to account for the variances in the ball COR. The BPF assumes that the BBCOR is independent of ball COR. According to Nathan [1.33], the scientific justification for this normalization has never been shown. It can be hypothesized, however, that for very stiff bats (wood) the BPF would be an appropriate normalizing procedure. The BBS formula can be normalized for ball COR by multiplying the BBCOR e_{BB} by the ratio of the nominal ball COR, e_n, to the measured ball COR e. The normalized BBCOR, e_{BBN}, is calculated as

$$e_{BBN} = e_{BB}\frac{e_n}{e}. \tag{1.28}$$

The normalized BBCOR is based on the same assumption as the BPF that the BBCOR is independent of the ball COR. The BBS formula also normalizes for ball weight. The nominal ball weight in the numerator of eq. 1.23 acts to normalize the ball weight to account for small differences from one ball to another. COR and weight normalization have not been experimentally verified. An aim of the current study is to investigate the validity of current normalizing procedures.

1.6 Dynamic Mechanical Analysis

Dynamic Mechanical Analysis (DMA) is often used to characterize viscoelastic materials. DMA can be simply described as applying an oscillating force to a sample and analyzing the material's response to that force [1.34]. The oscillating force creates a sinusoidal stress which in turn creates a sinusoidal strain response. By measuring the amplitude of the deformation at the peak of the sine wave and the lag δ between the stress and strain sine waves, the elastic modulus (E') and the imaginary loss modulus (E'') can be calculated. The elastic

storage modulus (E') is a measure of the material's ability to return or store energy while the loss modulus (E'') measures the ability to lose energy [1.34]. The storage and loss moduli are defined as

$$E' = \left(\frac{f_0}{bk} \right) \cos(\delta) \tag{1.29}$$

and

$$E'' = \left(\frac{f_0}{bk} \right) \sin(\delta), \tag{1.30}$$

respectively. In eqs. 1.29 and 1.30, f_0 is the force applied at the peak of the sine wave, b is the sample shape factor, k is the peak displacement, and δ is the phase angle. A physical example of the storage and loss modulus can be seen from the COR test. The speed at which the ball rebounds can be viewed as the storage modulus E' and the difference from the pitch speed to the rebound speed can be viewed as the loss modulus E". The loss modulus accounts for the energy lost to friction and internal vibrations. The ratio of E'' to E' is the loss tangent, $\tan\delta$, which is a measure of the damping in the material [1.34]. In equation form the loss tangent is given by

$$\tan(\delta) = \frac{E''}{E'}. \tag{1.31}$$

The complex modulus E^* is related to the storage and loss modulus by the equation

$$E^* = E' + iE''. \tag{1.32}$$

A useful diagram that relates eqs. 1.31 and 1.32 is shown in figure 1.3. As the material becomes elastic, δ becomes smaller and the complex modulus approaches the storage modulus.

Johnson [1.16] used the loss tangent to estimate the COR. The model assumes that the energy dissipated at impact is a small fraction of the kinetic energy of impact and that the period of cyclic strain is comparable with the contact time. Johnson states that the loading and

unloading during impact corresponds roughly to a half cycle, which allows the COR to be computed by the equation

$$e = (1 - \pi \tan(\delta))^{1/2}. \tag{1.33}$$

An advantage of DMA is that it allows a modulus to be measured at each cycle of oscillation in an environmentally controlled chamber. This allows a user to test a material at a variety of frequencies or temperatures. For example, at a frequency of 1 cycle per second (1 Hz) a temperature scan could be performed over a range of 200° F at 10° F per minute for an overall time of 20 minutes. On the other hand, a frequency scan from 0.1 Hz to 200 Hz could be tested at a constant temperature.

It is often desirable to investigate material properties at frequencies that exceed DMA capabilities and human patience. Since the behavior of viscoelastic materials is dependent on temperature, the Time Temperature Superposition Principle (TTSP) can be applied to solve this problem. The TTSP proposes that temperature effects may be described by altering the time scale of the viscoelastic response. The WLF equation, proposed by Williams, Landel, and Ferry, is the most widely used TTSP model and can be expressed as

$$\log a_t = \frac{-c_1(T - T_{ref})}{c_2 + T - T_{ref}}, \tag{1.34}$$

where a_t is the shift factor, c_1 and c_2 are material constants, T is the temperature, and T_{ref} is the reference temperature (both temperatures have units of Kelvin) [1.35]. Using this method, a frequency scan is performed at several temperatures. Shifting the frequency scan data relative to a reference temperature achieves the superposition. The resulting master curve covers a much broader frequency range compared to the original data.

1.7 Ball Modelling

Several people have modeled the ball in an effort to examine the safety of various types of balls. Crisco [1.36] used experimental quasi static ball compression tests to model the baseball properties. The derivative of the load-deformation curve yielded the ball stiffness as a function of compressive strain. An estimate of the elastic modulus was calculated using the assumption of the conservation of volume. The subsequent ball model was used to predict impact response of the head and chest. Many assumptions were made in this derivation and the ball model assumed a perfectly elastic collision (e=1). For the study of human response to impact, a perfectly elastic collision can be seen as a worst case scenario and therefore might not be a bad assumption.

Bathke [1.37] assumed that each constituent material in a multi layered baseball was elastic. The elastic properties of each layer of the baseball were determined using quasi-static compression displacement curves, and the overall ball was modeled with a combination of each layer. The commercial finite element code ABAQUS was used to model the multi-layered baseball impacting a rigid steel wall at several speeds. Although each material was modeled as linearly elastic, the COR was observed to decrease linearly with increasing pitch speed. Bathke attributed the loss in energy to internal vibrations within the baseball. Bathke's COR values appear to be much too high, but the slope of the COR vs. speed agrees well with experimental data from Hendee [1.9].

Mustone and Sherwood [1.38] modeled a baseball using LS-DYNA. The Mooney-Rivlin material model was used as it provided an option for the deformation behavior to be based on a quasi static compression displacement curve. The finite element model was calibrated to match the COR at 60 mph for a baseball. The subsequent ball model was used to predict batted ball

speeds from aluminum and wood baseball bats with a relative velocity of 140 mph (70 mph pitch, 70 mph swing speed). This study did not examine the rate effects of the baseball.

Shenoy [1.10], Sandmeyer [1.39], and Nicholls [1.40] modeled a baseball using the viscoelastic material model in LS-DYNA. The ball was modeled as a viscoelastic material, defined from a time dependent shear modulus as

$$G(t) = G_\infty + (G_0 - G_\infty)e^{-\beta \cdot t}, \tag{1.35}$$

where G_∞ and G_0 are the long term and instantaneous shear moduli, respectively, and β is the decay constant. Each researcher used different methods to obtain the model constants.

Shenoy used eight node solid elements to model a traditional and synthetic baseball. The constants G_0 and β were found by matching experimental force time data with that of finite element results. The remaining constant G_∞ was found from the equation

$$G_\infty = \frac{E_1}{2(1+\nu_1)}, \tag{1.36}$$

where the elastic modulus and Poisson's ratio were obtained from static tests. COR and dynamic compression simulations were carried out and compared to experimental data. Very good correlation was found between experimental and finite element predictions of impact force, COR, and contact time. The finite element results of the COR rate dependence agree with experimental results for both types of balls. Axtell [1.27], using Shenoy's baseball model, modeled the baseball collision against a rigid aluminum flat plate and found good correlation between the force time histories of the experimental and numerical model.

Sandmeyer [1.39] used eq. 1.35 to model softballs and baseballs impacting a rigid wall. The parameters in eq. 1.35 were found from reverse engineering. Using known COR and contact time values, the parameters were found through trial and error using finite elements. Although

an accurate baseball and softball model were simulated at 60 mph, Sandmeyer did not examine the rate effects of the model.

Nicholls [1.40] also used eq. 1.35 in LS-Dyna to model the viscoelastic behavior of baseballs. Nicholls proposed that the decay constant, β should be as close to the contact time as possible in order to account for the ball rate dependent behavior. G_∞ was found from quasi static compression tests and G_0 was found by trial and error. The quasi static compression tests were carried out to 50% of initial ball diameter, which is substantially more deflection than typical static compression tests require [1.26]. While 50% deflection may be typical of bat ball impacts [1.21], the rate dependence was not addressed. The rate of deflection in the finite element analysis was orders of magnitude greater than that of the static tests. The finite element results showed that the baseball COR increased with increasing pitch speed. This is contradictory to the experimental work of Axtell, Adair, Chauvin, Cross, Hendee, and Drane [1.27, 1.21, 1.6, 1.2, 1.9, 1.22]. The peak force increased while the contact time decreased with increasing pitch speed. This is in good agreement with experimental results.

Mase [1.41] modeled the COR and contact time for a golf ball using DMA experimental data. The resulting visco-hyperelastic material model accounts for the thermoplastic ball cover and the internal rubber core. DMA specimens were machined from the golf ball cover and rubber core. A sequence of relaxation tests were conducted at different temperatures allowing a master curve to be generated. The master curve was fit to a Prony series of the form

$$g(t) = \sum_{i=1}^{6} G_i e^{-\beta_i t} \,, \tag{1.37}$$

where *g(t)* is the relaxation function of the material, and G_i and β_i are parameters that are fit to the experimental data. The Prony series parameters were used in LS-Dyna, a commercially

available dynamic finite element software, to model the visco-hyperelastic behavior of the golf ball impacting a rigid steel wall. The finite element results of Mase agree with well with experimental COR and contact time results. The success of Mase leads one to believe that a similar study could be done for the polyurethane core of a softball.

Johnson and Lieberman [1.41] investigated several models of golf ball normal impact against a rigid steel surface. The first, known as the Simon model has the state-vector form

$$\dot{y}_1 = y_2 \tag{1.38}$$

and

$$\dot{y}_2 = -\frac{k}{m} y_1^{3/2}(1 + \alpha y_2) . \tag{1.39}$$

In eqs. 1.38 and 1.39, *m* is the mass of the ball, and k and α are experimentally determined parameters. Simon recommended that force vs. time data at two nominal approach velocities could be used to solve for the two parameters. The Simon model showed rebound velocities that were 5% high at 120 and 140 mph impacts. A five parameter model was also proposed by Lieberman and Johnson [1.41]. Two of the parameters, k_1 and α, come from quasi static compression tests. The other three parameters k_2, k_2, and c, are obtained from high speed impact tests. It is recommended that the latter three parameters be estimated by fitting the model COR at three different velocities to experimental data. The equations of motion in state vector space for the five parameter model are

$$\dot{y}_1 = y_2 , \tag{1.40}$$

$$\dot{y}_2 = -\frac{k_1}{m}|y_1|^a \operatorname{sgn}(y_1) - \frac{k_2}{m}|y_3|^\beta \operatorname{sgn}(y_3) , \tag{1.41}$$

and

$$\dot{y}_2 = -\frac{k_2}{c}\left|y_3\right|^{\beta}\,\mathrm{sgn}(y_3) + y_2\,, \tag{1.42}$$

where sgn($*$) has the value +1 or -1 depending on the sign of the argument. The five parameter model showed very good correlation with experimental data. The Simon and the five parameter model were only investigated for golf balls. No literature could be found that used eqs. 1.41-1.42 for softballs or baseballs.

1.8 Summary

The two properties currently used to characterize a softball are the COR and static compression. There is concern that current methods of measuring ball performance are not adequate. The COR and static compression are measured at speeds slower than seen in play. Much of the research that is published is related to the baseball, which uses a multi layer ball as opposed to the solid polyurethane softball. The properties of a softball can have a large effect on softball bat performance.

Despite many years of research, the COR remains a complicated subject. The COR has been found to depend on the speed, material properties, geometry, and the environment of the two colliding objects. While a handful of experimental COR studies have been performed relating to baseball, very little research has focused on the softball COR. It is unknown how the properties of the softball change over time and with repeated use.

Static compression is measured at a displacement rate that is 10,000 times slower than those seen in game play. A dynamic compression test has been shown to be feasible. Some researchers have found a linear correlation between static and dynamic compression while others have found the two measures of ball hardness to be independent. Impact force has been measured using load cells and pressure sensitive films. While more expensive, load cells have

been found to have increased reliability and accuracy. Again, very little data has been published with regards to softballs.

Softball bat performance measures such as the BBS and BPF are computed from a momentum balance of the bat-ball collision. Bat performance measures are adjusted to account for differences between measured and nominal ball COR and weight. There is a paucity of information, however, regarding the validity of these normalizing procedures.

An accurate finite element model of the ball is required in order to model the bat-ball collision. While several models of a sphere impacting a surface have been developed, much of the research has focused on modeling baseballs and has neglected to investigate the viscoelastic softball. The finite element models that exist have fit experimental COR data at only one speed while the rate dependence of the ball has not been investigated. The most common equation used to capture the viscoelasticity of the ball has not been investigated and it is unknown whether this model is sufficient. While most ball modeling has been done empirically, DMA has been used as an analytical tool. The material properties found from DMA are used in the finite element model. Researchers have found good correlation with experimental COR data using this technique. The multi layer construction of a baseball does not lend itself well to DMA, but it is unknown if DMA can be applied to the polyurethane core of a softball.

REFERENCES

[1.1] Barnes, G. *Study of collisions*. Am. J. Phys. **26**, p. 5-12. 1957.

[1.2] Cross, R. *The coefficient of restitution for collisions of happy balls, unhappy balls, and tennis balls*. Am. J. Phys. **68** (11), p. 1025-1031. 2000.

[1.3] ASTM F 1887-02. *Standard test method for measuring the coefficient of restitution of baseballs and softballs*. West Conshohocken, Pa. 2003.

[1.4] Barnes, G. *Study of collisions*. Am. J. Phys. **26**, p. 5-12. 1957.

[1.5] Brody, H. *The physics of tennis. III. The ball-racket interaction*. Am. J. Phys. **65** (10), p. 981-987. 1997.

[1.6] Chauvin, D.J., Carlson, L.E. *A comparative test method for dynamic response of baseballs and softballs*. International Symposium on Safety in Baseball/Softball. ASTM STP 1313, p. 38-46. 1997.

[1.7] Cochran, A.J. *Development and use of one dimensional models of a golf ball*. J. Sports Sciences. Taylor and Francis, Ltd. London, Uk. 2002.

[1.8] Heald, J.H., Pass, D.A. *Ball standards relevant to risk of head injury*. ASTM STP1229, p.223-238. 1994.

[1.9] Hendee, S.P., Greenwald, R.M., Crisco, J.J. *Static and Dynamic properties of various baseballs*. J. App. Biomech. **14**, p. 390-400. 1998.

[1.10] Shenoy, M.M. *Numerical simulation of baseball bat performance*. Masters thesis. Washington State University, 2000.

[1.11] Lu, C.J., Kuo, M.C. Coefficients of restitution based on a fractal surface model. J. Appl. Mech. **70**, p. 339-345. 2003.

[1.12] Stensgaard, I., Laegsgaard, E. *Listening to the coefficient of restitution-revisited*. Am. J. Phys. **69** (3), p. 301-305. 2001.

[1.13] Li, L-y., Thornton, C., Wu, C-y. *Impact behavior of elastoplastic spheres with a rigid wall*. Proc. Instn. Mech. Engrs. 214 (C). 2000.

[1.14] Hodgkinson, E. *On the collision of imperfectly elastic bodies*. Report of the fourth Meeting of the British Association for the Advancement of Science. 1835.

[1.15] Coaplen, J., Stronge, W.J., Ravani, B. *Work equivalent composite coefficient of restitution*. Int. J. of Impact Engrg. **30**, p. 581-591. 2004.

[1.16] Johnson, K.L. *Contact Mechanics*. Cambridge University Press, Cambridge. 1985.

[1.17] Thornton, C. *Coefficient of restitution for collinear collisions of elastic perfectly plastic spheres*. J. App. Mech. **67**, p. 383-386. 1997.

[1.18] Stronge, W. *Coupling of friction and internal dissipation in planar collision of compliant bodies. Proc. 2nd Int. Conf. on Contact Mechanics*. Plenum Press, p. 417-426. 1995.

[1.19] Kagan, D.T. The *effects of coefficient of restitution variations on long fly balls.* Am. J. Phys. **58** (2), p. 151-154. 1990.

[1.20] Dodd, M. *Verdict still out on effect of damp baseballs at Coors*. USA Today. pg. C.06. May 9, 2002.

[1.21] Adair, R.K. *The physics of baseball*. New York, Harper and Row, 3rd edition. 2002.

[1.22] Drane, P.J., Sherwood, J.A. *Characterization of the effect of temperature on baseball COR performance*. Proceedings from the Eng. of Sport 5. 2, p. 59-65. 2004.

[1.23] Moreland, J.C., Wilkes, G.L., Turner, R.B. *Viscoelastic behavior of flexible slabstock polyurethane foams as a function of temperature and relative humidity*. Polyurethanes World Congress. pp. 500-508. 1991.

[1.24] Giacobbe, P.A., Scarton, H.A., Lee, Y.S. Dynamic hardness (SDH) of baseballs and softballs. International Symposium on Safety in Baseball/Softball. ASTM STP 1313, p. 47-66. 1997.

[1.25] Aguiar, C.E., Laudares, F. *Listening to the coefficient of restitution and the gravitational acceleration of a bouncing ball*. Am. J. Phys. **71** (5), p. 499-501. 2002.

[1.26] ASTM F 1888-02. *Test method for compression-displacement of baseballs and softballs*. West Conshohocken, Pa. 2003.

[1.27] Axtell, J.T. *Experimental determination of baseball bat durability*. Masters thesis. Washington State University. 2001.

[1.28] Cross, R. *The bounce of a ball*. Am. J. Phys. **67** (3), p. 222-267. 1998.

[1.29] Vinger, P.F., Duma, S.M., Crandall, J. *Baseball hardness as a risk factor for eye injuries*. Arch. Ophthalmol. **117**, p. 354-358. 1999.

[1.30] Gobush, W. *Impact force measurements on golf balls*. Science and Golf: Proceedings of the First World Scientific Congress of Golf. Chapman and Hall, London. p. 219-224. 1990.

[1.31] ASTM F2219-02e1. *Standard test methods for measuring high speed bat performance factor*. West Conshohocken, Pa. 2003.

[1.32] ASTM F 1890-01. *Standard test method for measuring softball bat performance factor*. West Conshohocken, Pa. 2003.

[1.33] Nathan, A.M. Private communication. August, 2004.

[1.34] Menard, K.P. *Dynamic mechanical analysis-a practical guide*. CRC Press, New York. 1999.

[1.35] Williams, M.L., Landel, R.F., Ferry, J.D. *The temperature dependence of relaxation mechanisms in amorpous polymers and other glass forming liquids*. J. Am. Chem. Soc. **77**, p. 3701-3706. 1955.

[1.36] Crisco, J.J. *NCAA research program on bat and ball performance*. Final report to NCAA. 1997.

[1.37] Bathke, T. *Baseball impact simulation*. Senior mech. eng. thesis, Brown University. 1998.

[1.38] Mustone, T.J., Sherwood, J.A. *Using LS-Dyna to characterize the performance of baseball bats*. Unknown source.

[1.39] Sandmeyer, B.J. *Simulation of bat/ball impacts using finite element analysis*. Masters thesis, Oregon State University. 1994.

[1.40] Nicholls, R.L. *Private communication*. October, 2004.

[1.41] Mase, T., Kersten, A.M. *Experimental evaluation of a 3-D hyperelastic, rate dependent golf ball constitutive model*. Proceedings from the Eng. of Sport 5. **2**, p. 238-244. 2004.

[1.42] Johnson, S.H., Lieberman, B.B. *Normal impact models for golf balls*. The Engineering of Sport. Balkema, Rotterdam. 1996.

[1.43] Nathan, A.M. *Characterizing the performance of baseball bats*. Am. J. Phys. **71** p. 134-143. 2002.

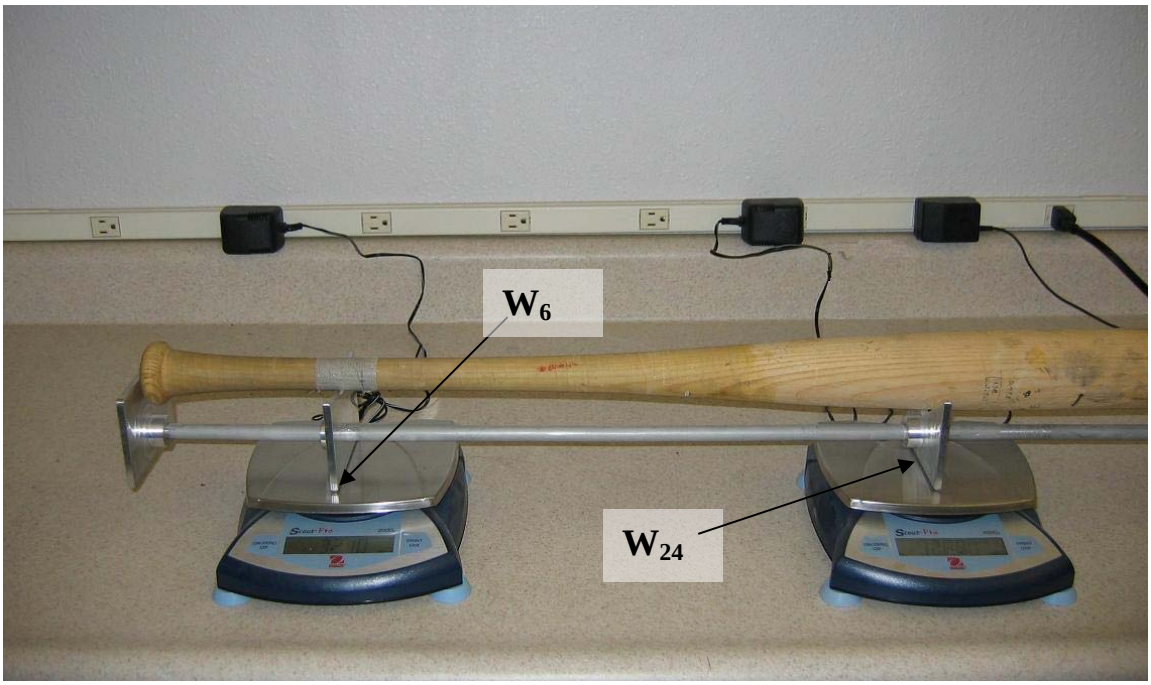

Figure 1.1: Fixture used to calculate the balance point of a bat. The weight at the 6" (W_6) and 24" (W_{24}) are recorded and eq. 1.16 is used to calculate the balance point.


Figure 1.2: Fixture used to measure the moment of inertia of a bat. The pivot clamp is located 6" from the knob end of the bat.

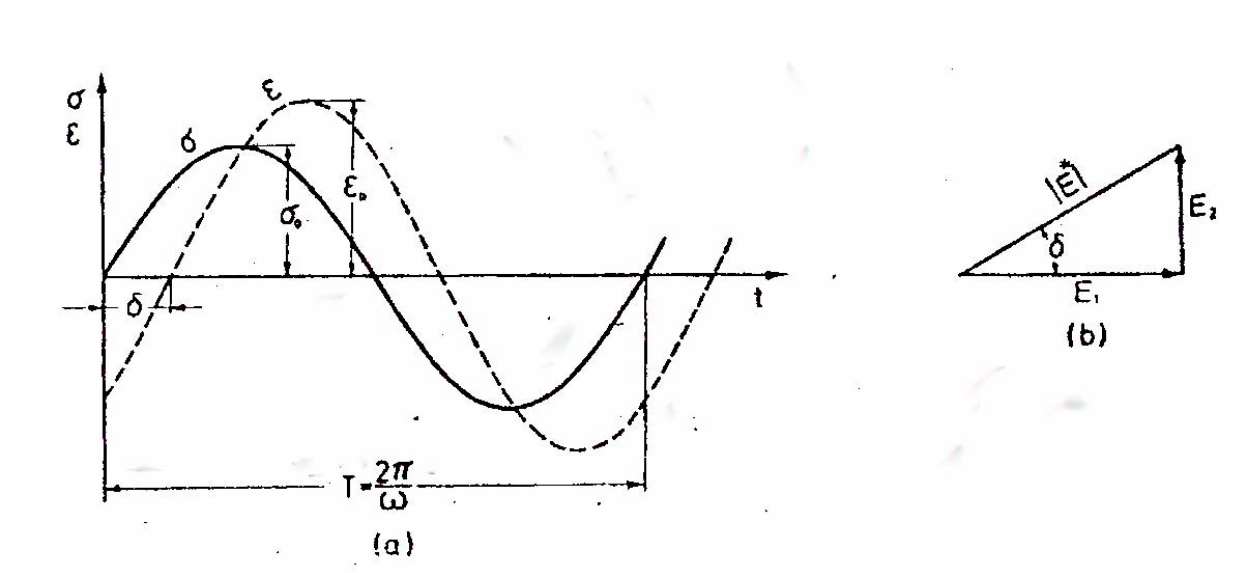

Figure 1.3: a) Physical relationships between stress, strain, and resulting phase angle. b) Visual representation of relationship between the complex modulus, the loss and storage moduli, and the phase angle. Copied from Menard [1.34].

CHAPTER TWO

EXPERIMENTAL RESULTS

2.1 Introduction

The two properties that are most commonly used to describe a softball are its coefficient of restitution (COR) and static compression [2.1, 2.2]. The COR is used to measure the energy of the ball that is lost during impact with a rigid wall [2.3], while compression is a measure of the ball's hardness. Both the ball COR and compression can affect a bat's hitting performance. The effect of compression on bat performance is primarily due to barrel deformation. Performance generally increases with barrel compliance. This so called trampoline effect is enhanced with increasing ball compression [2.4].

The vast majority of softballs are made from a polyurethane core with either a synthetic or leather cover. A cross section picture of the polyurethane ball is shown in figure 2.1. The synthetic core allows a wide range of ball COR and compression values to be achieved. The response of all viscoelastic materials is affected by the rate of loading, commonly referred to as rate dependence [2.5]. This work, however, is concerned with how the COR and the dynamic compression change with speed. Therefore, in this study, rate dependence will refer to the COR and dynamic compression changing with speed.

Softballs are typically denoted as XX/YY, where XX indicates the 60 mph ball COR and YY is the force in pounds needed to compress the ball ¼ inch and is a measure of ball hardness. The ball COR and compression are often used as another means of attempting to control bat performance and game play.

There is some concern whether the current practices of measuring ball properties adequately describe its response. The ball COR, for instance, is measured against a rigid and flat

surface at speeds that are lower than are used in play. It has been assumed without verification that this correctly represents play conditions. Ball compression is measured at a displacement rate that is 10,000 times slower than occurs in play. While the use of these methods represented a prudent starting point when they were introduced, little has been done to justify their continued use. There is also a paucity of information concerning how the properties of the ball change over time, with repeated use, humidity, or temperature. Much of the information that does exist is related to the baseball, which uses a multi layered ball of varying materials that can behave much differently than a polyurethane softball [2.4]. Figure 2.2 shows the cross section of a typical multi layer baseball.

The following will compare the response of softballs from several manufacturers, as a function of COR, compression, speed, and geometry. The effects of the number of impacts, temperature, and humidity/conditioning on its response will be considered as well. The appropriateness of normalizing bat performance data to account for differences in the balls will also be investigated.

2.2 Testing Aparatus

2.2.1 Ball Cannon

In order to test the properties of a softball and softball bat, it is necessary to propel the ball in an accurate, repeatable manner. A standard pitching machine could be employed, however, the variability in pitch speed, impact location, and spin of the ball pose multiple problems. To address this issue, an air cannon was designed that is capable of firing balls up to 150 mph accurately and without spin. A picture or the air cannon is shown in figure 2.3. A ball is placed in a sabot, and the ball/sabot combination is manually placed in the breach end of the cannon, as shown in figure 2.4. A sabot is used to hold the ball in place, without spinning, as it

travels down the barrel. Once the breach end plate has sealed the barrel shut, the valves on an air accumulator tank are opened and the sabot and softball ride together down the barrel until the sabot hits the arrestor plate. The arrestor plate functions to stop the sabot and allow the ball to continue traveling unobstructed towards a target (bat, load cell, or rigid wall).

Once the ball leaves the cannon, a series of three light curtains measure the speed of the ball before and after impact. A picture of the arrestor plate, light curtains, and rigid wall is shown in figure 2.5. The desired pitch speed is achieved by adjusting the pressure in the accumulator tank. The pitch speed was seen to increase proportionally to the air pressure inside the air accumulator tank. The accumulator tank is fed by a large air compressor that allows a wide range of pressures to be maintained. LabView version 7.1 (National Instruments, Austin, Texas) was used to control the pressure (pitch speed) and impact location of the cannon.

2.2.2 Sabot Development

Several iterations were required in the design of the sabot. The material chosen was required to withstand large impacts without failure and also could not damage the aluminum barrel. To manufacture the sabot, a solid cylindrical piece of material 5.5 inches in diameter and 3.0 inches thick was needed. The diameter of the sabot was turned down to match the inside diameter of the barrel. Material was removed from the inside of the sabot using a CNC milling machine and a CNC lathe. A picture of several sabot designs is shown in figure 2.6.

The initial sabot design, made of ultra high weight polyethelene (UHMWPE) would yield upon impact with the arrestor plate. After each impact this sabot required heat to reform the material inside the barrel. A picture of this initial design is shown in figure 2.6. The second sabot design utilized polycarbonate. Known for its ability to withstand large impacts, the polycarbonate proved to be a great improvement.

The bowl shape design of the sabot places a significant amount of mass in the bottom of the sabot. This mass is decelerated very quickly when the sabot hits the arrestor plate. The forces generated were large enough to initiate cracking in bottom of the polycarbonate sabot. Once a crack formed, it would spread to the side of the sabot and would continue to grow until the solid sabot was cracked in half. Several examples of damaged sabots are shown in figure 2.6.

To fix this problem, the one piece sabot was modified into a two piece design. The bottom of the sabot was removed using a lathe. The bottom surface was replaced by a thin fiberglass disk that was significantly lighter than the polycarbonate material it replaced. The new bottom plate was attached to the sabot using butyl tape. When the fiberglass plate cracks it is much easier and cheaper to replace than the entire sabot. A picture of the current sabot with the backing plate is shown in figure 2.7.

2.3 Static Compression

Static compression is the most common method used to measure the hardness of softballs. The standard test method to measure the static compression is outlined in ASTM F 1888-02. According to this method, a softball is placed between two flat plates and the peak force required to compress the ball ¼" over 15 seconds is recorded. The ball is rotated 90° and the ball is compressed again. The static compression is taken as the average of the two peak forces. A picture of the static compression test is shown in figure 2.8.

The static compression test is an application of Hertzian contact. For large deformations, the compressive force P is given by Tatara [2.6] as

$$P(R_1) = \frac{\sqrt{2}\pi E_1 R_1 U}{(1+\nu_1)} \left[\frac{1}{\frac{1}{2} - \sqrt{2} + 1 + 2\nu_1\sqrt{2} - 2\nu_1} \right], \tag{2.1}$$

where E_1, ν_1, and R_1 are the Young's modulus, Poisson's ratio, and radius of the ball, respectively. The lateral displacement U is measured from the center of the ball. From eq. 2.1, it can be seen that the compressive force increases as the radius of the ball increases. Therefore, it may not be appropriate to compare the static compression of balls of different diameter (eg. a baseball and a softball).

Cross, Hendee, and Mase [2.3, 2.7, 2.8] have shown that the load displacement curves of various types of sporting balls are nonlinear. Cross [2.3] reported that the force displacement relationship may also vary with frequency, which implies that the quasi static force versus compression curve may not be relevant to dynamic impacts. Nevertheless, a 44/375 ball from manufacturer A was compressed ¾" in 45 seconds and unloaded at the same rate. LabView was used to obtain the force displacement data from the load frame. The resulting curve is shown in figure 2.9. The loading portion of the curve appears to be linear while the unloading portion appears to be nonlinear. The ball remained deflected during the unloading phase, as evidenced by onset of zero force prior to the displacement returning to zero.

The area between the loading and unloading regions of the curve gives the energy loss [2.7]. Percent hysteresis was defined as the energy loss divided by the area under the loading portion of the curve, which was calculated to be 71.9%. This result was 10% higher than any found by Hendee [2.7] under similar loading conditions for baseballs.

With hopes of improving the current testing methodology, the properties of three different types of softballs from two manufacturers were studied. Table 2.1 gives a summary of the softballs used in the study. The average diameter of all the softballs was 3.77 inches (± 0.04), for which the diameter effects of eq. 2.1 will be neglected. The six dozen balls listed in table 2.1 were conditioned for two weeks in a 50% relative humidity environment prior to

static compression testing. The temperature in the humidity chamber was kept at $72^{\circ} \pm 2^{\circ} F$. Following the conditioning period, the static compression of each ball was measured. The average static compression for each ball type is shown in figure 2.10. The average static compression of the thirty-six balls from each manufacturer is also shown in figure 2.10. Manufacturer B had a 2.6% higher average static compression than the balls from manufacturer A.

Table 2.1: Types of softballs tested throughout the experimental study.

	Mnfc. A	Mnfc. B
Type of Ball	Quantity	Quantity
44/375	12	12
44/525	12	12
47/375	12	12

2.4 Coefficient of Restitution

2.4.1 Introduction

The COR of a softball, defined in eq. 1.2, is a measure of the energy loss during impact. The COR was experimentally obtained by firing a ball towards a rigid steel wall. The pitch and rebound speeds were measured from the light gates. The experimental setup is shown in figure 2.11. The air cannon allowed control over which surface of the ball was impacted. To minimize contact with the ball laces, only the four main faces, or ears, were impacted. The ball was rotated 90° after every impact so that each face of the ball was impacted one in four times.

The COR can have a large effect on bat performance. For a typical bat, a 2.0% increase in the COR can raise the calculated BBS by 0.7 mph. Governing bodies have set bat performance at a limit, so a small change can become important. It has also been found that the COR can have an appreciable affect on actual game play [2.9].

2.4.2 COR Rate Dependence

Experimental data has previously shown that the COR decreases linearly with increasing pitch speed [2.4, 2.7, 2.10]. The slope and intercept of this line, however, are not accounted for in current testing methods because the softball COR is only measured at one speed, 60 mph. There is no requirement on the COR at higher or lower speeds. This allows a ball manufacturer to control the rate dependence of the COR. In contrast, Japanese COR testing is done over several speeds [2.4]. Chauvin stated, "A multiple speed test could provide organizations a better view of how certain ball constructions will actually affect their game."

The COR of one dozen 44/375 softballs was impacted at 60, 90, and 110 mph. Each ball was impacted ten times at each speed with a maximum testing frequency of 1 impact per minute. The COR is plotted vs. impact speed in figure 2.12. There is a nearly linear trend of decreasing COR with increasing pitch speed. A 16.5% decrease in COR was observed between the 60 mph and 110 mph impacts.

To investigate the effect further, five 44/375 balls from four different manufacturers were impacted against a flat plate at speeds ranging from 50-110 mph. The COR was plotted against pitch speed in figure 2.13 and the results show clearly that the softball COR decreases nearly linearly with pitch speed. Chauvin [2.4] attributes the increased loss of energy to increased deformation of the ball at higher speeds. Chauvin explains that a ball that losses energy as it deforms will expend increasingly more energy with greater deformation.

The slope and intercept of a straight line fit of the data in figure 2.13 is shown below in table 2.2. Although each ball tested was a 44/375, the results show that there are differences in the slope and y-intercept from one manufacturer to the next. The differences shown in the COR at 60 mph could result in as much as 15ft of ball travel [2.9].

Table 2.2: Slope and y-intercept of the straight line fit for each manufacturer in figure 2.8. Each value has been multiplied by 10,000 for easier comparison.

	Slope 1/mph (x10,000)	y-intercept (x10,000)
Mnf. A	-13.48	5288
Mnf. C	-14.46	5491
Mnf. D	-13.33	5197
Mnf. E	-14.61	5223
Average	-13.97	5300

The COR at 60 and 90 mph was measured for each of the softballs in table 2.1. Each ball was impacted ten times at 60 and 90 mph. The average COR of all 36 balls was calculated for each impact speed. Figures 2.14 and 2.15 display the average COR vs. impact number at 60 and 90 mph, respectively. The average COR of all the balls was found to decrease by 11% from 60 to 90 mph. The 90 mph COR vs. 60 mph COR is plotted in figure 2.16. Each point is the average of 10 impacts. Although there is scatter in the data, a linear correlation was observed between the COR and speed, which is consistent with figures 2.12 and 2.13.

2.4.3 COR Test Speed

The 60 mph rigid wall COR value is used to calculate bat performance over a wide range of bat-ball collision speeds. For example, the ASA bat certification test requires that a softball be fired at 110 mph at an initially stationary bat. The USSSA and ISF bat certification test requires that a ball be fired at 60 mph at the same stationary bat. The fifty mph difference in pitch speed will clearly change the energy losses seen by the ball. However, the same 60 mph ball COR value is used in all bat performance calculations, regardless of the bat-ball collision speed. An improved COR test speed may be needed. The speed at which the COR should be measured may be found by assuming that the ball momentum change in a rigid wall COR impact is equal to that with the bat-ball impact. The momentum balance for a ball impacting a rigid wall is

$$Ft = m\left(v_i - v_r\right), \tag{2.2}$$

where m, v_i, and v_r are the ball mass, inbound, and rebound speed and the quantity Ft is the impulse of the impact. The inbound and rebound speeds are taken to be negative and positive, respectively. F is the impact force and t is the contact time. Figure 2.13 shows how the COR (ratio of rebound to inbound speed) changes with speed. From this data the inbound and rebound speeds will be found that solve the momentum balance. Solving eq. 2.2 for F yields

$$F = \frac{m(v_i - v_r)}{t}. \tag{2.3}$$

The momentum balance for a ball impacting a bat is

$$Ft = m(v - BBS), \tag{2.4}$$

where v is the pitch speed, m is again the ball mass, BBS is the batted ball speed, and t is the contact time. The pitch speed is given as $v = 25$ mph. For a 110 mph collision, the BBS will have a range of values from 88 mph (wood bat) to 104 mph (high performing bat). Solving equation 2.4 for F yields

$$F = \frac{m(v - BBS)}{t}. \tag{2.5}$$

Equating the forces in eqs. 2.3 and 2.5 gives

$$\frac{m(v_i - v_r)}{t} = \frac{m(v - BBS)}{t}. \tag{2.6}$$

The contact time t for a ball impacting a rigid wall is assumed to be approximately equal to the contact time t for the ball impacting a bat. Algebraic simplification results in the equation

$$v_i - v_r = v - BBS. \tag{2.7}$$

The quantity on the right hand side of eq. 2.7 is assumed to be a constant with the BBS ranging from 88 mph (wood bat) to 104 mph (high performing bat). The correct COR pitch speed v_i will be calculated for the range of BBS 88 to 104 mph. The average of the data in figure 2.13 gave a

best fit linear equation for the COR vs. impact speed. The resulting empirical equation relating the COR to pitch speed is

$$e = -0.001397 v_i + 0.5300 . \tag{2.8}$$

Using the definition of the COR in eq. 1.2, eq. 2.8 can be written as

$$-v_r = -0.001397 v_i^2 + 0.53 v_i . \tag{2.9}$$

Solving equation 2.7 for the rebound speed and plugging this result into eq. 2.9 gives

$$v - BBS = const = -0.001397 v_i^2 + 1.53 v_i . \tag{2.10}$$

Solving eq. 2.10 for BBS's of 88, 98, and 104 mph yields nominal COR pitch speed values of 69, 75, and 79 mph, respectively. Since most modern bats perform near 98 mph, the median pitch speed value of 75 mph is recommended. In figure 2.13, the COR was observed to decrease by 4.62% from 60 to 74 mph. Therefore, measuring the COR at 60 mph for a 110 mph bat ball impact may not be appropriate given the decrease in COR.

2.5 Dynamic Compression

2.5.1 Background

The effect of ball hardness can be viewed from the perspective of impact force. This has been achieved by firing balls toward a rigidly mounted flat plate attached to a load cell, as shown in figure 2.17 [2.4, 2.7, 2.10, 2.11]. The force is measured as a function of time from the ball impacting the load cell. The peak force during contact is denoted as the dynamic compression. The dynamic compression is relevant to bat performance since it governs the deformation that would occur in a bat.

The focus of past work has been toward human safety, and developing numerical models. A result of this work was the observed linear correlation between the dynamic and static compression [2.4, 2.7, 2.10, 2.11]. This observation will be explored further in the current study.

Two different types of load cells were used to measure the dynamic compression. A strain gage load cell (Model 41/E367-01, Sensotec) was initially used. The strain gage load cell used in the current work had a deflection of 0.003 inches at maximum load. It was found that electrical noise and vibrations in the impact made it difficult to locate the peak force and calculate the impulse of the impact. A representative plot of the force vs. time from the strain gage load cell is shown in figure 2.18. A filter was required to remove some of the electrical noise and mechanical vibrations. Filtered strain gage load cell force-time data of a 44/375 ball impacted at 60 and 90 mph is shown in figure 2.19. The filtered data resulted in a much smoother curve when compared to the raw data in figure 2.18.

A piezoelectric load cell (Model 208C05, PCB Piezotronics, Depew, New York) was found to have a deflection of 0.0008 inches at maximum load. The inherently stiffer piezoelectric structure was found to reduce the vibrations and electrical noise in the signal. Three piezoelectric load cells were mounted in an equilateral triangle directly behind the point of impact. The individual load cell signals were combined using a a four channel summation amplifier (Model 482M66, PCB Piezotronics, Depew, New York). A picture of the load cell setup is shown in figure 2.20. A plot of the unfiltered force vs. time data is shown in figure 2.21. When comparing figures 2.18 and 2.21, it is clear that the piezoelectric load cell created a much cleaner signal with smaller vibration effects.

The two types of load cells provided a check on one another, and dynamic compression values were found to be similar. The data that was initially measured with the strain gage load cell was therefore not repeated with the piezoelectric load cell.

2.5.2 Impulse COR

It is possible to perform ball COR measurements using light curtains while measuring dynamic compression. There is concern, however, that the compliance of the load cell could affect the COR measurements. To address this issue, 12 balls were impacted ten times against a strain gage load cell. After ten days, the same 12 balls were impacted against the rigid wall. The average COR of the 12 balls impacted with the strain gage load cell decreased 0.7% in comparison to their rigid wall COR value (which is within the repeatability of the COR measurement). The COR vs. impact surface is shown in figure 2.22. Results from the stiffer piezoelectric load cell agree with the strain gage results. Therefore, the effect of the load cell on ball COR measurements for the current work was considered negligible.

The area under the curves in figures 2.18, 2.19, and 2.21 is the impulse imparted to the ball from the collision. The relative speeds before and after impact can be found from a momentum balance using the equation

$$(v_i - v_r) = \frac{Ft}{m}. \tag{2.11}$$

Since the quantity $\frac{Ft}{m}$ is known from the force time data and ball mass, the left hand side of eq. 2.11 can be used as a relative measure of the speed of the ball before and after impact. This impulse COR can be compared to the COR measured using the light curtains.

The light curtain COR and the impulse COR (from the strain gage load cell) are shown in figure 2.23 for 60, 90, and 110 mph impacts. The average momentum from the load cell and the light curtains were within 1% of each other. The electrical noise and vibration of the load cell increased the variation by a factor of ten over the light curtains, however.

The impulse COR measurements were repeated using the piezoelectric load cells. The average momentum measured from the light curtains and the piezoelectric load cells is shown in figure 2.24. The impulse COR was observed to be within 0.7% of the light curtain COR. The reliability of the piezoelectric impulse COR showed great improvement, as the variation was less than that of the light curtains. The variation in each momentum measurement was less than one mph.

2.5.3 Dynamic Compression Rate Dependence

The dynamic compression was measured for the balls in table 2.1 at 60 and 90 mph. Each ball was fired ten times at each speed at 1 impact per minute. The average dynamic compression vs. impact number is shown in figures 2.25 and 2.26. There does not appear to be a trend in the dynamic compression data over the ten impacts. It is concluded therefore, that a testing frequency of one impact per minute over ten minutes does not change the dynamic compression of the ball. This will be important in the discussion of ball degradation. The average dynamic compression at 60 and 90 mph was found to be 2940 and 4400 lbs, respectively, for a 49.5% increase.

Three 44/375 balls from four manufacturers were used to measure the dynamic compression at speeds of 50, 60, 74, 90, and 110 mph. The data is plotted in a bar chart in figure 2.27 for easy comparison of dynamic compression between the different manufacturers and speeds. Although not shown, the data was also evaluated on a scatter plot. The dynamic compression of each manufacturer was observed to increase linearly with increasing pitch speed. The slopes and y-intercepts of the straight line fits for each manufacturer are shown in table 2.3. The y-intercept data appears reasonable since the value should be zero.

Table 2.3: Slope and y-intercept data for the dynamic compression vs. speed of different manufacturers.

	Slope lbs/mph	y-intercept (lbs)
Mnf. A	56.641	29.844
Mnf. C	56.425	34.536
Mnf. D	57.962	2.4036
Mnf. E	54.061	126.86
Average	56.27225	48.4109

It was shown above that the momentum change in a 75 mph rigid wall COR test is the same as a 110 mph bat-ball impact. According to figure 2.27, a bat will therefore will see approximately 4200 lbs of force in a typical bat-ball collision. The effect of the cylindrical bat surface on impact force will be discussed below in section 2.7.

2.5.4 Dynamic and Static Compression

Dynamic compression is shown as a function of static compression for three ball types from two ball manufacturers in figure 2.28. A linear correlation between the two measures of ball hardness is consistent with previous observations of baseballs [2.7]. The dynamic compression presented in figure 2.28 has been normalized with the ball momentum to remove the effects of variation in pitch speed and ball mass using the equation

$$F_N = \frac{F}{v_i m}, \tag{2.12}$$

where F_N is the normalized dynamic compression (1/s), F is the dynamic compression, v_i is the pitch speed, and m is the ball mass. The normalization also allows direct comparison of results measured at different pitch speeds. Results from tests conducted at 90 mph, for instance, agree closely with those shown for 60 mph, as shown in figure 2.29.

It should be noted that an extrapolation of the data in figures 2.28 and 2.29 produces a non-zero y-axis intercept. This may be expected since a ball of negligible hardness will still

produce an impact force when delivered at a high speed. This implies that static and dynamic compression should not be taken as directly proportional (an offset is needed).

Figure 2.30 presents the data of figure 2.28 in a different way. The static and dynamic compression are plotted vs. ball type using a column chart. An approximately constant offset between static and dynamic compression is associated with balls of similar nominal ball hardness. However, when comparing a 44/375 ball with a 44/525 ball, the offset is not constant. It may not be appropriate, therefore, to use static compression as a predictor of impact force for balls of varying ball hardness.

2.6 Multi Layer Softball Design

A multi layer softball has recently been introduced that appears to have a large effect on the performance of softball bats. The ball is designed with a soft foam outer shell approximately 1/8" thick. The inner sphere is made of a harder foam. A cross section picture of the ball showing the different layers is shown in figure 2.31. Since static testing is done over ¼" (1/8" on each side of the ball), the soft outer shell governs the measured ball compression. In a bat-ball impact, the ball can deform up to 50% of its initial diameter [2.9]. Therefore, a typical bat-ball impact will engage both the soft and the hard layer of the ball. For this multi layered ball, the static compression is effectively measuring an artificial ball hardness.

Several tests were performed on six 44/375 multi layer balls, and table 2.4 summarizes the order in which the tests were performed. For direct comparison, six traditional 44/375 balls were tested concurrently with the multi layer balls.

The multi layered and traditional balls had an average ¼" static compression value of 318 and 365 lbs, respectively. After a 24 hour recovery, each ball was tested for dynamic compression and COR at 60, 90, and 110 mph using the flat plate impact surface. Following the

dynamic testing, a ½" static compression test was carried out on the multi layer and traditional balls. Table 2.5 summarizes the results of each test, and the average static compression, COR, and dynamic compression are shown in figures 2.32, 2.33, and 2.34, respectively.

When only looking at the ¼" static compression and the COR, it would appear that the multi layer ball is the same as the traditional ball. In fact, the multi layer ball has a very similar COR but a lower static compression, so it would be appropriate to assume that the multi layer ball would result in a lower BBS than the traditional ball. However, figure 2.34 shows that the dynamic compression of the multi layer balls is as much as 13.9% higher than the traditional balls.

The ½" static compression test was better able to characterize the hardness of the multi layer ball than the ¼" test. In the ¼" test, the static compression of the traditional ball was observed to be higher than the multi layer ball. In the ½" test, which engages both the soft and the hard layer of the ball, the traditional ball was observed to have a smaller static compression value than the multi layer ball.

To quantify the effect of the increased dynamic hardness, six multi layered 44/375 balls were used to test the performance of a 2004 ASA certified composite bat according to ASTM 2219. The properties of the bat are shown in table 2.6. The BBS was calculated via eq. 1.25. As a benchmark, the bat was also tested with six traditional 44/375 balls. The average COR, static compression, and dynamic compression of the balls used to test the composite bat are shown in table 2.5.

The bat was scanned in ½" increments to find the location of maximum BBS. The resulting curve of BBS vs. impact location is shown in figure 2.35. Using the multi layer balls, the maximum BBS, measured at the 20.5" location (from the pivot point), was found to be 102.7

mph. The standard 44/375 balls yielded a maximum BBS of 96.2. The 6.5 mph increase in performance with the multi layer balls shows that current methods of measuring ball performance may not be adequate. The dynamic properties of the ball are not completely captured with current methods. The dynamic compression and the ½" static compression were the only methods that were able to distinguish the multi layer ball from the traditional ball.

Table 2.4: Testing order of nine multi layer and Traditional softballs.

Multi Layer and Traditional 44/375 Softballs		
Testing Order:	Test	Notes:
1	Static Compression	1/4"
2	Dynamic Compression/COR	60 mph
3	Bat Test	110 mph
4	Dynamic Compression/COR	90,110 mph
5	Static Compression	1/2"

Table 2.5: Average values of the tests outlined in table 2.4. Six balls of each type were used in the study.

Test:	Standard Ball	Multi Layer Ball
1/4"Static Compression (lbs)	365	318
60 mph COR	0.442	0.44
60 mph DC (lbs)	3208	3654
BBS (mph)	96.2	102.7
90 mph COR	0.395	0.4
90 mph DC (lbs)	5070	5473
110 mph COR	0.37	0.373
110 mph DC (lbs)	6196	6544
1/2" Static Compression (lbs)	640	739

Table 2.6: Properties of the composite bat used to test the performance of the traditional and multi layered balls.

Bat Material:	Weight (oz):	Length (in):	Balance Point (in)	COP (in)
Composite	28.825	33.9375	20.035	21.972

2.7 Cylindrical Impact Surface

Some believe that ball COR should be measured against a rigidly mounted cylindrical surface to better simulate bat testing and game conditions. The effect of a rigid cylindrical surface was considered by attaching a solid steel half cylinder of 2 ¾" diameter (analogous to a

baseball bat barrel) to the piezoelectric load cells. Three load cells were mounted in an equilateral triangle. A picture of the experimental setup is shown in figure 2.36.

The dynamic compression vs. time is shown in figure 2.37 for a ball from manufacturer B impacting a flat plate and a cylindrical surface. In figures 2.38 and 2.39, the 90 mph ball COR and dynamic compression were observed to decrease by 6.5% and 7.8%, respectively due to the cylindrical impact surface. The cylindrical impact surface effectively reduces the contact area of the ball at impact. The reduced area results in greater local deformation inside the ball, which contributes to the energy loss or reduced COR. The reduction in dynamic compression is also associated with increased local ball deformation, as evidenced by a 7.5% increase in contact duration between the flat and cylindrical contact surfaces.

To study the effect of diameter on the COR and dynamic compression, a second half cylinder of 2 ¼" diameter (analogous to a softball bat barrel) was also investigated. A fourth load cell was added in the center of the equilateral triangle to increase the stiffness. Six balls from manufacturer A were impacted eight times on both cylindrical surfaces. The ½" reduction in the diameter did not appear to have a measurable effect on the COR or dynamic compression as the data was within 0.6% of each other.

The rate dependence of the COR and dynamic compression on the cylindrical surface was investigated using three 44/375 balls from four manufacturers. Each ball was fired eight times at speeds of 60, 90, and 110 mph. Figure 2.40 shows the average COR vs. pitch speed for each manufacturer. The slope of the COR vs. pitch speed on the cylindrical impact surface was observed to decrease by 27% compared to the flat plate, as shown in figure 2.41. Using this result and following a similar derivation to that of section 2.4.3, a more appropriate speed to

measure the COR for a 110 mph bat-ball impact was found to be 80 mph (compared to the 75 mph calculated for the flat plate).

The dynamic compression vs. pitch speed is shown in figure 2.42. The dynamic compression was observed to increase proportionally with pitch speed, and was found to be 14.7% less than that for the flat plate. The impulse COR calculated from these results was observed to be 2.8% higher than that from the light curtain COR.

The results show that current measures of ball COR are higher than would occur in a bat-ball impact. Ball COR tests using a cylindrical surface were shown to be feasible and added minimal effort to the test. It should be noted, however, that standard ball pitching machines would not likely have the accuracy needed for cylindrical surface COR measurements.

2.8 Degradation

2.8.1 Consecutive and Alternating Impact Study

Most test standards and protocols limit the number of impacts that a ball can undergo before being deemed unsuitable to measure bat performance [2.12, 2.13]. These limits remain in place despite results that show baseball COR and compression are constant through 100 impacts [2.10]. Synthetic softballs can have greater temperature and viscoelastic effects than the natural materials they replaced. Little information exists concerning the durability of synthetic softballs.

The dynamic compression and COR of three softballs impacted 100 times at 90 mph consecutively (within 120 minutes) are presented in figure 2.43. The data appear to suggest a significant change in response as the ball was impacted. The ball surface temperature was measured after each impact using an infrared temperature gauge (Model: MiniTemp, Raytek). The temperature increase can be seen graphically in figure 2.44 which shows the average

temperature vs. impact number. The ball temperature increased by 10° F degrees over the 100 impacts.

To separate the effects of temperature and ball impacts, another group of balls was tested intermittently. The procedure involved 10 consecutive impacts, followed by a minimum 60 minute pause for the ball to return to lab temperature. The average temperature per ten impacts vs. the intermittent impact number is shown in figure 2.45. The ball temperature increased approximately 5° F during the 10 impacts over 10 minutes. As shown in figure 2.46, the dynamic compression and COR appear relatively independent of impact number. This suggests that ball temperature and testing frequency may play a more important roll in measuring bat performance than limiting the number of ball impacts. Similar results were obtained from a group of balls impacted repeatedly against a cylindrical surface.

As shown in Fig. 2.43, the ball COR was observed to decrease by 0.001 over the first 10 impacts. Using 0.001 as a maximum that a test should affect the ball, it is recommended that a ball should not be impacted more than 10 times in one hour, or more than one impact per minute. Balls that are to be reused in subsequent bat tests should be given a minimum of one hour in standard laboratory conditions to recover following a sequence of impacts before they are to be used again.

As observed in Fig. 2.14 and 2.15, a pattern is apparent when the first 4 impacts are compared to the subsequent impacts. The plot suggests that after each face has been impacted once, the COR increases. Temperature effects could be responsible for the change in COR. In figure 2.47, the ball surface temperature was measured using an infrared temperature gauge and was plotted against impact number. The surface temperature of the softball was seen to increase $1.5^{\circ}F$ after the fifth impact, which corresponds to the increase in the COR. However, the effect

of increasing temperature would be to soften the polyurethane core of the softball. A softer ball will deform more, and a reduction in the COR would be predicted. It is possible that the increase in COR after the fourth impact is related to the viscoelastic response of the synthetic core. If the ball has not returned to its original shape before the second impact on a face, the ball would in effect be preloaded in compression. Again, using Chauvin's reasoning, a harder ball will deform less and more kinetic energy will be retained It is advisable, therefore, that both internal heating and viscoelastic effects should be considered when evaluating allowable ball test frequencies.

The current procedure for measuring the ball COR requires that the first six valid impacts be taken as the average value. Due to the increase in the COR after the fourth impact however, this method may not give the most accurate number. It is recommended that the first four impacts be discarded and the COR be taken as the average of the last six of ten impacts.

2.8.2 Long Term Ball Study

A long term ball study has been carried out to examine how the properties of softballs change over time. Twenty-four 44/375 balls from manufacturer A were used to study the COR and static compression. Balls were initially tested out of the box at an unknown moisture content at room temperature. After the initial test, the balls were placed in a conditioning chamber at 50% relative humidity. Thereafter, six balls were tested for COR and another six balls were tested for static compression on a monthly basis. The weight of these twelve balls was monitored as well. A control group was established with the remaining twelve balls. Six COR control balls were tested for the COR initially out of the box. Three of these balls were placed at 50% and left untouched for the remainder of the study. The other three balls were placed in a

vacuum bag and were also untouched. The six static compression control balls followed the same procedure.

The average COR and static compression of the long term ball study are shown in figure 2.48. The initially low values of the COR and static compression correspond to the pre conditioning values. It is interesting to note that every ball in this study was observed to lose weight in the conditioning chamber, indicating that the balls were at greater than 50% relative humidity prior to arriving in Pullman, Wa.

The fluctuation in the static compression was found to be primarily related to the test room environment. A $4^{\circ}F$ change in the lab temperature resulted in approximately 20 lbs change in the static compression value. The last static compression data point was observed to increase significantly, but ongoing research is needed to determine if this increase is permanent. The COR was found to vary by less than 1.0%. It is hypothesized that this variation in the COR over time is within the experimental error of the COR test.

It is recommended that the long term ball study be continued to gain a better understanding of how the ball properties change over time. Also, introducing a dynamic compression group may give additional evidence.

2.8.3 Conditioning

Conditioning requirements are often placed on balls before they may be tested. The effect of ball conditioning was examined by monitoring the weight gain of five balls taken from a 30% RH environment to 50% RH. Figure 2.49 shows the percent weight gain as a function of time. It was observed that the balls require approximately 14 days to reach equilibrium. The effect of humidity was further examined by comparing the COR and dynamic compression of a dozen balls conditioned at 30%RH and 55%RH. Going from the dry to humid environments, ball COR

and dynamic compression were observed to increase by less than 1%. Static compression, however, decreased by 21% over the same change in humidity, as shown in figure 2.50. This suggests that the rate effects of softballs may depend on their moisture content.

2.9 Ball Homogeneity

Preliminary experimental COR and static compression testing was performed that suggested the ball properties were independent of the cover. In these studies, the COR and static compression were observed to remain constant with and without the leather cover. However, subsequent experimental testing has shown that the cover may affect the performance of the ball.

Four 44/375 balls from manufacturer A were tested with the cover on for COR and dynamic compression at 60 mph. After a one hour rest, the cover was removed from the balls and the COR and dynamic compression were measured again. When the cover was removed, the COR was observed to increase by 4.2% while the dynamic compression decreased by 16.6%, as shown in figures 2.51 and 2.52.

If the leather cover had a negligible mass, one would expect the dynamic compression to increase when the cover was removed due the core being much harder than the cover. However, the leather cover and stitches were found to weigh approximately 1.43 oz, which accounts for 21% of the total ball weight. The dynamic compression results with and without the cover were normalized with the ball momentum according to eq. 2.12. The normalized dynamic compression of the ball without the cover was observed to increase by 4.38% when compared to that with the cover, indicating that the core of the ball is harder than the core with the cover. Therefore, the decrease in the dynamic compression is a direct result of Newton's second law.

The decrease in the dynamic compression also causes the ball to deflect less. This reduced deflection is responsible for the increase in the COR, since less energy is expended in

the compression and expansion phases of the impact. Also, the soft cover material may cause additional energy loss in the softball.

It is possible that removing the cover could affect the rate dependence of the COR and dynamic compression. To investigate this effect, six 44/375 balls from manufacturer A were experimentally tested at 60, 90, and 110 mph with and without the leather cover. In figures 2.53 and 2.54, the average COR and dynamic compression with and without the cover were plotted vs. the pitch speed. At each speed, impacts with the cover on had lower COR and higher dynamic compression values than the ball without the cover. However, a constant offset at each speed was not observed in either figure. The slopes of the COR and dynamic compression vs. pitch speed of balls with and without covers were observed to remain approximately constant, indicating that the rate dependence was not affected by the removal of the cover.

The design of the softball may have an effect on the homogeneity of the softball. The properties of the polyurethane core vary from one type of ball to the next. The type of bond, thickness, and material (synthetic or leather) of the cover may also have an effect. The type of ball used in the preliminary study was not documented, but it is possible that a combination of these factors caused the ball COR and static compression to remain constant with and without the cover.

2.10 Normalizing

The softball COR, weight, and hardness can have a large effect on bat performance. A 2% change in ball COR results in a 0.7 mph change in the BBS. A 2% change in ball weight can result in a 0.4 mph change in BBS. The change in bat performance due to ball hardness (static or dynamic) is bat dependent, and is difficult to quantify. The dynamic compression, however, was seen to have a large effect on the BBS in section 2.6.

In order to have accurate and reproducible bat performance data, balls with very tight property tolerances are required. However, softballs are manufactured to be used in a game, where slight differences in the ball are not as critical as in the laboratory. It is difficult and time consuming, therefore, to find a ball that fits laboratory criteria. A balance between laboratory accuracy and ball testing time must be placed in the ball property tolerances. The ASA requires that each ball used in a bat certification test have a 60 mph COR equal to $0.44 \pm .005$, a ¼" static compression between 350-375 lbs, and a weight greater than 6.75 oz. The dynamic compression is not currently controlled. The small differences in these balls can still lead to measurable differences in bat performance. It is desirable, therefore, to adjust the bat performance to account for differences between the balls. This method, known as normalizing, is currently used to account for differences in ball COR and weight. The ASA normalizes for the ball COR and weight in equations 1.24 and 1.23, respectively. The ISF and USSSA normalize for ball COR in equation 1.21.

A normalizing study was performed to investigate the validity of normalizing for ball COR and weight, and to quantify the effects of ball hardness. Three groups of three balls were used that had specific properties. For the COR group, denoted as COR, the COR was varied while keeping the static compression and weight approximately constant. For the compression group, denoted as COMP, the static compression was varied while keeping the COR and weight approximately constant. For the weight group, denoted as WGT, the weight was varied while keeping the COR and static compression approximately constant. Each group (COR, COMP, WGT) had a low, medium and high value for the respective varying parameter. For example, the COR group had a low COR ball, a medium COR ball, and a high COR ball with the weight and static compression for these three balls held approximately constant. The properties of each

group are listed in table 2.7. Figures 2.55, 2. 56, and 2. 57 show the relative change of each parameter for the COR, COMP, and WGT groups, respectively.

Finding the balls to be used in the study was not a simple task. Hundreds of balls were surveyed to find the nine balls used in the study. An effort was made to keep the tolerance as tight as possible for the two constant properties in each group. All constant properties within a group varied by less than 2.5%, except for the "High" ball in the WGT group which had a COR 4.0% higher than that of the other two balls.

Care was taken in selecting the bats for the normalizing study. A low performing bat has a high barrel stiffness while a high performing bat has a low barrel stiffness [2.14]. A bat with a high barrel stiffness (wood or low performing aluminum) causes the ball to deform more than does a bat with a low barrel stiffness. The ball will lose more energy as it deforms. Therefore, it is important to investigate the validity of normalizing on bats of varying performance.

Four bats of increasing performance were used to investigate normalizing. Each bat was initially tested for performance using standard softballs at 90 mph and the BBS was computed. A wood bat, a low performing aluminum bat, a good composite bat, and a very high performing composite bat were used in the normalizing study. Each bat had progressively higher performance. The BBS vs. impact location is shown for each bat in figure 2.58. The wood, low performing aluminum, good composite, and very high composite bat had maximum BBS's of 87, 91, 98, and 104 mph respectively.

Each bat was impacted five times in the maximum BBS location with each of the nine balls. Impacting the bat at the maximum BBS location is important because energy losses in the bat can be neglected at this point [2.15]. Due to high ball hardness values, the pitch speed had to be reduced from 110 mph to 90 mph (tests at 110 mph caused damage in the aluminum and

composite bats). A 90 mph pitch will increase the calculated BBS compared to a 110 mph pitch. However, the important aspect in this study was the relative change in bat performance with the different types of balls.

The BBS of each bat vs. the COR group is shown in figures 2.59 and 2.60. In figure 2.61 the BBS is normalized for the ball weight and COR while in figure 2.60 the BBS was normalized for the ball weight only. Since the weight of the COR group balls was virtually the same, the weight normalization should have a negligible effect.

In figure 2.59, it appears that the COR normalization technique over corrects and results in a BBS that is too high. This over correction implies that the current technique of COR normalization may not be accurate. The BBS data that was only normalized for ball weight should increase with increasing COR. In figure 2.60, however, only the two low performing bats showed this trend. The "low COR" ball showed higher performance than that of the "med" and "high" COR balls on the two higher performing bats, despite the weight and static compression remaining constant. Upon further investigation, it was found that the dynamic compression of the "low" COR ball was 20% higher than the other two. This is further evidence that static compression may not be capable of predicting dynamic ball hardness.

The BBS vs. the compression group is shown in figures 2.61 and 2.62. Increasing the static compression was observed to increase the BBS for the two high performing bats while it made little difference in the low performing bats. The increase in performance in the high performing bats is attributed to the trampoline effect. Since the COR was nearly constant in this group, normalizing for the ball weight only did not have a significant effect on the BBS results in figure 2.61.

In figures 2.63 and 2.64, the BBS is plotted vs. the weight group. The "high" weight ball had a 2.8% lower COR than the other two balls. The BBS normalized for the COR and weight in figure 2.63 again overcorrected the BBS due to the decrease in the COR for the "high" weight ball. The data normalized for the ball weight only in figure 2.64 showed very good results, indicating that the weight normalizing technique is appropriate.

Table 2.7: Normalizing study ball data. Nine balls were used overall.

	Low	Medium	High
	Changing COR		
COR	0.4114	0.4586	0.5088
Compression (lb)	466	457	468
Weight (oz)	6.72	6.715	6.72
	Changing Compression		
COR	0.436	0.441	0.449
Compression (lb)	341	391	452
Weight (oz)	6.975	6.955	6.925
	Changing Weight		
COR	0.462	0.468	0.4489
Compression (lb)	452	455	448
Weight (oz)	6.43	6.78	7.04

2.11 Summary

A cannon was developed that is capable of firing softballs accurately and without spin at speeds ranging from 0-150 mph. A critical aspect of this design was the polycarbonate sabot, which holds the ball as it travels down the barrel. A series of three light curtains were used to measure the pitch and rebound speeds of the softball. The cannon was utilized in this study to measure the COR and dynamic compression as a function of speed, geometry, time, and environmental conditions.

Ball hardness is currently measured in a quasi static compression test, where the displacement rate is 10,000 times slower than game or testing conditions. Also, the current testing method only requires ¼" displacement, which is significantly less deformation compared to game conditions. For balls of similar design, the static compression was observed to correlate

well with dynamic compression. An offset associated with the ball's momentum was observed in the correlation, however.

The COR was observed to decrease proportionally with increasing pitch speed. Since current COR testing is only performed at one speed, the slope of the COR vs. pitch speed was observed to be manufacturer dependent. It is recommended, therefore, that the softball COR be measured at more than one speed. The data from 60 mph COR tests are used in the bat-ball performance equations. There is concern, however, that the ball momentum change in a 60 mph impact is significantly less than that seen in a 110 mph bat-ball impact. For a flat and rigid impact surface, 75 mph was calculated to be a more appropriate COR pitch speed.

Simultaneous ball COR and dynamic compression measurements appear feasible and were shown to have a negligible effect on the COR measurements. A strain gage load cell and a piezoelectric load cell were both used to measure the impact force, but the piezoelectric force sensors had significantly less electrical and vibrational noise in the signal. The COR calculated from the impulse was found to be in good agreement with that from the light curtains. The dynamic compression was observed to increase proportionally with increasing pitch speed.

A multi layer softball has recently been manufactured that has a very large effect on bat performance. This ball conforms to current ASTM softball COR and static compression test standards, but was observed to cause a 6.5 mph increase in BBS compared to a standard softball. The dynamic compression of this multi layer ball was observed to be 13.9% higher than a traditional ball. A ½" static compression test was able to better characterize the hardness of the multi layer ball than the typical ¼" test. It appears that current softball testing methods may not be adequate, and that dynamic or ½" compression tests may be needed.

A cylindrical impact surface was used to measure the COR and dynamic compression. The cylindrical impact surface was observed to decrease the COR and dynamic compression and increase the contact time. Two diameters were investigated (2 ¾" and 2 ¼"), and the small diameter change between these two cylinders was observed to have a negligible effect on the COR and dynamic compression. Impulse COR measurements on the cylindrical impact surface were within 2.8% of the light curtain results.

Test induced internal heating of the ball was observed to affect its dynamic compression and COR value. A ball test frequency of 10 impacts per hour is recommended to reduce this effect in determining bat performance. A recoverable viscoelastic effect was apparent when the first impact of a ball's surface was compared to subsequent impacts of that surface. Test standards should consider this fact for balls impacted multiple times. A $4^{\circ}F$ increase in the laboratory was observed to decrease the static compression approximately 20 lbs. Static compression was also observed to decrease with increasing humidity. Humidity did not appear to have a measurable effect on the dynamic compression and COR.

The effect of the leather cover was investigated by testing the COR and dynamic compression with and without the cover. The COR was observed to increase by 4.2% while the dynamic compression decreased 16.6% when the cover was removed. The decrease in the dynamic compression is due to 21% of the ball weight being removed in the cover and stitches. The increase in the COR is attributed to the reduced dynamic compression which results in less deformation of the ball. Also, the cover is softer than the core material, causing increased energy loss in the ball when the cover is present.

The validity of normalizing bat performance to account for differences in the softball was investigated. It was found that the current method of normalizing for the COR may not be valid,

while normalizing for ball mass appeared to work very well. Increasing ball hardness was observed to increase bat performance, especially for high performing bats whose barrel stiffness is low.

REFERENCES

[2.1] ASTM F 1887-02. *Standard test method for measuring the coefficient of restitution of baseballs and softballs*. West Conshohocken, Pa. 2003.

[2.2] ASTM F 1888-02. *Test method for compression-displacement of baseballs and softballs*. West Conshohocken, Pa. 2003.

[2.3] Cross, R. *The bounce of a ball*. Am. J. Phys. **67** (3), p. 222-267. 1998.

[2.4] Chauvin, D.J., Carlson, L.E. *A comparative test method for dynamic response of baseballs and softballs*. International Symposium on Safety in Baseball/Softball. ASTM STP 1313, p. 38-46. 1997.

[2.5] Gibson, R.F. *Principles of composite material mechanics*. McGraw-Hill, New York. 1994.

[2.6] Tatara, Y. *On comparison of rubber elastic spheres over a large range of displacements. part 1. theoretical study*. J. Engineering. Materials and Technology; Transactions of the ASME. 113 (3), p. 285-291. 1991.

[2.7] Hendee, S.P., Greenwald, R.M., Crisco, J.J. *Static and Dynamic properties of various baseballs*. J. App. Biomech. **14**, p. 390-400. 1998.

[2.8] Mase, T., Kersten, A.M. *Experimental evaluation of a 3-D hyperelastic, rate dependent golf ball constitutive model*. Proceedings from the Eng. of Sport 5. **2**, p. 238-244. 2004.

[2.9] Adair, R.K. *The physics of baseball*. New York, Harper and Row, 3rd edition. 2002.

[2.10] Axtell, J.T. *Experimental determination of baseball bat durability*. Masters thesis. Washington State University. 2001.

[2.11] Giacobbe, P.A., Scarton, H.A., Lee, Y.S. *Dynamic hardness (SDH) of baseballs and softballs. International Symposium on Safety in Baseball/Softball*. ASTM STP 1313, p. 47-66. 1997.

[2.12] ASTM F2219-02e1. *Standard test methods for measuring high speed bat performance factor*. West Conshohocken, Pa. 2003.

[2.13] NCAA. *National collegiate athletic association provisional standard for testing baseball bat performance*. 1999.

[2.14] Russell, D. *Private communication*. July, 2003.

[2.15] Cross, R. *The sweet spot of a baseball bat*. Am. J. Phys. **66** (9), p. 772-779. 1998.

CHAPTER TWO FIGURES

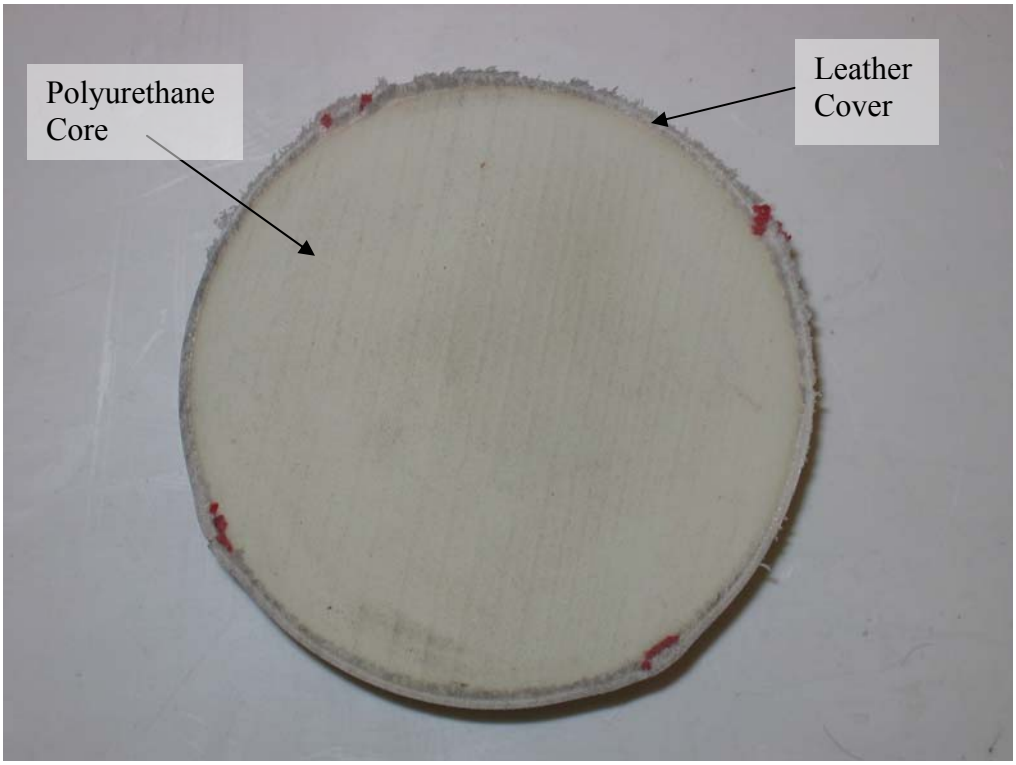

Figure 2.1: Cross section view of a typical polyurethane core softball.

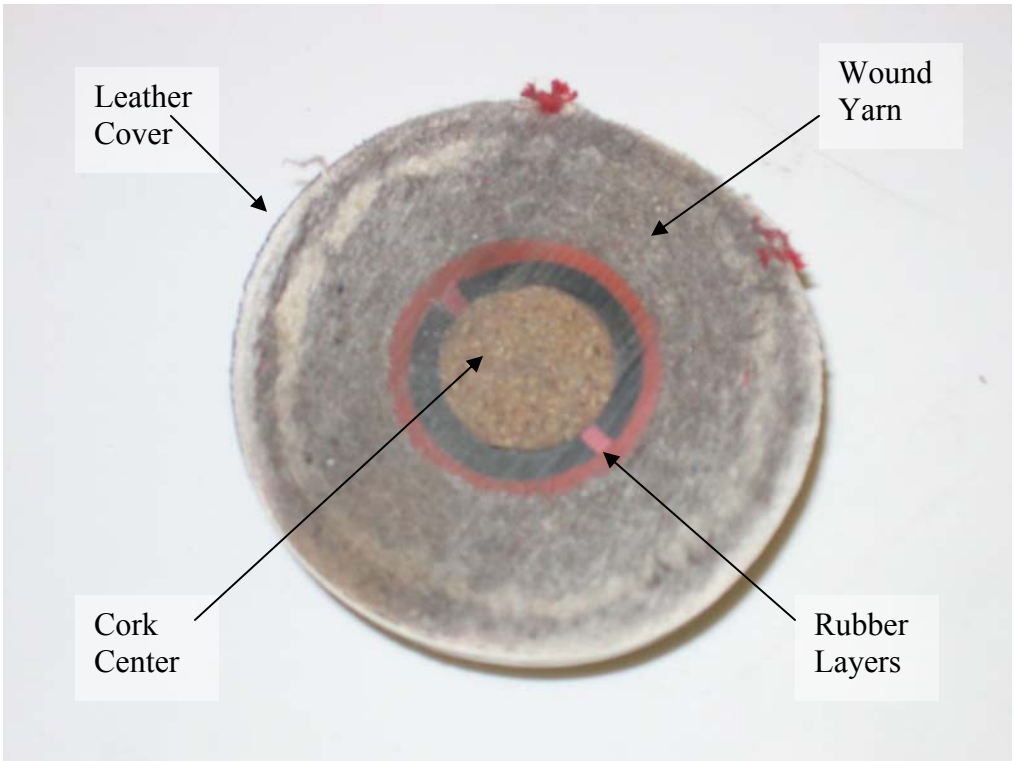

Figure 2.2: Cross section view of a typical NCAA or major league baseball.

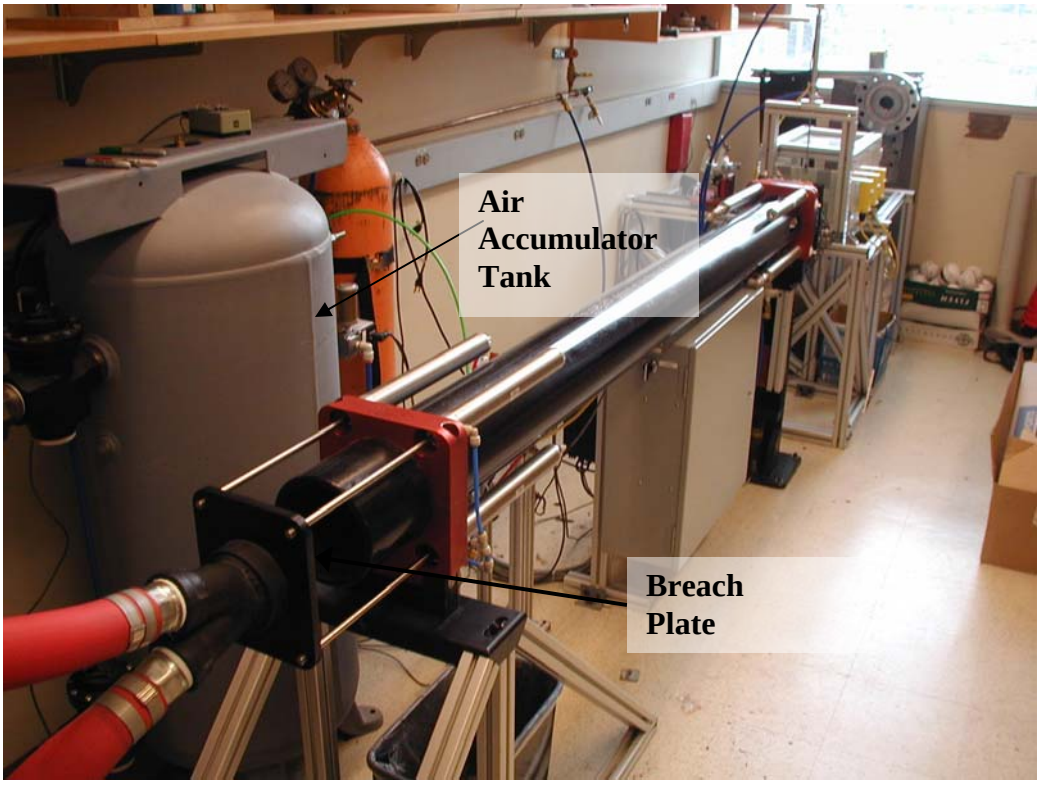

Figure 2.3: Picture of the cannon used for experimental testing. The barrel has a length of eight feet.

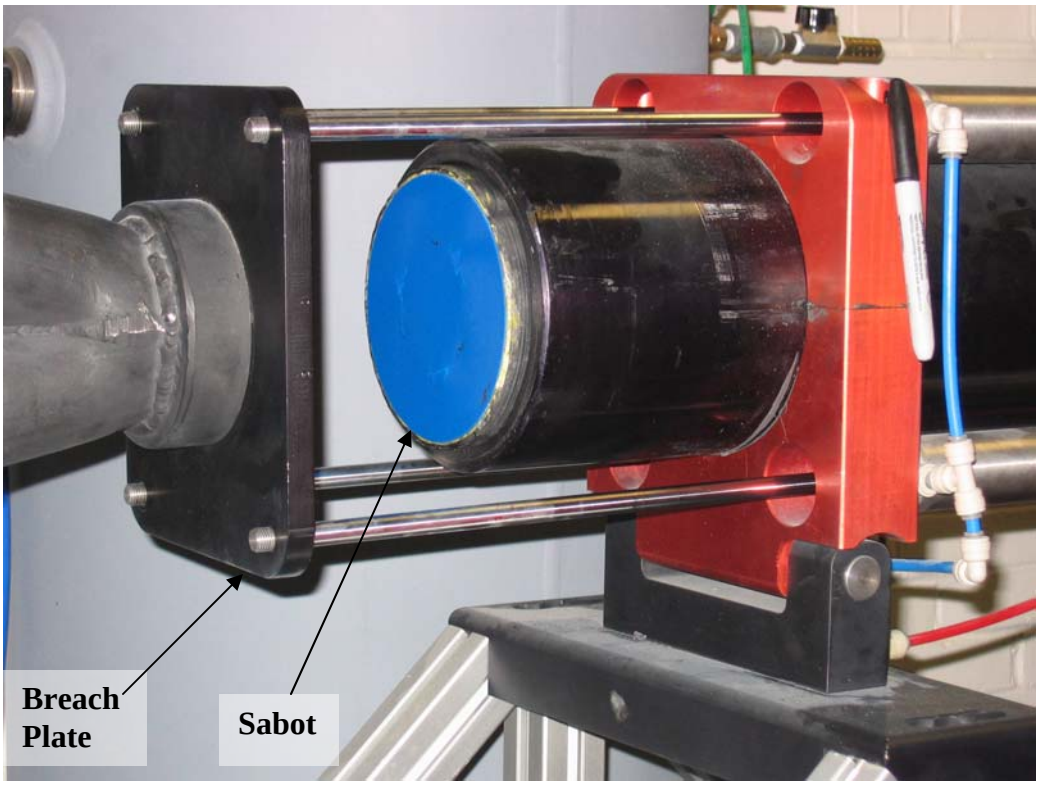

Figure 2.4: Picture of the breach end of the cannon with the sabot inserted. The pneumatic cylinders open and close the breach.

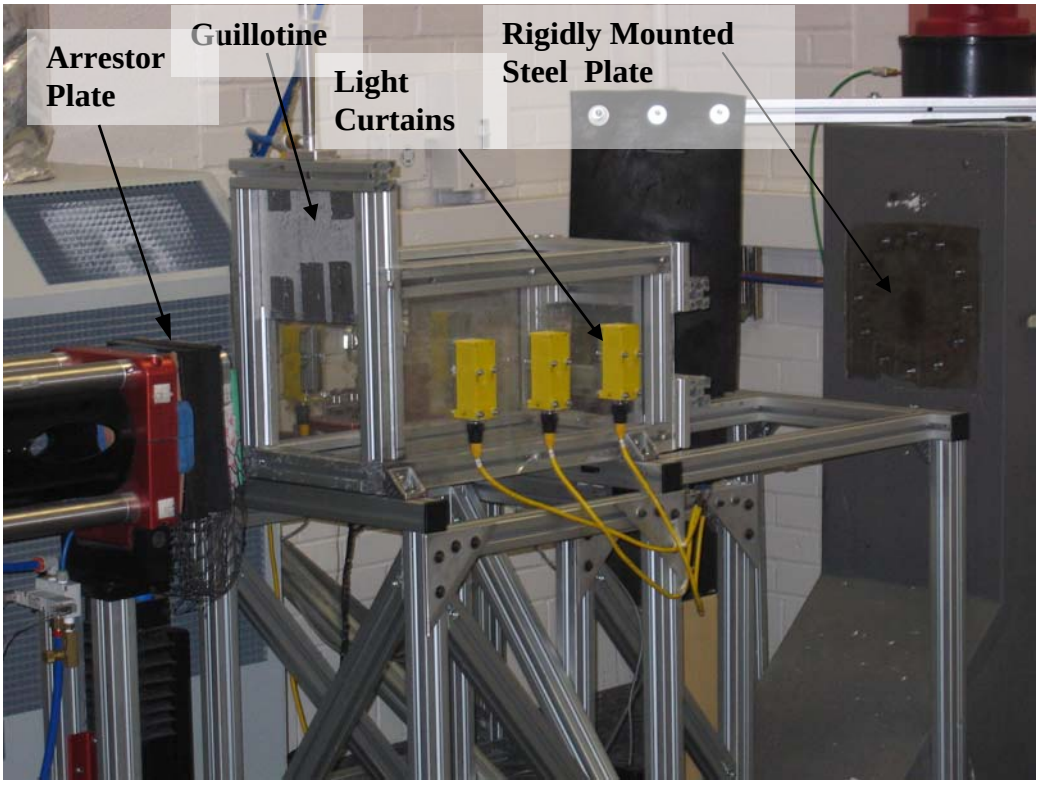

Figure 2.5: Picture of the end of the barrel, the arrestor plate, the guillotine, light curtains, and the rigid steel plate embedded in a concrete wall.


Figure 2.6: Several sabot designs that failed with repeated impacts. The original UHMWPE design is shown in the upper left. The others are made of polycarbonate.

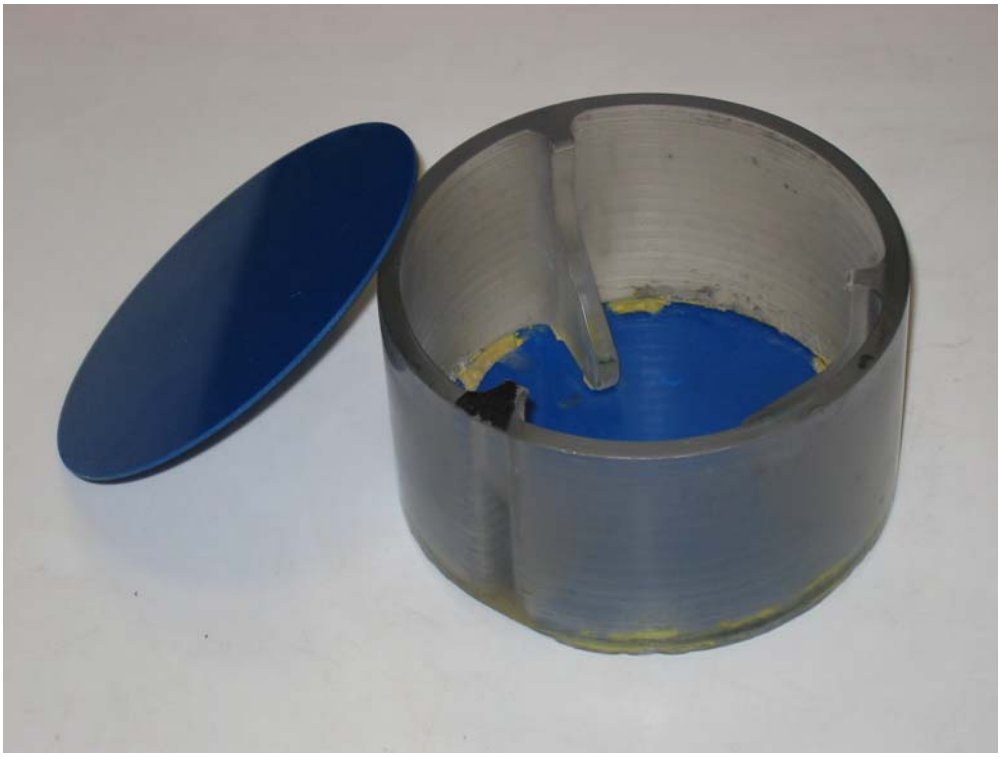

Figure 2.7: Picture of the current sabot design with the fiberglass bottom plate. An example of the 1/16" backing plate is shown also.

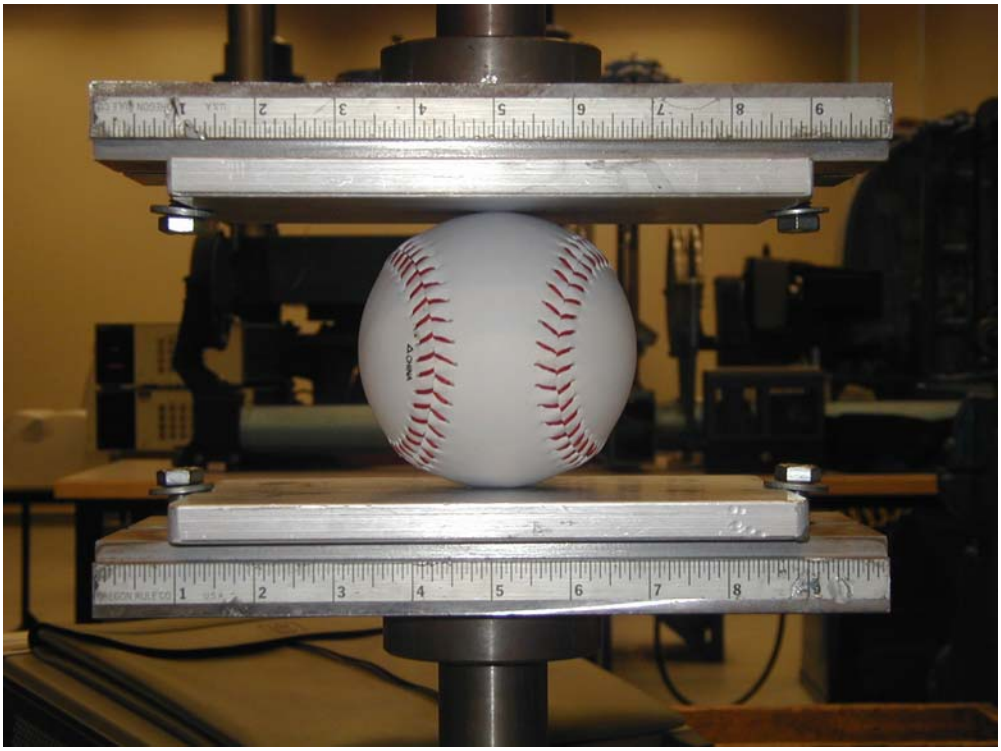

Figure 2.8: Picture of static compression load frame (MTS Systems Corporation, Minneapolis, MN).

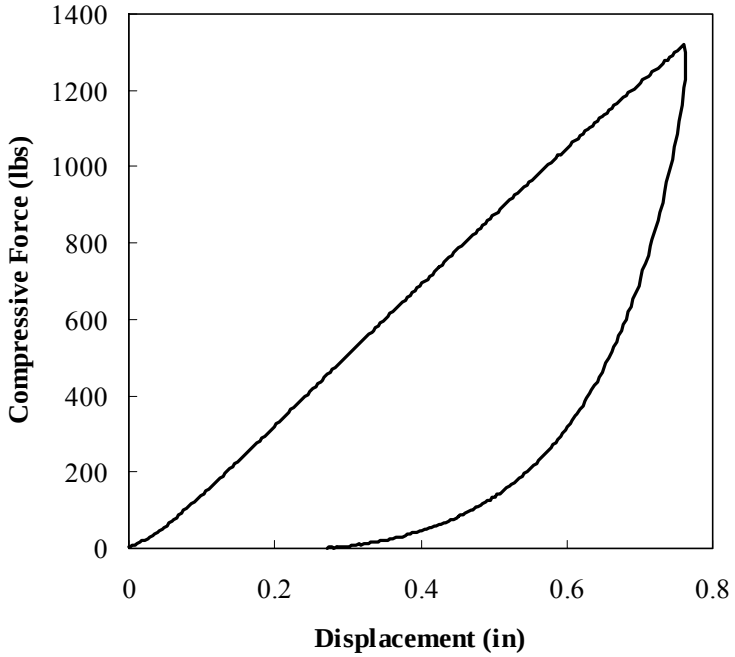

Figure 2.9: Load-displacement curve of a 44/375 ball compressed ¾" between two flat steel platens.

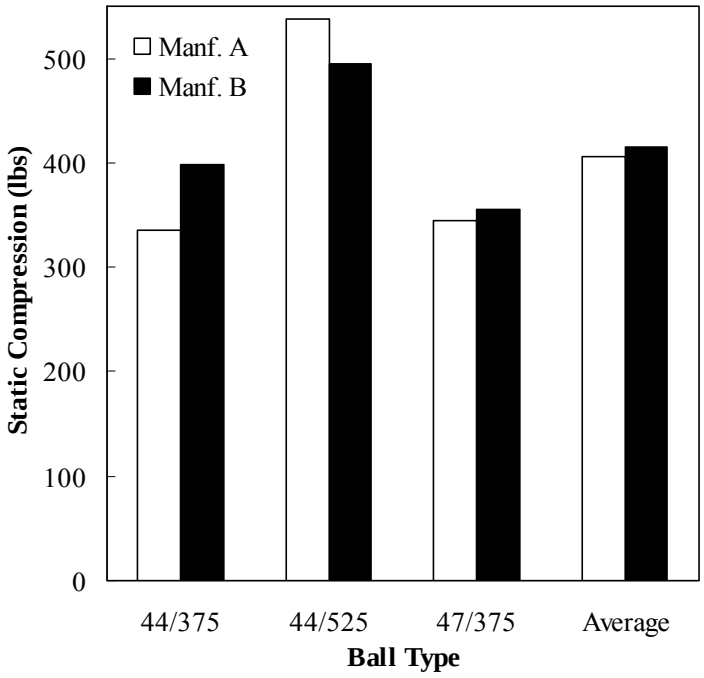

Figure 2.10: Average static compression measured per ASTM F 1888-02 vs. the ball type. The average static compression of each manufacturer is shown on the far right of the plot. Balls were conditioned for two weeks before testing.

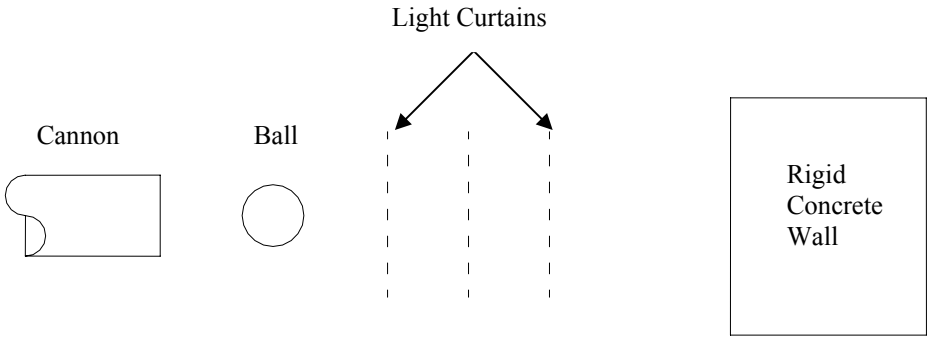

Figure 2.11: Test setup for measuring the coefficient of restitution.

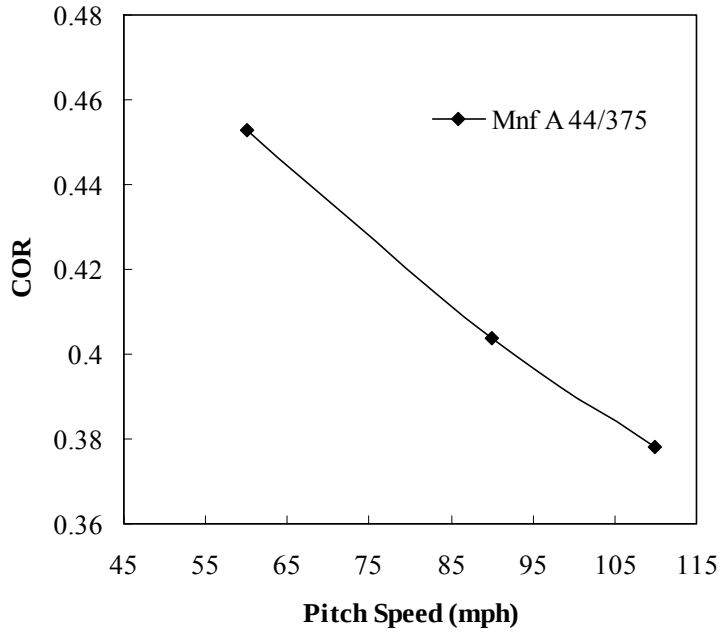

Figure 2.12: Average coefficient of restitution vs. pitch speed for one dozen 44/375 balls from manufacturer A. Each ball was impacted ten times at each speed.

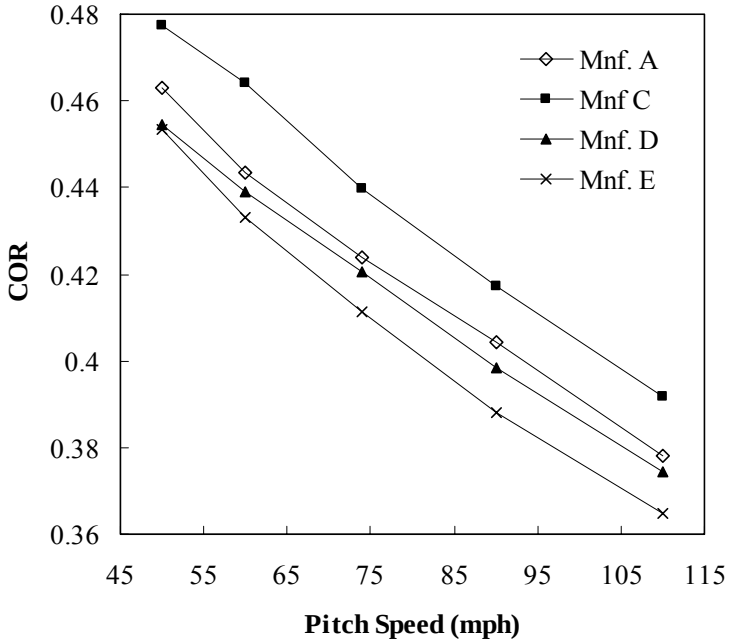

Figure 2.13: COR vs. pitch speed (40-110 mph) of 44/375 balls from four manufacturers. Each data point is the average of three balls fired six times.

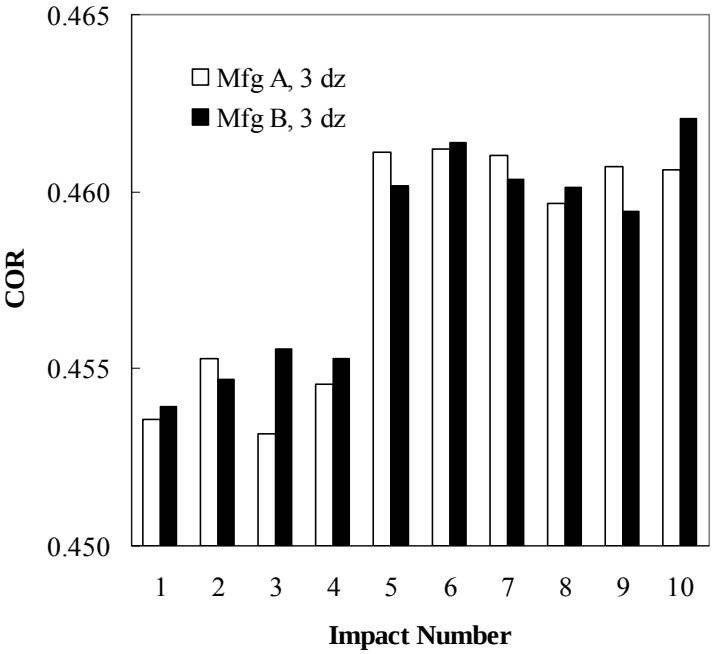

Figure 2.14: Average coefficient of restitution at 60 mph vs. impact number for three dozen balls from manufacturer A and B.

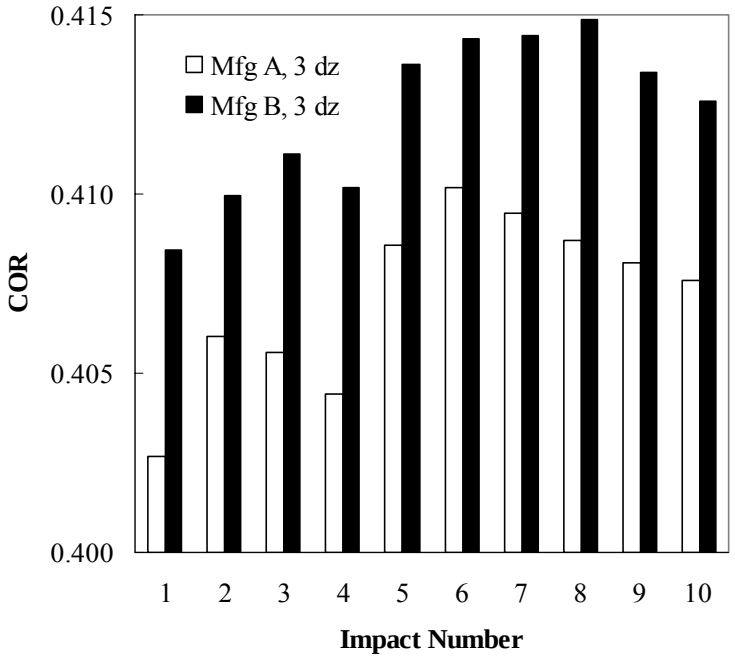

Figure 2.15: Average coefficient of restitution at 90 mph vs. impact number for three dozen balls from manufacturer A and B.

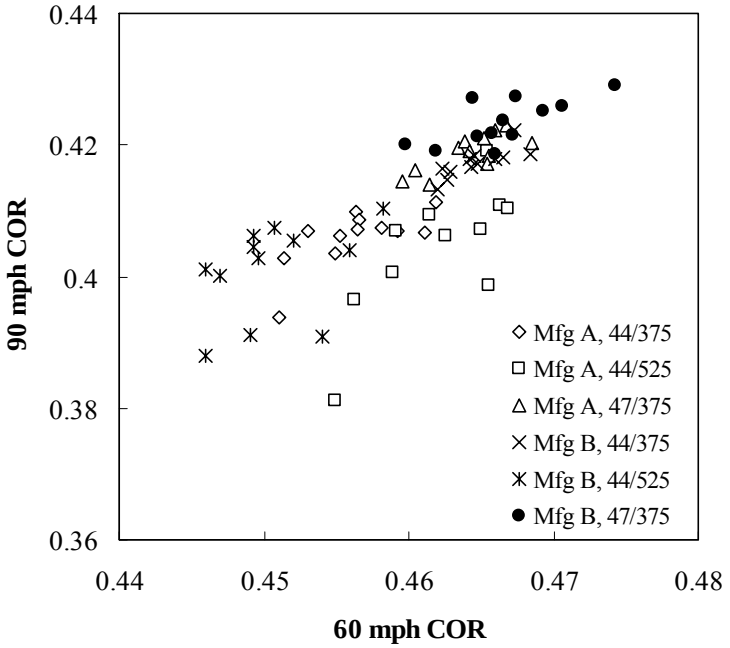

Figure 2.16: 90 mph COR vs. 60 mph COR. Each point is the average of ten impacts. 12 balls of each manufacturer and model are shown.

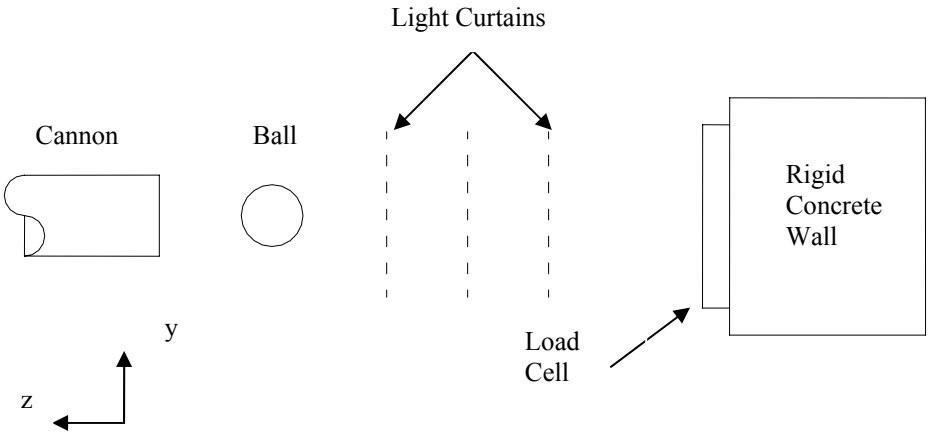

Figure 2.17: Experimental test setup for dynamic compression.

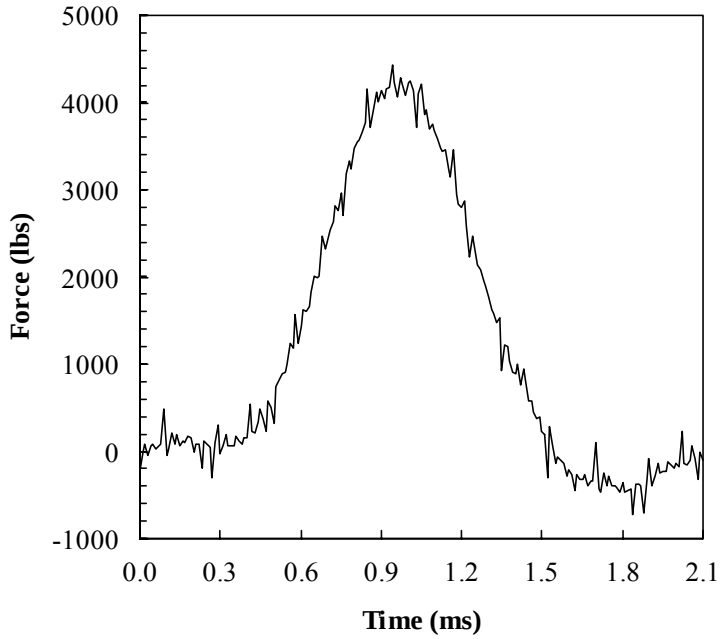

Figure 2.18: Impact force of a 44/375 ball from manufacturer A at 90 mph against a flat surface using the strain gage load cell. The data shown is unfiltered.

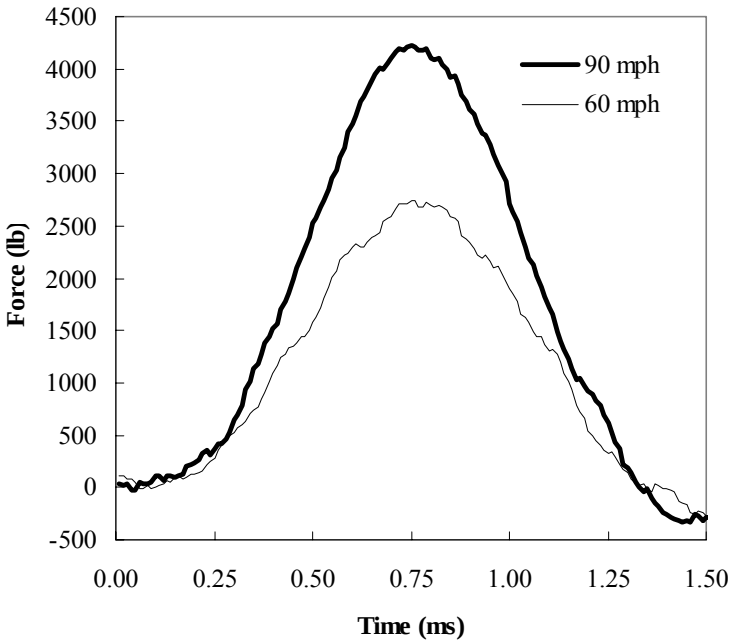

Figure 2.19: Filtered strain gage load cell data for a 60 and 90 mph impact vs. time. A 44/375 ball from manufacturer A was used.

Figure 2.20: Picture of piezoelectric load cell experimental setup. The load cells are mounted in an equilateral triangle with a common side length of two inches.

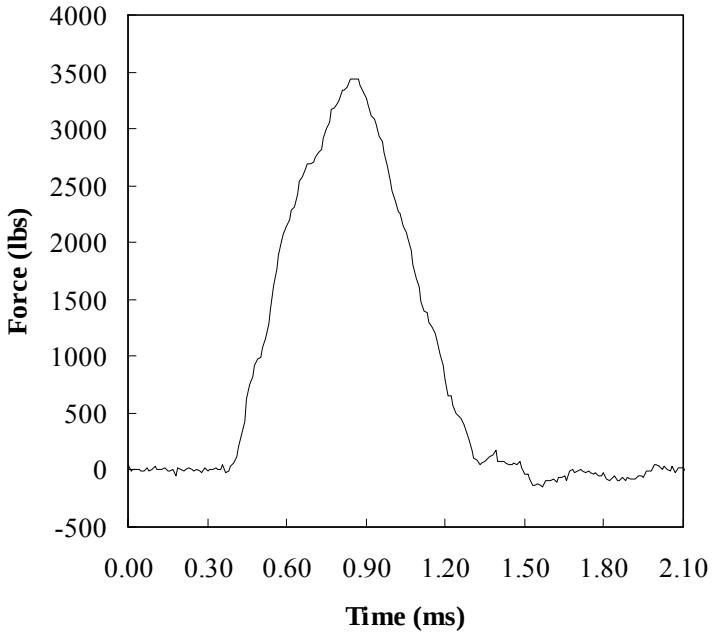

Figure 2.21: Piezoelectric force vs. time curve of a 44/375 ball from manufacturer A. The data shown is for a 60 mph impact.

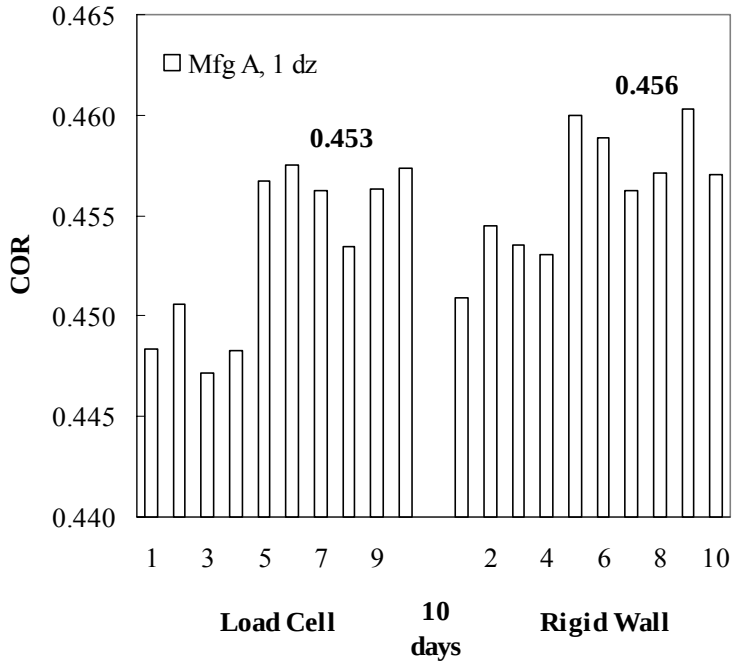

Figure 2.22: One dozen 44/375 balls were fired at a load cell with a flat plate and after ten days they were fired again against a rigid steel plate. The COR vs. impact surface is plotted.

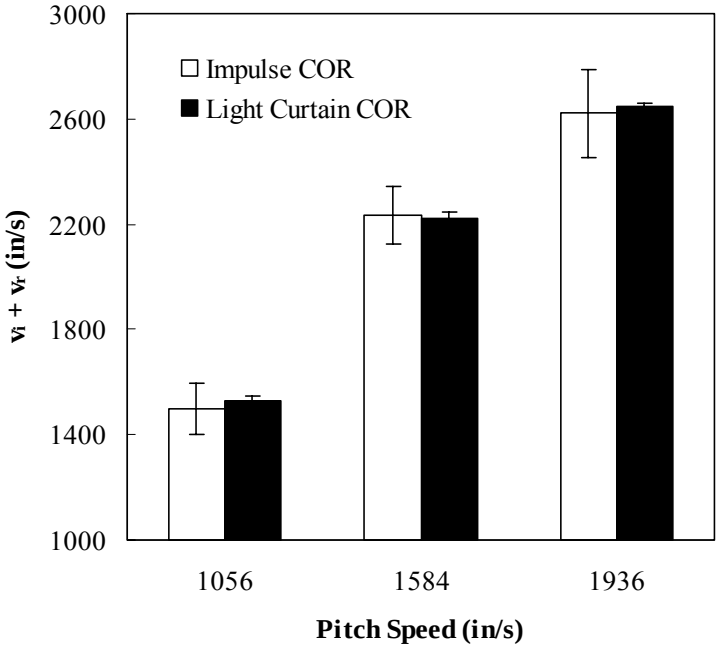

Figure 2.23: Strain gage impulse COR and light gate COR for one dozen 44/375 balls from manufacturer A. Each ball was impacted ten times at 1056, 1584, and 1936 in/s (60, 90, 110 mph)

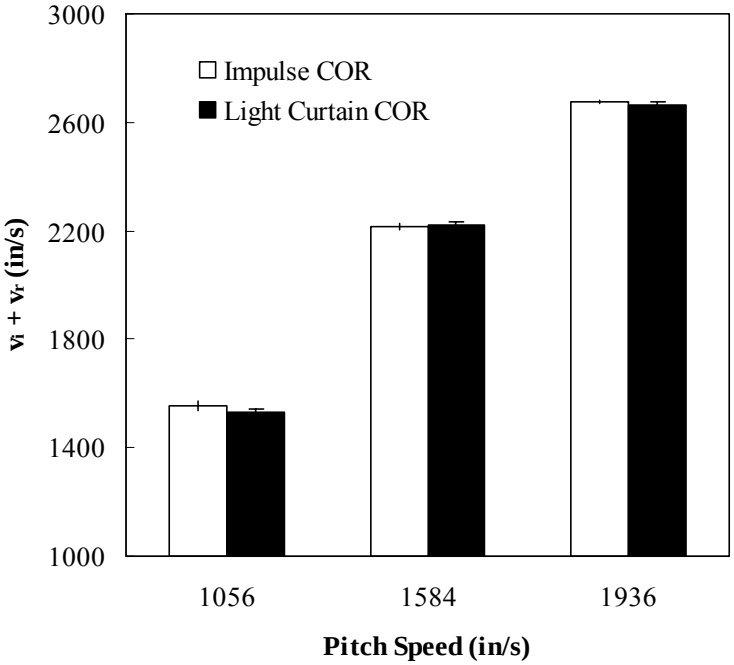

Figure 2.24: Piezoelectric load cell impulse COR and light gate COR of three 44/375 balls from manufacturer A. Each ball was impacted ten times at 1056, 1584, and 1936 in/s (60, 90, 110 mph).

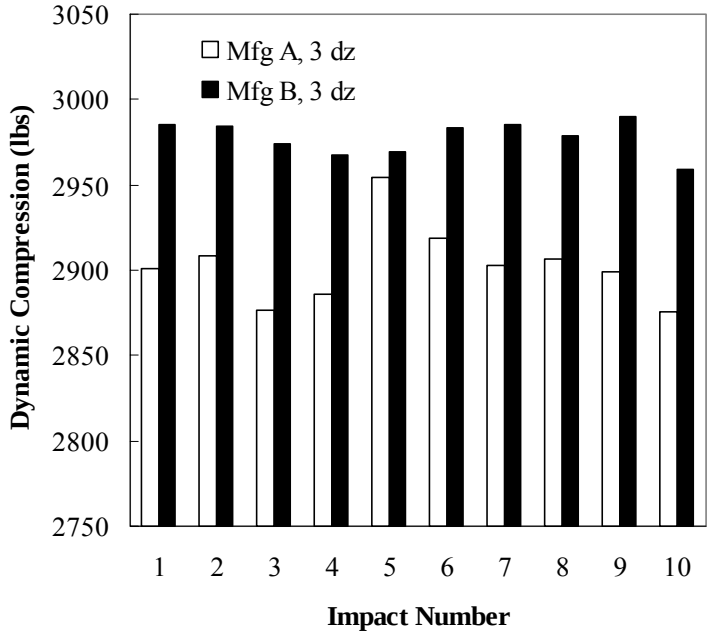

Figure 2.25: Dynamic compression at 60 mph vs. impact number for three dozen balls from manufacturer A and B.

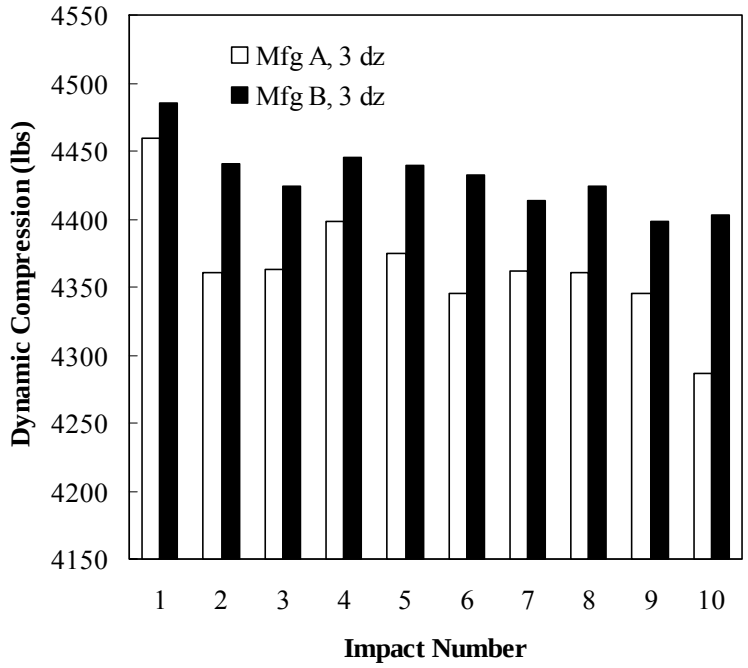

Figure 2.26: Dynamic compression at 90 mph vs. impact number for three dozen balls from manufacturer A and B.

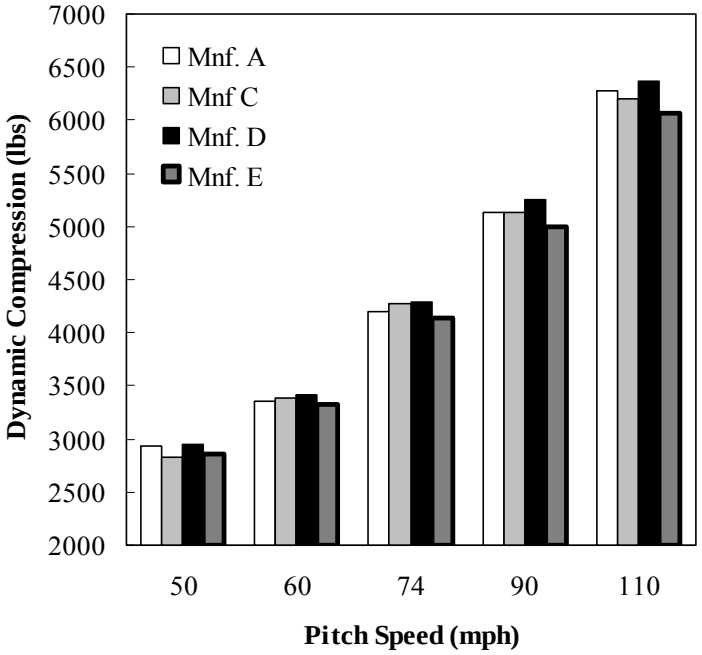

Figure 2.27: Dynamic compression vs. pitch speed from four manufacturers. Each data point is the average of three balls fired six times at each speed.

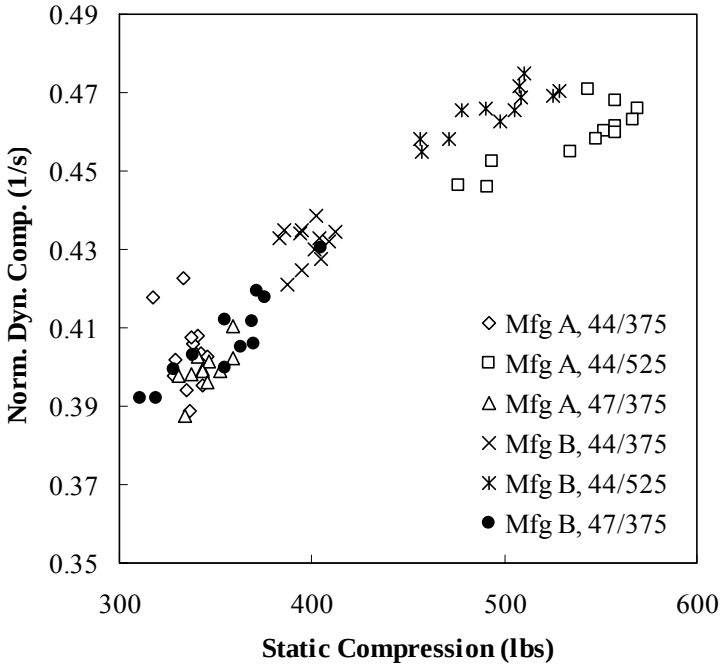

Figure 2.28: Normalized dynamic compression at 60 mph vs. static compression. The dynamic compression is the average of ten impacts for each data point.

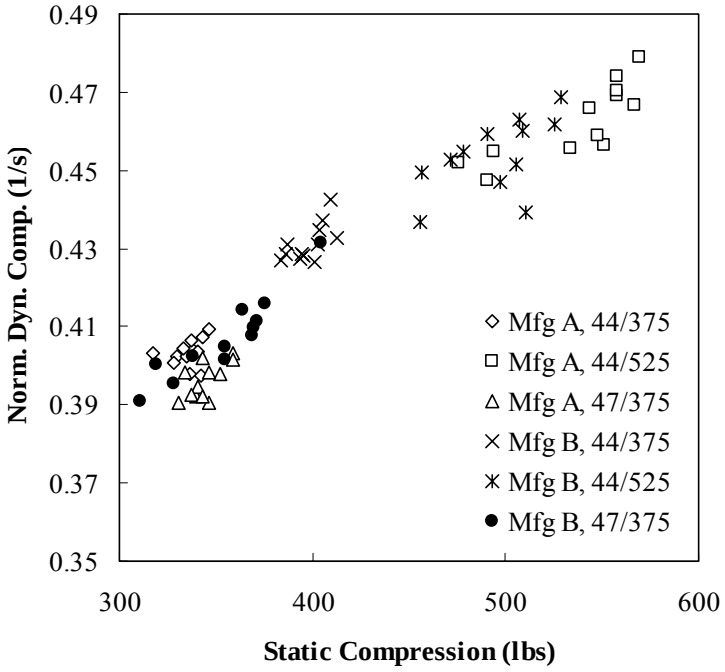

Figure 2.29: Normalized dynamic compression at 90 mph vs. static compression. The dynamic compression is the average of ten impacts for each data point.

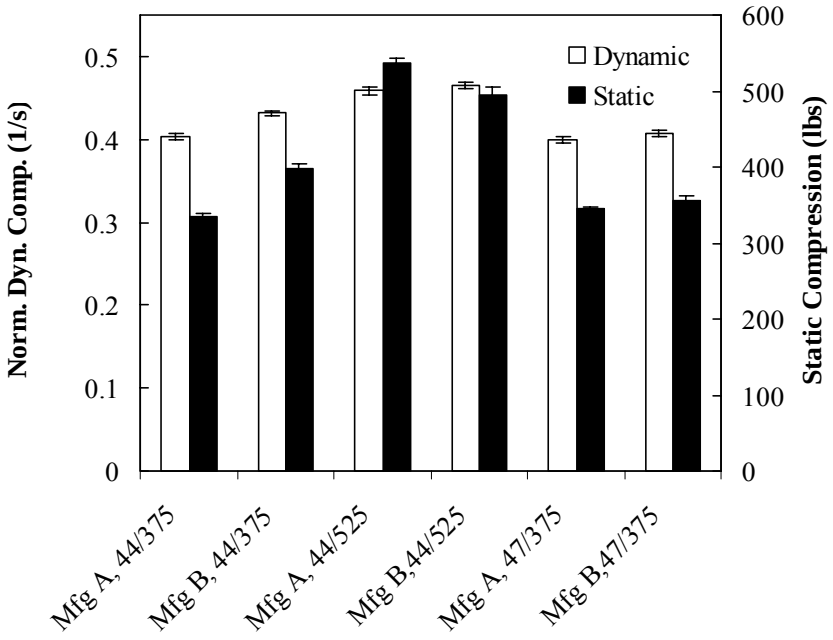

Figure 2.30: Normalized dynamic compression at 60 mph and static compression plotted against the different ball types. The dynamic compression is the average of ten impacts of twelve balls.

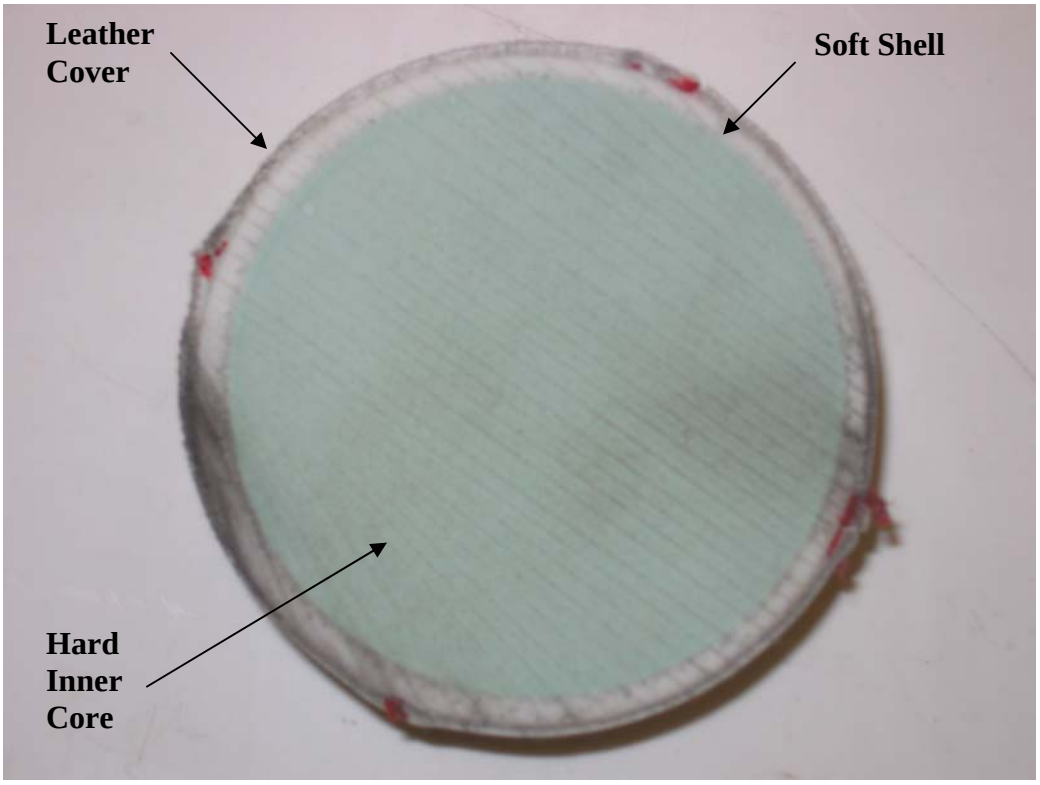

Figure 2.31: Cross section view of multi layer ball showing the leather cover, soft outer shell, and the hard inner core.

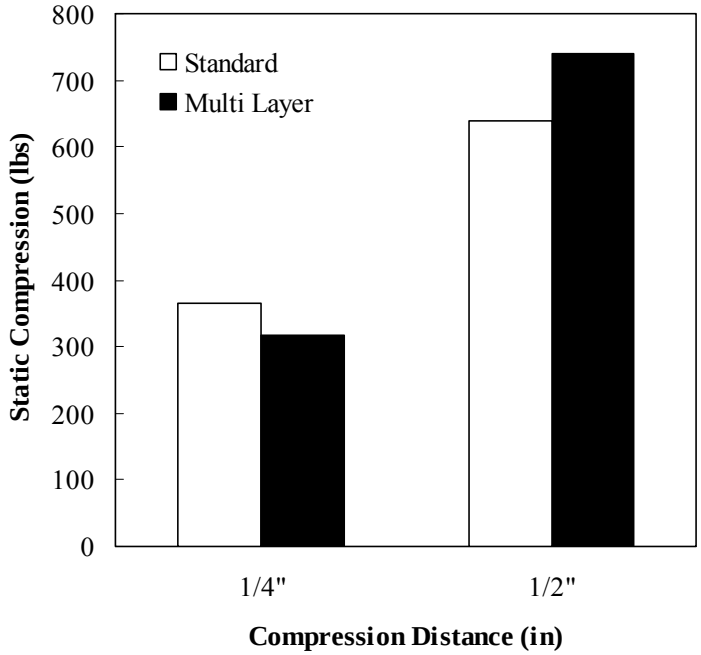

Figure 2.32: Static compression vs. compression distance for the standard and the multi layered ball.

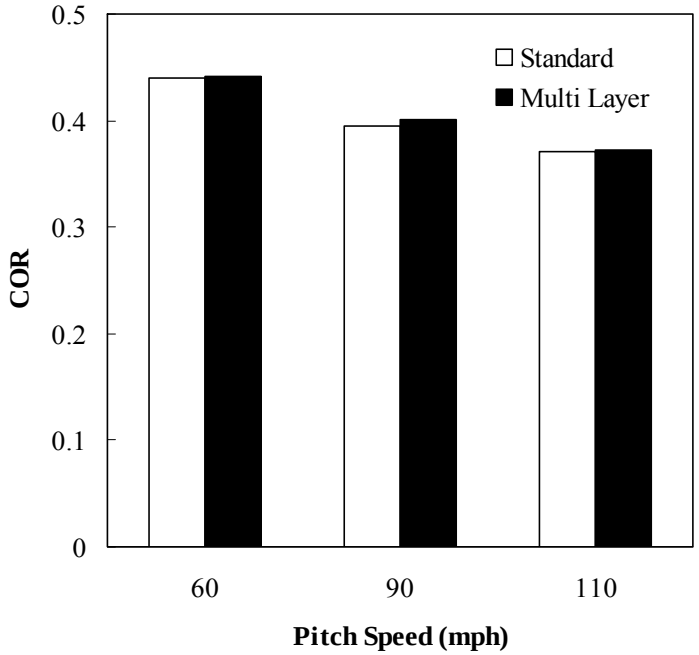

Figure 2.33: Average COR of vs. pitch speed of six traditional and multi layer balls.

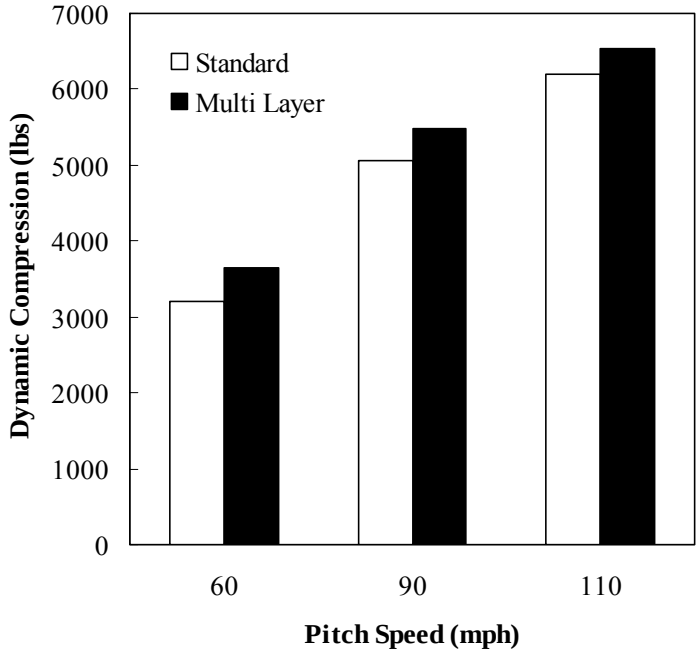

Figure 2.34: Average dynamic compression vs. pitch speed of six traditional and multi layer balls.

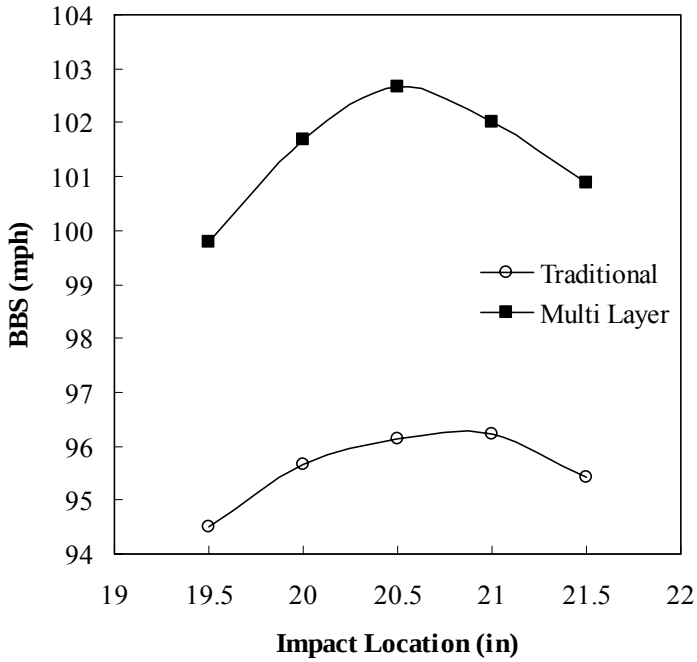

Figure 2.35: Calculated BBS vs. impact location for the traditional and multi layer 44/375 ball. Each point is the average of six balls. The bat was initially stationary and the ball was fired at 110 mph.

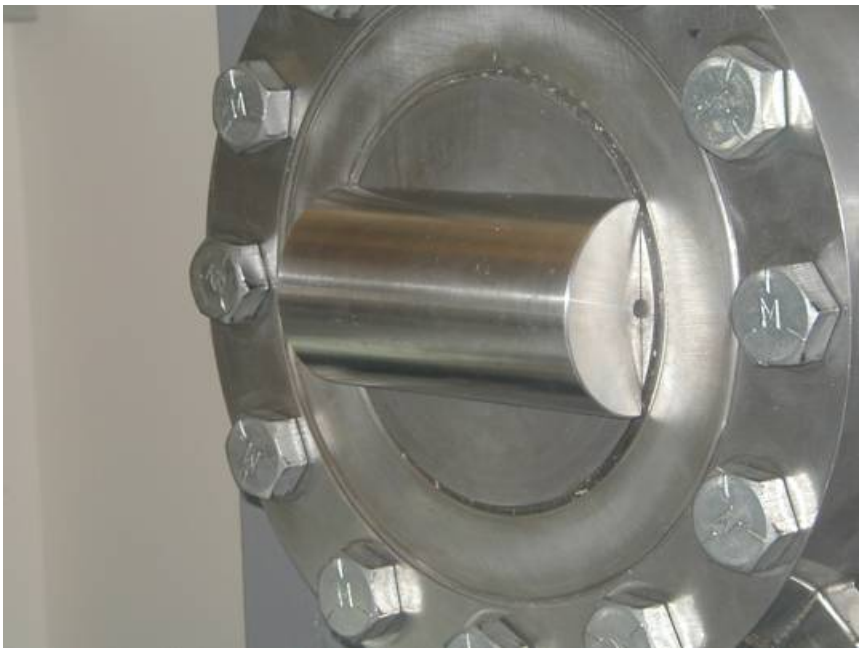

Figure 2.36: Picture of cylindrical impact surface attached to strain gage load cell. Cylindrical impact tests were also performed using piezoelectric load cells.

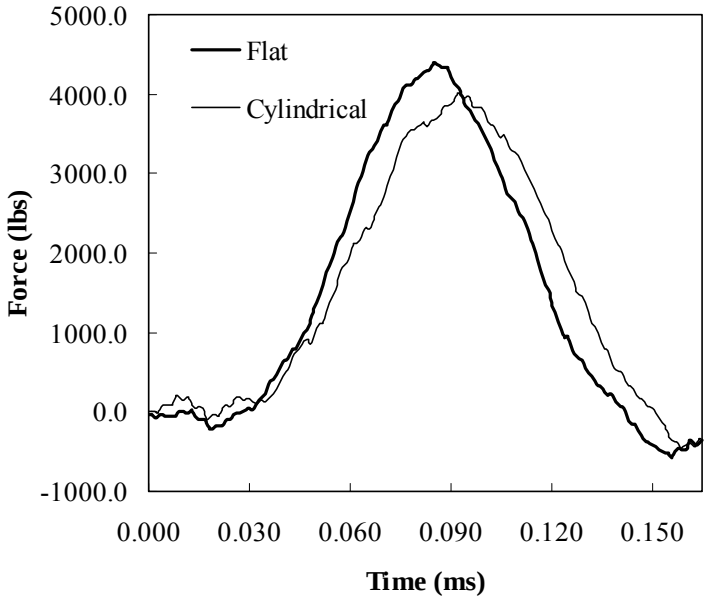

Figure 2.37: 90 mph impact Force vs. time for a 44/375 ball from manufacturer B. The ball was fired against the flat and cylindrical load cell surfaces.

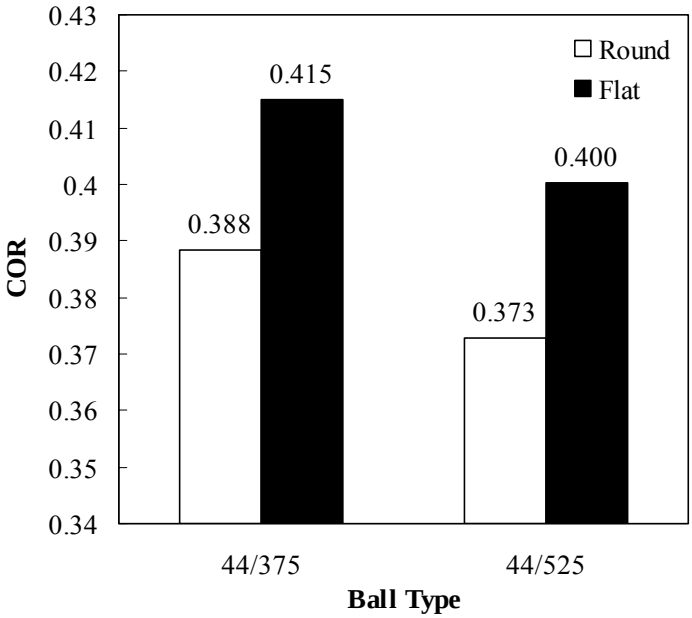

Figure 2.38: 90 mph COR vs. ball type (manufacturer B) for balls tested on flat and round surfaces. The values are the average of twelve balls of each ball type.

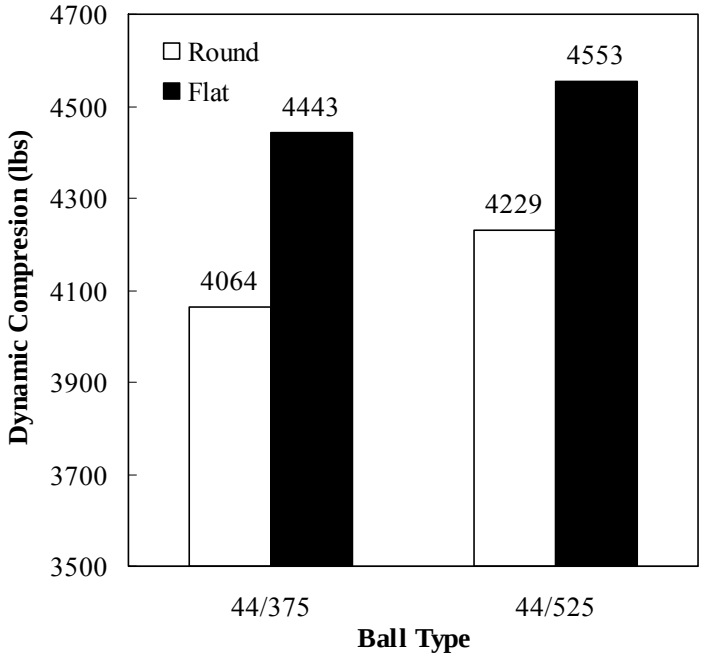

Figure 2.39: 90 mph dynamic compression vs. ball type (manufacturer B) for balls tested on flat and round impact surfaces. The values are the average of twelve balls of each ball type.

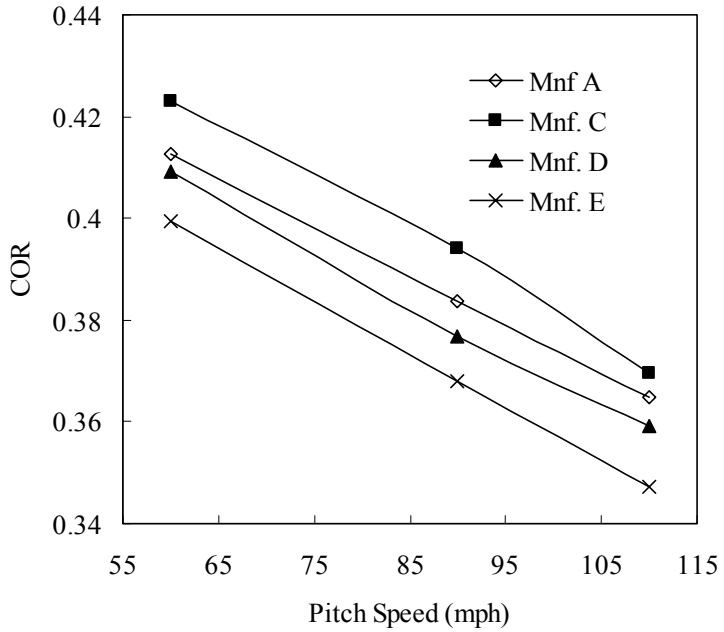

Figure 2.40: Average COR vs. pitch speed against a 2 ¼" cylindrical impact surface of four different manufacturers. Each data point is the average of three balls fired eight times.

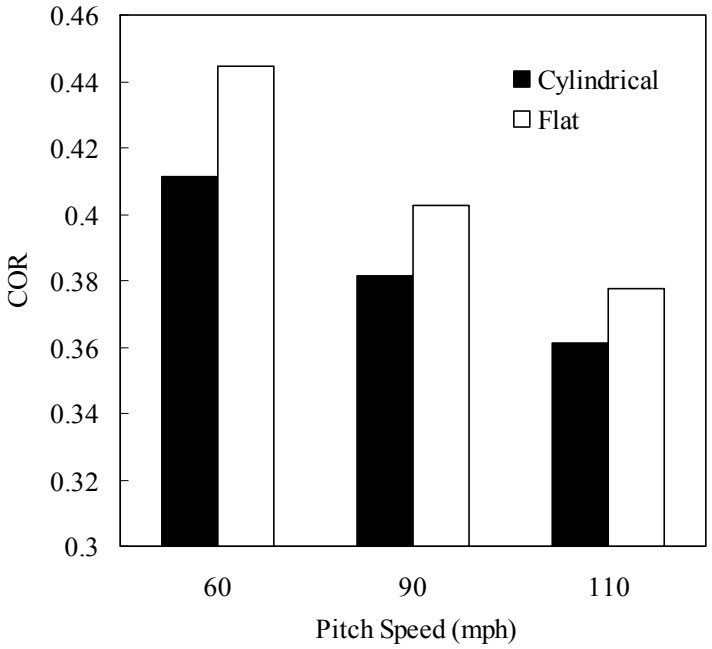

Figure 2.41: COR vs. pitch speed for flat and cylindrical impact surfaces. The data shown is the average of three 44/375 balls from manufacturer A, C, D, and E. Each ball was fired eight times at each speed on each impact surface.

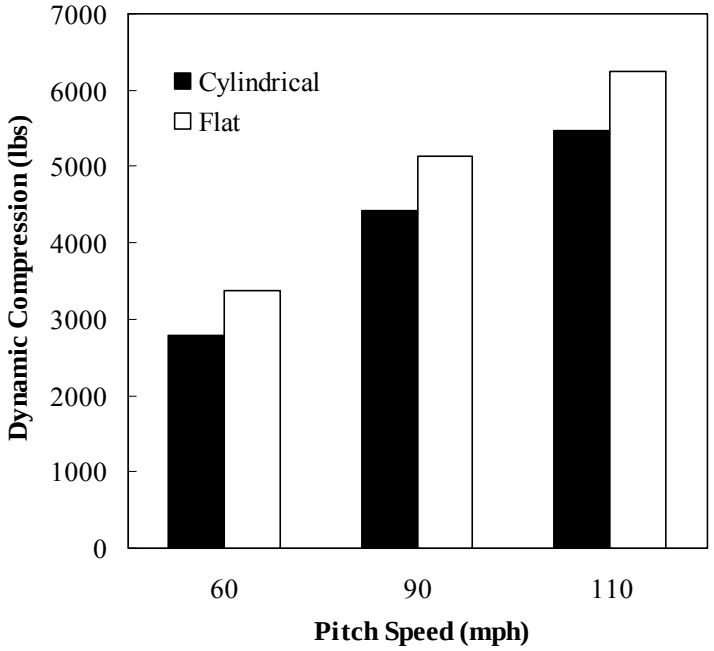

Figure 2.42: Dynamic compression vs. pitch speed for flat and cylindrical impact surfaces. The data shown is the average of three 44/375 balls from manufacturers A, C, D, and E. Each ball was fired eight times at each speed.

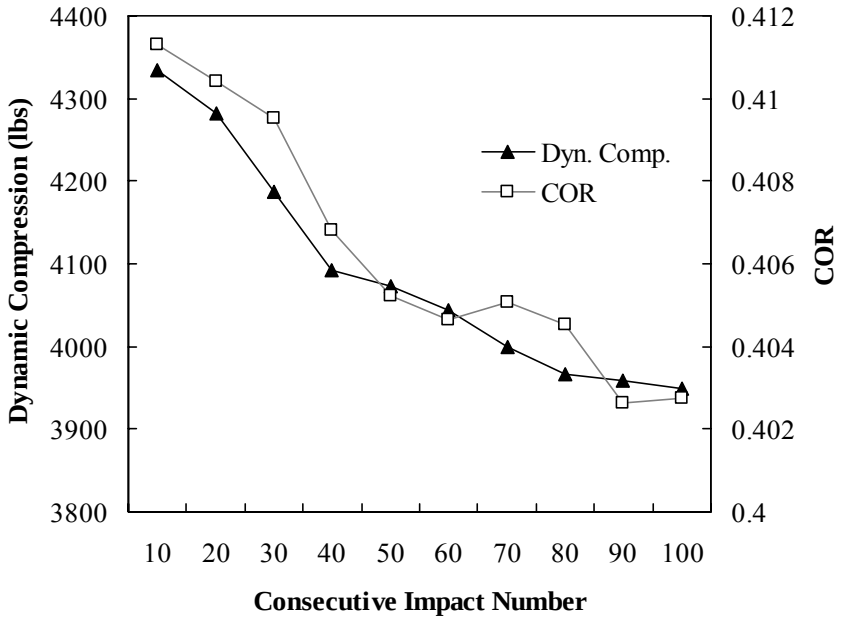

Figure 2.43: Dynamic compression and COR as a function of consecutive impact number (90 mph, two 44/375 balls). Each data point is the average of ten impacts per ball.

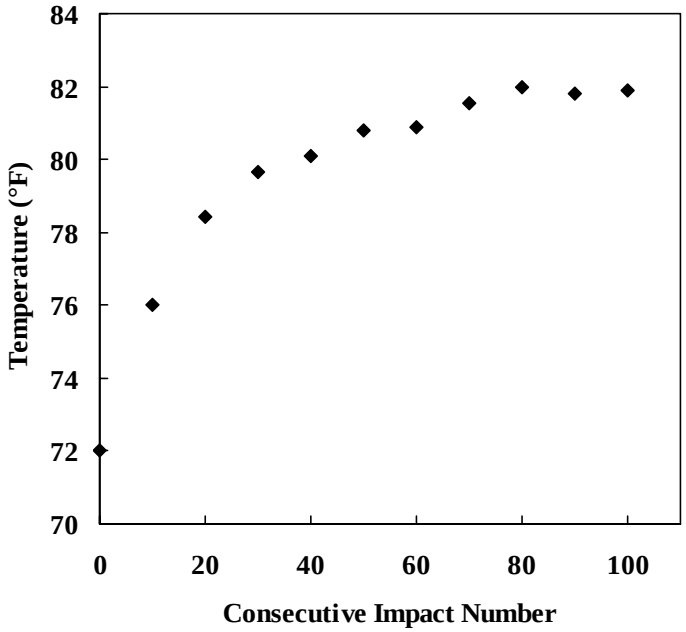

Figure 2.44: The temperature was measured of the balls impacted 100 times consecutively.

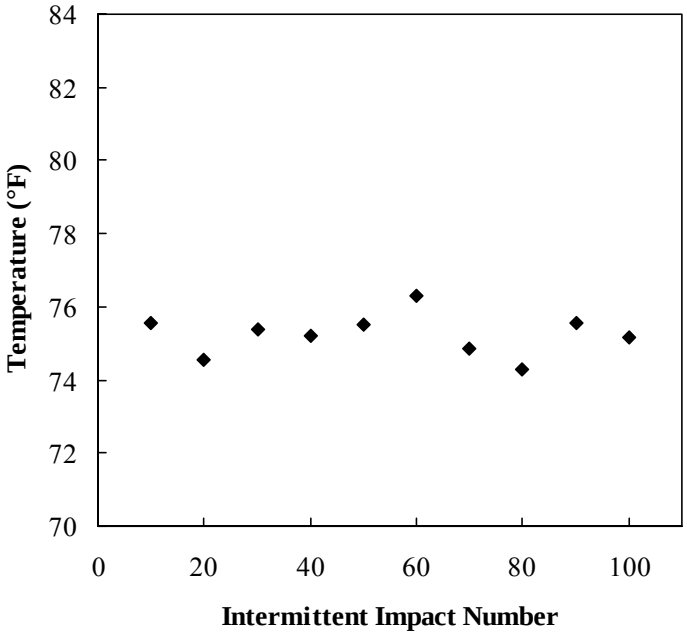

Figure 2.45: The temperature was measured of the balls impacted 100 times intermittently.

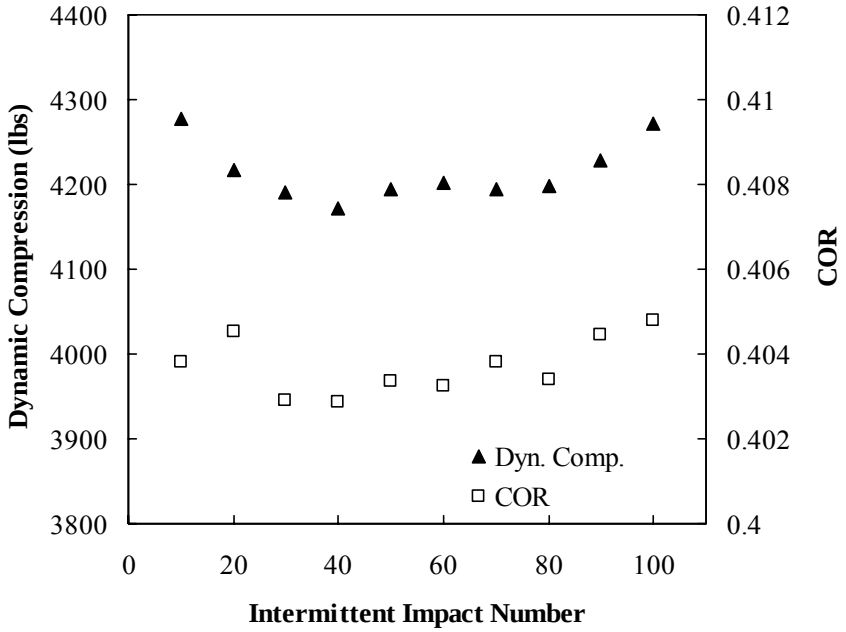

Figure 2.46: Dynamic compression and ball COR as a function of intermittent impact number (90 mph, two 44/375 balls). Each point is the average of ten impacts from each ball, where balls were allowed to recover every 10 impacts.

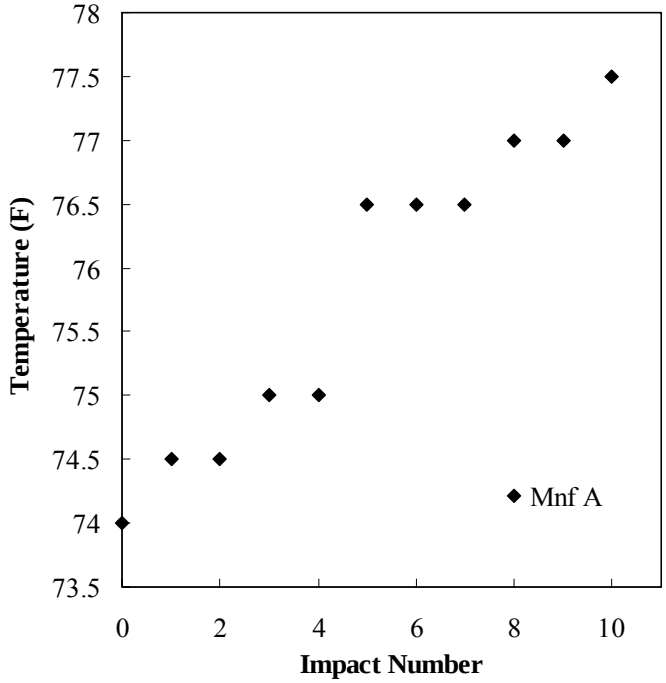

Figure 2.47: Temperature vs. impact number for one dozen 44/375 balls from manufacturer A at 90 mph.

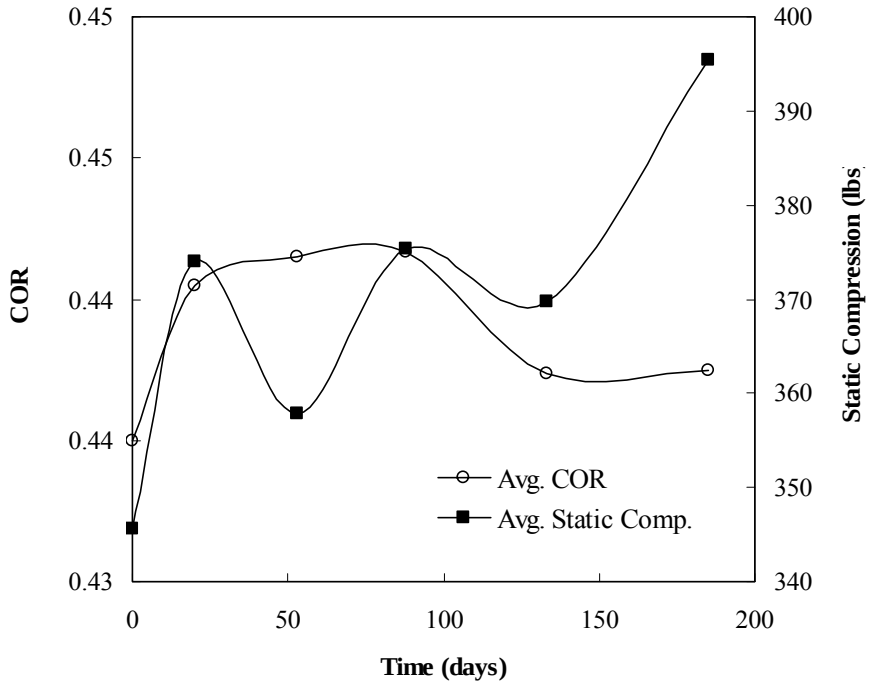

Figure 2.48: Average COR and static compression vs. time for the long term ball study.

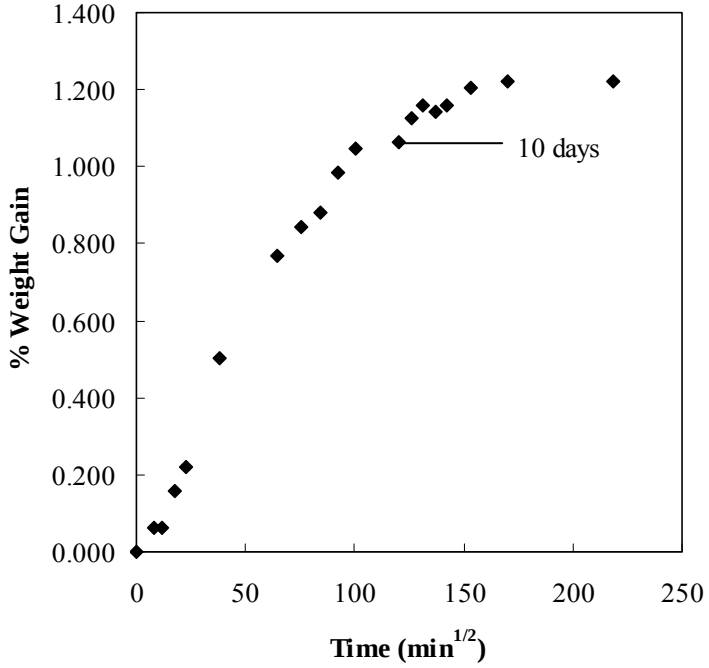

Figure 2.49: Weight gain was measured for one dozen 44/375 balls placed into a 50% relative humidity chamber. The balls were kept in this environment for 30 days and moisture saturation was reached at 14 days.

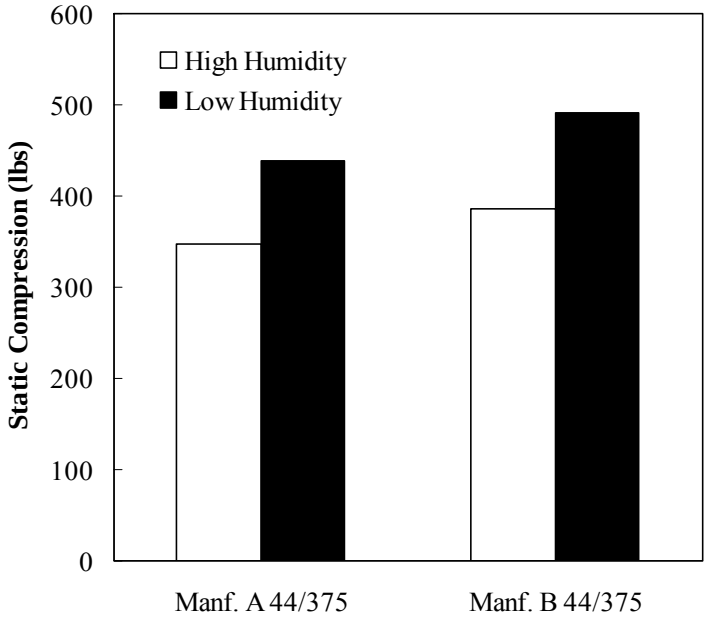

Figure 2.50: Static compression vs. ball type for balls tested at high and low humidity. Each column is the average of twelve balls. Each ball was conditioned at each level for a minimum of fourteen days.

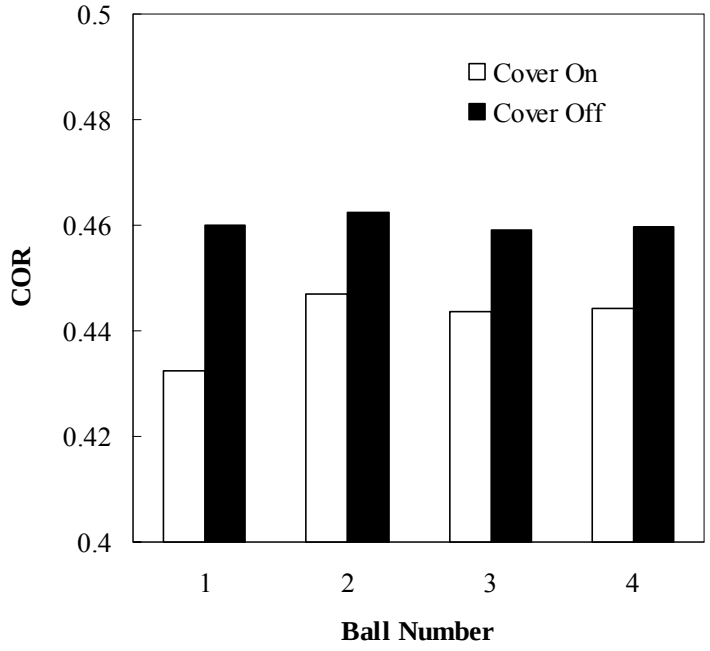

Figure 2.51: 60 mph COR of four balls from manufacturer A. Each ball was impacted six times with the cover on and with the cover removed.

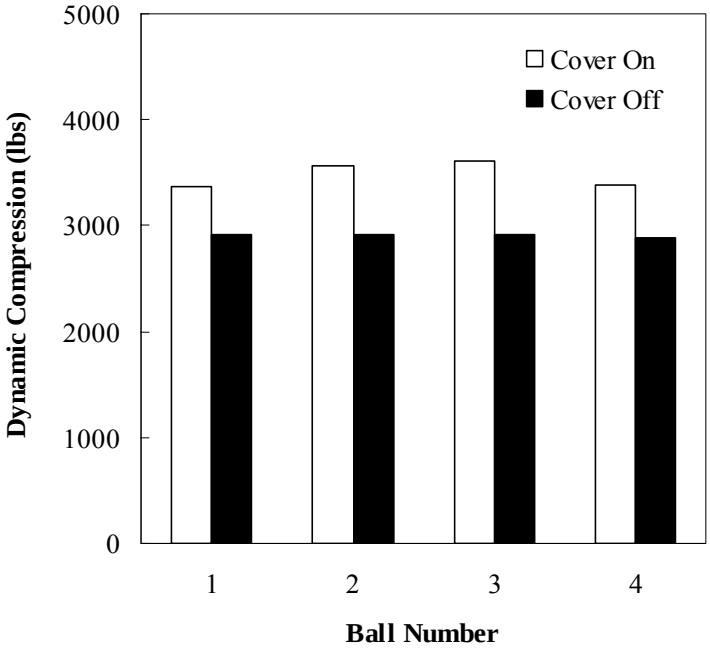

Figure 2.52: 60 mph dynamic compression of four balls from manufacturer A. Each ball was impacted six times with the cover on and with the cover removed.

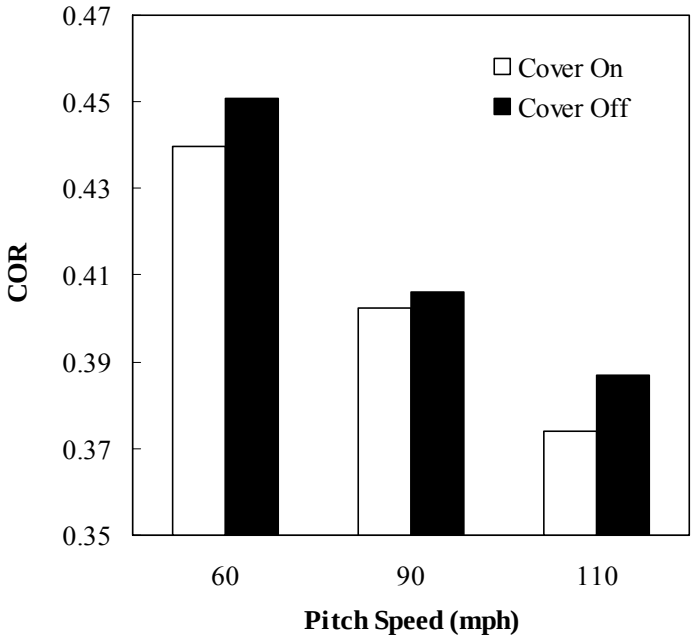

Figure 2.53: COR vs. pitch speed for three balls from manufacturer A. Each ball was tested with the cover on and with the cover removed.

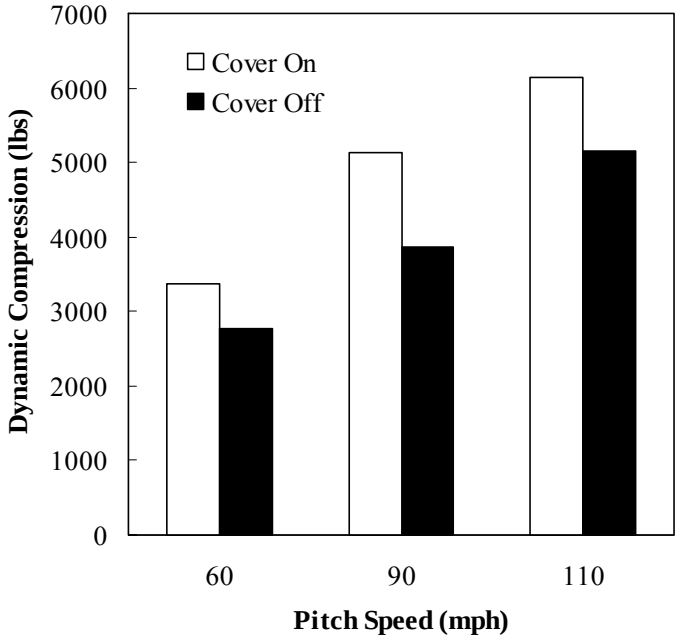

Figure 2.54: Dynamic compression vs. pitch speed for three balls from manufacturer A. Each ball was tested with the cover on and with the cover removed.

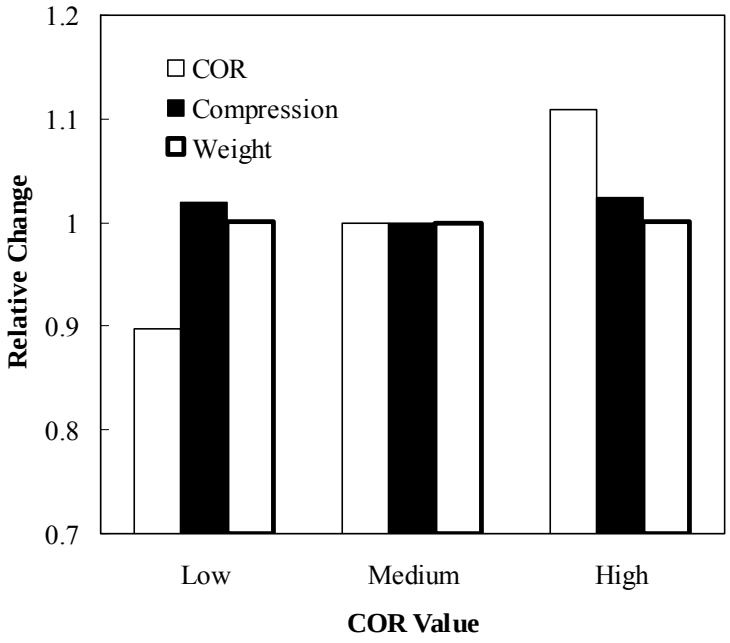

Figure 2.55: Relative change of ball properties for the varying COR group. The COR value is increasing while the static compression and weight are held approximately constant.

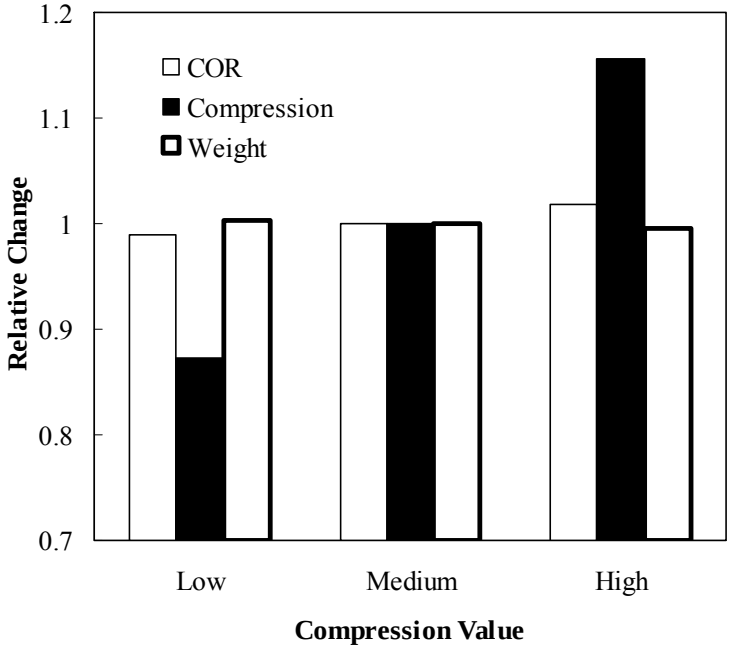

Figure 2.56: Relative change of ball properties for the varying compression group. The compression value is increasing while the COR and weight are held approximately constant.

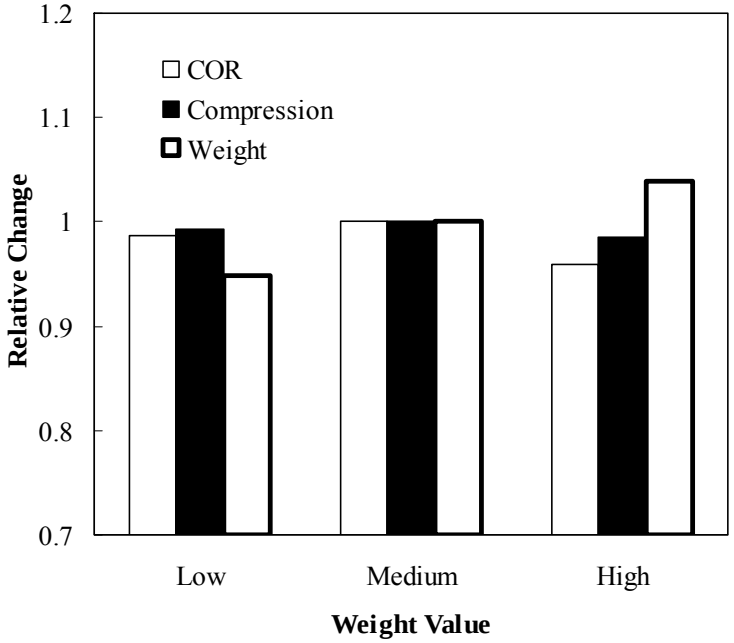

Figure 2.57: Relative change of ball properties for the varying weight group. The weight value is increasing while the COR and static compression are held approximately constant.

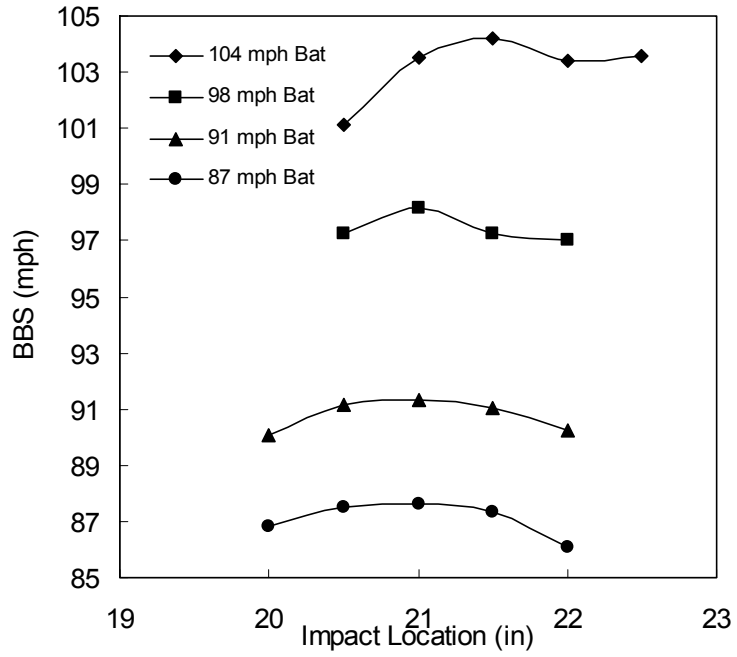

Figure 2.58: BBS vs. impact location for the four bats used in the normalizing study. Each bat was tested with six traditional 44/375 balls at 90 mph.

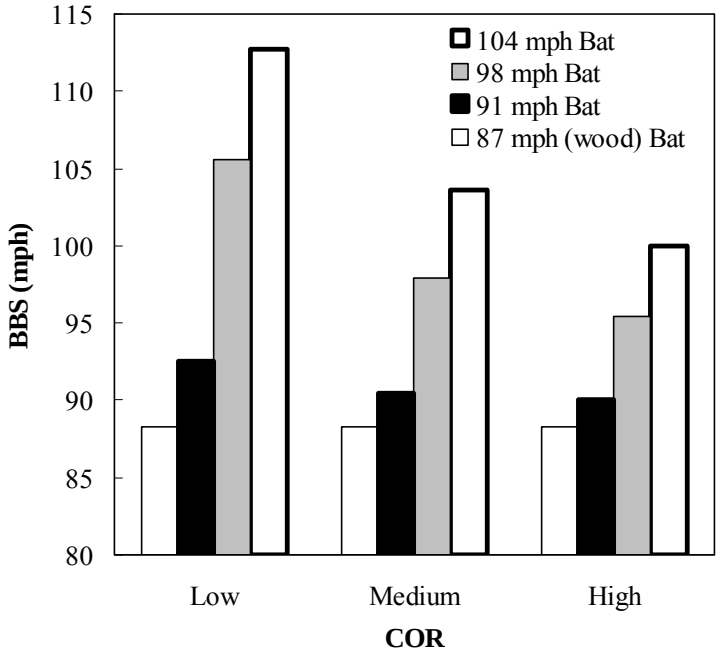

Figure 2.59: BBS vs. varying ball COR. The BBS is normalized for ball weight and COR.

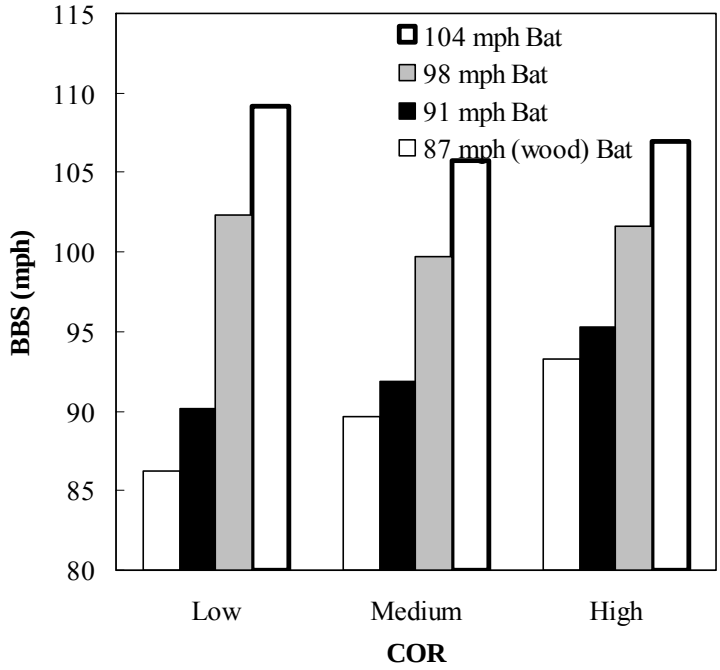

Figure 2.60: BBS vs. varying ball COR. The BBS is normalized for ball weight only.

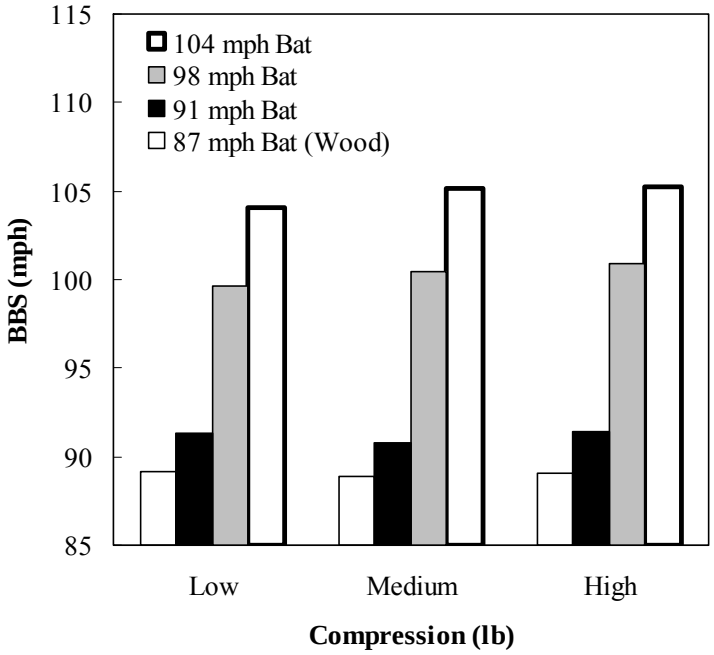

Figure 2.61: BBS vs. varying ball compression. The BBS is normalized for ball weight and COR.

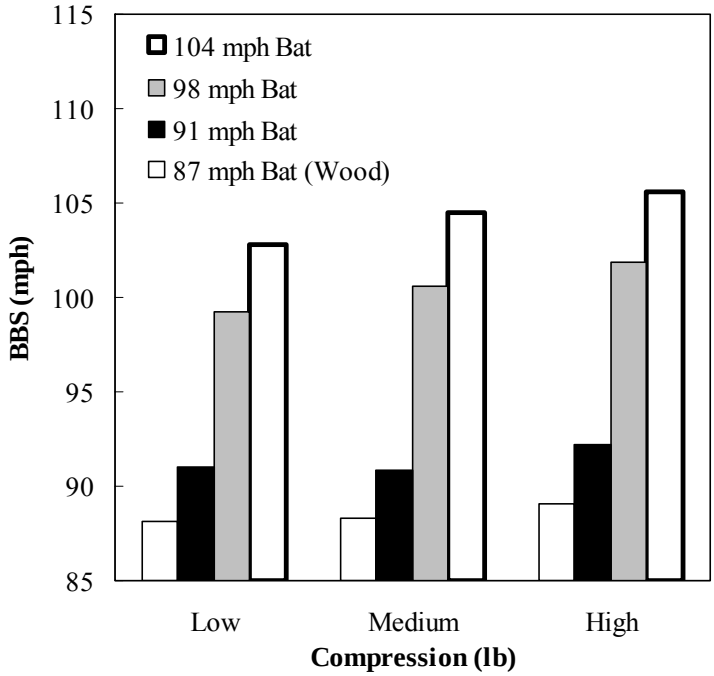

Figure 2.62: BBS vs. varying ball compression. The BBS is normalized for ball weight only.

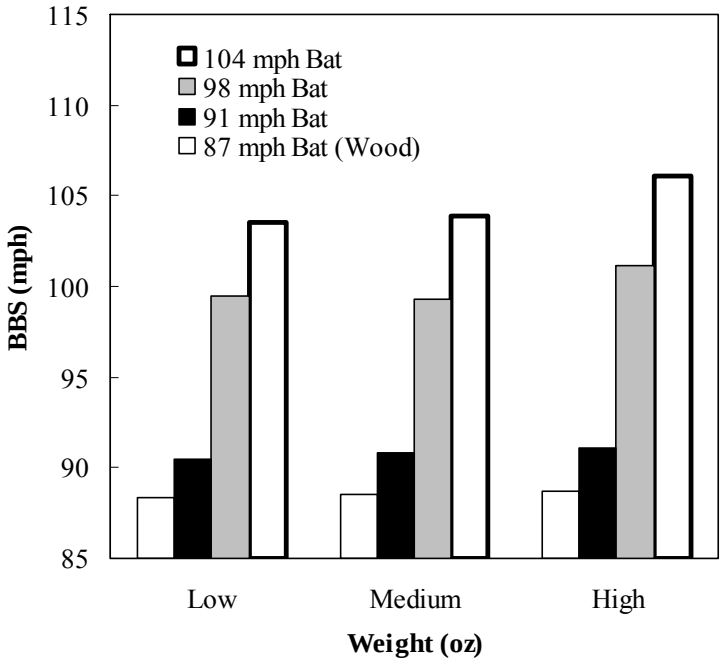

Figure 2.63: BBS vs. varying ball weight. The BBS is normalized for ball weight and COR

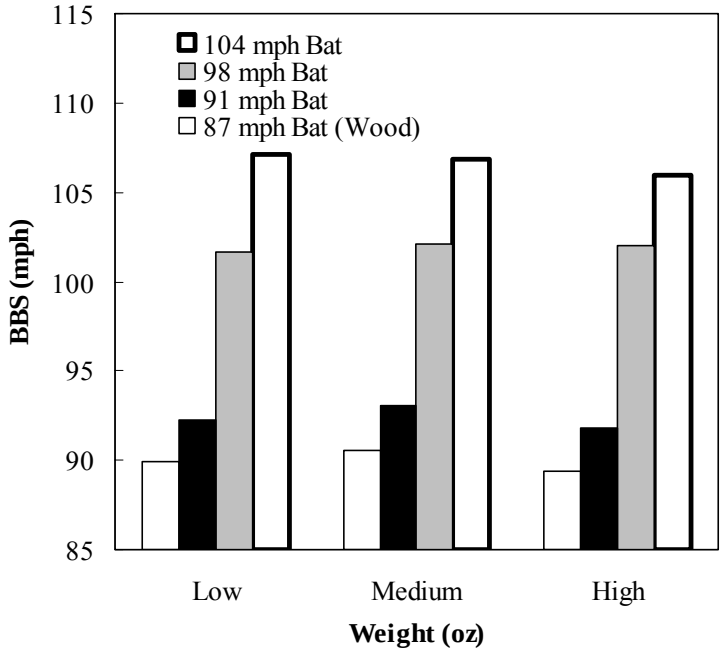

Figure 2.64: BBS vs. varying ball compression. The BBS is normalized for ball weight only.

CHAPTER 3

BALL MODELING

3.1 Introduction

The softball can have a large effect on the performance of a softball bat. While many baseball models have been developed [3.1, 3.2, 3.3], the softball has received very little attention. There is a need from a research and development standpoint to be able to accurately predict softball bat performance and simulate laboratory tests. An accurate model of the viscoelastic softball is needed to predict bat performance. The model of the softball must describe the rate dependence of the COR, dynamic compression, and contact time.

In past research, quasi static ball tests have been used in finite element models. While the data for these tests are relatively easy to obtain, the resulting models are not always accurate due to the large difference in the loading rate. Smith [3.4] found that quasi static load displacement curves input in a finite element model resulted in a plastic collision with excessive amounts of ball deformation.

In chapter 2, experimental data showed that the softball COR was less than unity. An elastic model, therefore, would not describe the energy dissipated during impact. While a variety of techniques could be used to account for energy losses, the polymeric core of the softball lends itself well to viscoelastic material modeling. In the following, two viscoelastic material models are investigated. The experimental results discussed in chapter 2 are used for finite element model verification.

Although the ball was modeled as a homogenous sphere, the diameter and weight of softball model are consistent with those of a softball with the cover on. Therefore, the decrease in the dynamic compression due to the weight should not affect the finite element model.

Further, it is hypothesized that the observed increase in the COR without the cover on is primarily due to the reduced dynamic compression. The COR, therefore, may only be affected a small amount due to the homogeneity of the model.

A three parameter power law viscoelastic material model, using a time dependent shear modulus to account for energy losses, was investigated. It is currently unknown if the softball rate dependence of the COR and dynamic compression can be adequately modeled using this simple viscoelastic model. Therefore, a parameter study was performed to determine the effect each parameter has on the COR and the dynamic compression. The rate dependence of several combinations of the parameters was also examined. The results of this parameter study are not limited to softballs or baseballs, but can be generalized to any spherical object impacting a flat or cylindrical surface.

A general viscoelastic material model was also investigated. This model uses a relaxation curve to account for energy losses in the ball. The curve was generated from experimental DMA data obtained from a coupon made of the polyurethane core of the softball. The accuracy and the ability to describe the rate dependence were investigated for this model.

3.2 Finite Element Analysis Background

The experimental COR, dynamic compression, and cylindrical impact tests were modeled using the dynamic finite element code LS-DYNA (Version 970, LSTC, Livermore, Ca). The softballs were modeled as homogenous spheres with isotropic properties. The analyses were performed on a 3.06 GHz Pentium 4 processor with 512 MB of RAM.

The ball properties of interest in this study were the COR, dynamic compression, contact time, and impulse COR. The COR was defined using eq. 1.2 as the ratio of the rebound speed to the pitch speed. The pitch speed was entered in the finite element input file (.dyn) in LS-DYNA

and the rebound speed was found in an output file (nodout) following the finite element analysis. The reference node was chosen at the center of the sphere. The data in the output file was used to plot the velocity vs. time, as shown in figure 3.1.

In figure 3.1, the initial flat negative region is the pitch velocity of the ball prior to impact. The steep slope corresponds to the compression and expansion phases of the ball during impact, where the ball velocity changes from negative to positive. The subsequent positive flat portion of the curve represents the rebound velocity of the ball. Rebound speeds were generally constant, varying by less than one inch per second.

When the ball comes into contact with the rigid wall or the cylindrical surface, a force is generated. The magnitude of this force depends on the hardness, mass, and speed of the colliding bodies. This contact force exists from the point of initial contact to the time the ball rebounds off of the plate. In LS-Dyna, the contact force time history was available in the output file (rcforc). The dynamic compression value was determined by finding the peak force in the force vs. time curve, as shown in figure 3.2. The contact time was also found from the force vs. time curve. The contact time was defined as the time from the first nonzero force to the last nonzero force. In some instances the impulse was used to obtain a second measure of the relative speeds before and after impact. This impulse COR can be compared to the standard COR by summing the pitch and rebound speeds used in eq. 1.2, as described in section 2.5.2.

3.3 Convergence Study

The mesh density can have a significant effect on the accuracy of the finite element model. A refined mesh will converge to the true mathematical solution while a mesh density that is too low will not accurately describe the conditions being modeled [3.5]. As the mesh density increases the computation time increases as well. Also, many finite element codes have a

maximum amount of elements that a model can have. In this work, the educational version of LS-Dyna was used which limits the number of elements to 10,000.

An important consideration in this work was that the ball model developed was to be subsequently used in a bat-ball collision model where the bat contains 4500 elements. This limited the number of elements in the ball model to 5500. The ball model used in this study had to have a short simulation time due to the large number of models investigated. Also, the bat-ball collision model takes several hours to run when a conservative ball mesh density is used. Increasing the number of elements in the ball could add significant computation time in the bat model. Despite this, two mesh densities were applied to the softball and impact surfaces to quantify the effect of the mesh density on the values of the COR, dynamic compression, contact time, and impulse COR.

The softball was modeled using eight-node solid elements. The standard and fine softball mesh contained 2,816 and 4096 elements, respectively. Symmetry was used in the fine mesh with ¼ of the ball being modeled. Therefore, the fine mesh can be thought of as having 16,384 elements. Two views of each softball mesh density are shown in figures 3.3 to 3.6.

The convergence study was performed using the flat and cylindrical impact surfaces. The mesh density of the impact surfaces was increased as the ball mesh density increased. The rigid, flat wall with dimensions of 4x4x1 inches was modeled using four node shell elements with 400 and 1600 elements for the standard and fine mesh densities, respectively. The standard mesh cylindrical surface was modeled using 1296 eight node solid elements, which had 288 elements at the contact surface. The fine mesh cylindrical impact surface was modeled using 1600 four node shell elements. Each cylinder had a diameter of 2 ¼" and a length of four inches. The standard and the fine mesh cylindrical impact surfaces are shown in figure 3.7 to 3.9. The flat

plate and the cylindrical surface were both given the properties of steel and were constrained in the x, y, and z directions to assure a rigid impact surface.

The standard mesh required less than one minute computation time, while the fine mesh required approximately eight minutes. Each model was run for three milliseconds (0.003 s), which was sufficient time for the ball to impact and rebound off the plate and reach a steady state velocity, as shown in figure 3.1.

For impacts against a flat plate, it was found that the standard mesh produced COR and dynamic compression results within 5.1% and 1.0 %, respectively, of the fine mesh (on average). The cylindrical impact surface showed similar trends with the COR increasing by 4.3% and the dynamic compression varying by 1.1%. The COR was observed to be systematically higher for the fine mesh density, while the dynamic compression did not show a consistent trend.

The difference between the fine and standard mesh COR values were observed to decrease with increasing pitch speed. The impulse COR was observed to be lower than the COR calculated from eq. 1.2 for both mesh densities. The standard mesh density impulse COR varied from the eq. 1.2 COR by 3.8% (standard deviation = 0.02) while the fine mesh density impulse COR varied by 2.7% (standard deviation = .01). Therefore, it appears that as the mesh density becomes more refined, the impulse COR is approaching the eq. 1.2 COR.

The force time curve was observed to be noticeably smoother for the fine mesh compared to the standard mesh density due to an increased amount of nodes coming into contact during the collision. The contact time varied on average by 1.35% from the standard to the fine mesh density. Values of the COR, dynamic compression, impulse, and contact time at 60, 90, and 110 mph impact speeds are shown for the fine and standard mesh densities for several models in tables 3.1and 3. 2.

The results show that the COR is strongly affected by the mesh density while the dynamic compression, impulse COR, and contact time appear to be less sensitive. Due to element and time limitations, the differences between the two mesh densities were neglected and the standard mesh density was used for the parameter study. The parameter values used in this study were not absolute material properties, and therefore, the results are still valid since experimental calibration is necessary.

Table 3.1: Values of the COR, dynamic compression, impulse, and contact time for several models at varying speeds for the standard mesh density.

Model	Impact Surface	Pitch Speed in/s (mph)	Standard Mesh				
			Rebound Speed (in/s)	COR	Dyn. Comp. (lbs)	Impulse (in/s)	Contact Time (ms)
1	Flat	1056 (60)	467	0.4422	2820	1465	1.17
1	Flat	1584 (90)	650	0.4102	4480	2147	1.04
1	Flat	1936 (110)	754	0.3895	6270	2588	1.00
2	Flat	1056 (60)	469	0.4441	3070	1467	1.11
2	Flat	1584 (90)	655	0.4133	5048	2153	1.00
2	Flat	1936 (110)	762	0.3938	6775	2593	0.94
3	Flat	1056 (60)	468	0.4434	2860	1465	1.16
3	Flat	1584 (90)	655	0.4136	4500	2153	1.05
3	Flat	1936 (110)	765	0.3952	6070	2598	0.99
6	Flat	1056 (60)	469	0.4443	2280	1466	1.41
6	Flat	1584 (90)	657	0.4150	3830	2155	1.27
6	Flat	1936 (110)	766	0.3954	5150	2597	1.20
7	Flat	1056 (60)	473	0.4476	2490	1470	1.30
7	Flat	1584 (90)	665	0.4199	4170	2162	1.18
7	Flat	1936 (110)	777	0.4014	5280	2609	1.12
1	Cylindrical	1056 (60)	497	0.4708	2510	1493	1.28
1	Cylindrical	1584 (90)	706	0.4454	4060	2201	1.17
1	Cylindrical	1936 (110)	831	0.4293	5240	2661	1.11
2	Cylindrical	1056 (60)	498	0.472	2660	1495	1.25
2	Cylindrical	1584 (90)	709	0.4476	4360	2204	1.13
2	Cylindrical	1936 (110)	836	0.432	5900	2666	1.06
3	Cylindrical	1056 (60)	490	0.4638	2580	1486	1.26
3	Cylindrical	1584 (90)	698	0.4405	4170	2194	1.15
3	Cylindrical	1936 (110)	827	0.4274	5210	2657	1.10

Table 3.2: Values of the COR, dynamic compression, impulse, and contact time for several models at varying speeds for the fine mesh density.

Model	Impact Surface	Pitch Speed in/s (mph)	Fine Mesh				
			Rebound Speed (in/s)	COR	Dyn. Comp. (lbs)	Impulse (in/s)	Contact Time (ms)
1	Flat	1056 (60)	491	0.4646	2824	1505	1.16
1	Flat	1584 (90)	671	0.4239	4840	2195	1.04
1	Flat	1936 (110)	780	0.4027	6200	2641	0.98
2	Flat	1056 (60)	491	0.4650	2820	1505	1.11
2	Flat	1584 (90)	677	0.4271	5190	2200	0.99
2	Flat	1936 (110)	790	0.4078	6821	2651	0.93
3	Flat	1056 (60)	500	0.4733	2821	1514	1.16
3	Flat	1584 (90)	686	0.4333	4920	2209	1.04
3	Flat	1936 (110)	798	0.4121	6280	2660	0.99
6	Flat	1056 (60)	517	0.4892	2365	1530	1.44
6	Flat	1584 (90)	709	0.4475	3864	2231	1.29
6	Flat	1936 (110)	822	0.4245	5102	2683	1.21
7	Flat	1056 (60)	508	0.4811	2436	1522	1.32
7	Flat	1584 (90)	697	0.4403	4209	2220	1.19
7	Flat	1936 (110)	809	0.4179	5382	2671	1.13
1	Cylindrical	1056 (60)	523	0.4954	2514	1536	1.33
1	Cylindrical	1584 (90)	727	0.4592	4147	2249	1.20
1	Cylindrical	1936 (110)	852	0.4403	5484	2713	1.14
2	Cylindrical	1056 (60)	520	0.4926	2687	1533	1.28
2	Cylindrical	1584 (90)	726	0.4584	4526	2248	1.15
2	Cylindrical	1936 (110)	853	0.4406	5894	2714	1.09
3	Cylindrical	1056 (60)	534	0.5053	2461	1547	1.33
3	Cylindrical	1584 (90)	746	0.4709	4152	2267	1.21
3	Cylindrical	1936 (110)	876	0.4523	5440	2735	1.14

3.3 Power Law Viscoelastic Model

3.3.1 Introduction

The viscoelastic material model within LS-DYNA (material #6) was used to model the polyurethane core of a softball. The Power law viscoelastic material model is defined by a time dependent shear modulus as

$$G(t) = G_\infty + (G_0 - G_\infty)e^{(-\beta t)}, \tag{3.1}$$

where G_∞ is the long term shear modulus, G_0 is the short term shear modulus, and β is the decay constant. The model is a spring (G_∞) in parallel with a spring (G_0) and damper (β) as shown in figure 3.10. Linear viscoelasticity is assumed for the deviatoric stress tensor σ'_{ij}, which can be calculated from the Jaumann rate integral (also known as the hereditary or convolution integral) as

$$\sigma'_{ij} = 2\int_0^t G(t-\tau) D'_{ij} d\tau \,, \tag{3.2}$$

where D'_{ij} is the deviatoric strain tensor and τ is time [3.6]. The stress state can be decomposed into a hydrostatic pressure component and a change in shape component. The deviatoric stress refers to the change in shape component, which is equal to the total stress minus the hydrostatic pressure component. The deviatoric strain refers to the total strain minus the volumetric strain.

A recursion formula is used to compute the new value of the Jaumann rate integral at time t^{n+1} from its value at time t^n. Inspection of eq. 3.1 reveals that at $t = 0$, the short term shear modulus governs the material behavior while at $t = \infty$ the long term shear modulus becomes dominant. At times between these two extremes, each shear modulus contributes. The rate at which the long term modulus governs material behavior is dependent on the value of the decay constant β. The larger the value of β, the quicker the long term shear modulus governs material behavior.

3.3.2 Viscoelastic Parameter Study

While several baseball models have used eq. 3.1 in the past, it is unknown how the viscoelastic parameters affect the rate dependence of the ball. The most common approach to finding the parameters in past models has been through reverse engineering. The parameters were adjusted until the model was in satisfactory agreement with the experimental data. Several very different values of the parameters have been used, as shown in table 3.3. It is hypothesized that although a wide range of parameter values can model the ball sufficiently at one impact speed, some combinations may model the rate dependence more accurately. In the current study, a systematic approach was taken to examine how the parameters of eq. 3.1 and the bulk modulus affect the COR and dynamic compression of the softball.

Table 3.3: Viscoelastic material model parameters (eq. 3.1) used by several different researchers to model the baseball or softball.

Model:	Researcher:	k psi (Pa)	G_0 psi (Pa)	G_{inf} Psi (Pa)	β Hz
Baseball	Nicholls [3.1]	?	6.29 ($43.4x10^3$)	0.0552 (381)	$1.428x10^3$
Soft Baseball	Nicholls [3.1]	?	$41.9x10^3$ ($28.9x10^3$)	0.013 (93.4)	$1.428x10^3$
Baseball	Sandmeyer [3.2]	$4.0x10^6$ ($27.57x10^9$)	245 ($1.689x10^6$)	850 ($5.86x10^6$)	850
Softball	Sandmeyer [3.2]	$4.0x10^6$ ($27.57x10^9$)	125 ($861.8x10^3$)	450 ($3.102x10^6$)	950
Baseball	Shenoy [3.3]	$13.488x10^3$ ($93x10^6$)	$4.496x10^3$ ($31.0x10^6$)	$1.45x10^3$ ($10.0e^6$)	$11.0x10^3$
Rubber Baseball	Shenoy [3.3]	$2.755x10^3$ ($19.0x10^6$)	290 ($2.0x10^6$)	145 (1.0x106)	$1.25x10^3$

The four parameters that were investigated in this study were the bulk modulus k, long term shear modulus G_∞, short term shear modulus G_0, and the decay constant β. The mass density was kept constant at 0.0000372 $lb \cdot s^2 / in$. Each parameter was varied to see how changing one value affects the COR and dynamic compression. Caution had to be taken in the values chosen to model the ball, as some combinations led to instability and errors in the finite element results. Of main concern was the Poisson's ratio υ, related to the shear and bulk modulii by the equation

$$\upsilon = \frac{3G - 2k}{6G - 2k}, \tag{3.3}$$

where G is either the long or short term shear moduli and k is the bulk modulus. If either shear or bulk modulii value causes eq. 3.3 to become negative or greater than 0.5, the finite element model becomes unstable and an error occurs. The values used in the study, therefore, were limited by these conditions.

At each value of the bulk modulus, the long and short term shear moduli and the decay constant were varied. Table 3.4 gives a summary of the values of each parameter used in the study. For each value of the long and short term shear modulii and the bulk modulus, the decay constant was varied over several decades. While most models result in stable solutions, it is possible to change a parameter too much and cause the ball to deform in complex shapes. An example of this is shown in figure 3.11.

Table 3.4: Values of each parameter used in the study. The plots of the COR and dynamic compression vs. the decay constant for the models listed below are in appendix one.

k (psi)	G_0 (psi)	G_{inf} (psi)	β (Hz)
$10.0x10^3$	$5.0x10^3$	$1.0x10^3$	$100\text{-}2.0x10^6$
$10.0x10^3$	$5.0x10^3$	$1.6x10^3$	$100\text{-}2.0x10^6$
$10.0x10^3$	$5.0x10^3$	$2.0x10^3$	$100\text{-}2.0x10^6$
$10.0x10^3$	$10.0x10^3$	$0.1x10^3$	$10\text{-}500.0x10^3$
$10.0x10^3$	$10.0x10^3$	$1.3x10^3$	$10\text{-}2.0x10^6$
$10.0x10^3$	$10.0x10^3$	$2.0x10^3$	$10\text{-}2.0x10^6$
$10.0x10^3$	$15.0x10^3$	$1.7x10^3$	$100\text{-}2.0x10^6$
$10.0x10^3$	$15.0x10^3$	$2.0x10^3$	$100\text{-}2.0x10^6$
$200.0x10^3$	$10.0x10^3$	$0.1x10^3$	$10\text{-}2.0x10^6$
$200.0x10^3$	$10.0x10^3$	$1.3x10^3$	$10\text{-}2.0x10^6$
$200.0x10^3$	$250.0x10^3$	$0.1x10^3$	$10\text{-}2.0x10^6$
$200.0x10^3$	$250.0x10^3$	$1.3x10^3$	$10\text{-}2.0x10^6$
$200.0x10^3$	$250.0x10^3$	$50.0x10^3$	$10\text{-}2.0x10^6$
$1.0x10^6$	$10.0x10^3$	$0.1x10^3$	$10\text{-}2.0x10^6$
$1.0x10^6$	$10.0x10^3$	$1.3x10^3$	$10\text{-}2.0x10^6$
$1.0x10^6$	$1.0x10^6$	$0.1x10^3$	$10\text{-}6.0x10^6$
$1.0x10^6$	$1.0x10^6$	$1.3x10^3$	$10\text{-}8.0x10^6$
$1.0x10^6$	$1.0x10^6$	$50.0x10^3$	$10\text{-}2.0x10^6$
$1.0x10^6$	$1.0x10^6$	$500.0x10^3$	$10\text{-}2.0x10^6$
$10.0x10^6$	$10.0x10^3$	$0.7x10^3$	$10\text{-}5.0x10^6$

For each value of the bulk and short term modulus, the COR and dynamic compression vs. the decay constant for different values of the long term shear modulus were plotted. Representative examples are presented below, details of which are presented in appendix one.

3.3.3 Model Variations

While investigating the parameters in table 3.4, several softball models were found that fit experimental COR and dynamic compression data for a 60 mph impact with a 44/375 ball. Table 3.5 gives the values of the parameters and the resulting COR and dynamic compression values for each softball model. It should be noted that an infinite number of parameter combinations may exist to model the 44/375 ball. It is hoped that the models found contain a representative sample of the population of models.

It is desirable to know how changing one parameter affects the values of the COR and dynamic compression. In models 1, 2, and 3 of table 3.3, three of the four parameters $(k, G_0, G_\infty, \beta)$ were held constant while the fourth was varied over several decades. The results of this study can be generalized for any spherical object impacting a rigid wall, such as a tennis or golf ball.

Table 3.5: Values of parameters, COR, and dynamic compression of each model of the 44/375 ball at 60 mph.

	k (psi)	G_0 (psi)	G_{inf} (psi)	β (Hz)	COR	Dynamic Compression (lbs)
Model 1	200.0×10^3	250×10^3	1.3×10^3	1.0×10^6	0.4422	3118
Model 2	200.0×10^3	10.0×10^3	1.3×10^3	32.5×10^3	0.4441	3187
Model 3	1.0×10^6	1.0×10^6	1.3×10^3	4.35×10^6	0.4434	3370
Model 4	10.0×10^3	10.0×10^3	1.3×10^3	23.2×10^3	0.4408	3228
Model 5	10.0×10^6	10.0×10^3	1.3×10^3	38.2×10^3	0.4391	3152
Model 6	10.0×10^6	10.0×10^3	0.7×10^3	68.0×10^3	0.4443	2633
Model 7	10.0×10^6	1.0×10^6	0.9×10^3	6.0×10^6	0.4476	2859
Model 8	10.0×10^3	10.0×10^3	10.0×10^3	12.0×10^3	0.4517	3050
Model 9	1.0×10^6	10.0×10^3	1.3×10^3	35.0×10^3	0.4441	3220
Model 10	10.0×10^3	15.0×10^3	1.7×10^3	30.0×10^3	0.4565	3610

In figures 3.12 and 3.13, the COR and dynamic compression of models 1, 2, and 3 are plotted against the long term shear modulus G_∞. The COR and dynamic compression were found to be very sensitive to the value of the long term shear modulus. This implies that the exponential term of eq. 3.1 causes the sum to decay quickly, leaving only the long term shear modulus for a large portion of the simulation. As the long term shear modulus increased, the COR and dynamic compression increased as well. This could be expected because as the shear modulus increases, the ball becomes incompressible. An incompressible ball has a very short contact time and only a small amount of energy is expended during the compression and expansion phases of the impact, leading to high COR and dynamic compression values.

At low values of G_∞ a plastic collision was approached (COR = 0) and the dynamic compression leveled out at approximately 2,000 lbs. At high values of G_∞ the impact appeared

to be approaching an elastic collision (COR = 1.0), while the dynamic compression appeared to be steadily increasing. At values between these two extremes, the COR and dynamic compression appeared to increase linearly with increasing long term shear modulus. In figures 3.12 and 3.13, the values of models 1, 2, and 3 almost fall on top of each other for values of $G_\infty <$ 5,000. At values larger than this the curves begin to separate. The separation could be a result of the values of the short term shear modulus or the decay constant, as the positioning of the curves agrees with the order of these two values in each model.

The COR and dynamic compression vs. the short term shear modulus G_0 is shown in figures 3.14 and 3.15. Models 1 and 3 had similar curves for the COR and dynamic compression, while model 2 deviated from the others. The COR curve of model 2 had a minimum while models 1 and 3 were observed to decrease with increasing short term shear modulus. The dynamic compression of model 2 was initially flat, however, and as G_0 increased a linear increase in the dynamic compression was observed. The dynamic compression of models 1 and 3 remained nearly flat for all values of G_0 investigated. The behavior of the curves for larger values of the short term shear modulus is undefined, as the Poisson's ratio limited the range of values that could be investigated.

In figure 3.16, the shear relaxation modulus vs. the short term shear modulus is shown for models 1, 2, and 3. The relaxation modulus was evaluated at one half of the contact time for each data point. In models 1 and 3, the decay constant is so large that it causes the exponential term in eq. 3.1 to go to zero at small time values regardless of the value of the short term shear modulus, giving the shear relaxation modulus a constant value equal to the long term shear modulus. The decay constant of model 2 is small enough that it allows the exponential term to add to the long term shear modulus when the short term shear modulus is sufficiently large. For

models 1 and 3, the shear modulus remains constant at $G_\infty = 1300$ Psi for all values of G_0 while the relaxation modulus of model 2 begins to increase after $G_0 = 50{,}000$ Psi, which corresponds to the minimum COR value seen in figure 3.14.

The shear modulus shown in figure 3.16 was observed to be proportional to the dynamic compression and inversely proportional to the contact time, as shown in figures 3.15 and 3.17, respectively. For large values of the short term shear modulus, the shear modulus was also proportional to the COR. For smaller values of G_0, the COR approached an elastic collision since the ability for viscoelastic energy loss diminishes as G_0 approaches G_∞. As the relaxation modulus of model 2 began to increase in figure 3.13, the COR and dynamic compression increased and the contact time decreased due to the ball becoming harder. For models 1 and 3, the relaxation modulus remained constant as did the dynamic compression and contact time.

In model 2, the short term shear modulus values to the right of the minima caused the ball to remain deflected after impact. As the ball continued to move away from the impact surface, the ball would return to round. The reason for this behavior is not well understood, though it is possibly due to the Poisson's ratio approaching zero with increasing short term shear modulus. In figures 3.18 and 3.19, a representative picture of a round post impact ball is shown along with the flat post impact ball of model 2.

Figures 3.20 and 3.21 show the COR and dynamic compression vs. decay constant for models 1, 2, and 3. The COR curves were observed to have a minima while the dynamic compression appeared to be decreasing with increasing decay constant. The location of the minimum values in the COR curve appear to be proportional to G_0. The minimum value is significant because the value of the decay constant can be chosen so that the desired COR can be

on either side of the minimum value. This allows two choices for the dynamic compression value associated with a COR value.

The COR value appeared to be approaching an elastic collision as the decay constant approached zero. This is due to the exponential term decaying slowly, so that the impact is complete before the material time dependence begins. In figure 3.22, the shear modulus vs. the decay constant is shown. The shear modulus was evaluated at the contact time for each data point. Figure 3.22 suggests that for very low decay constant values, the shear modulus approaches the short term shear modulus.

As the decay constant increased, the COR in figure 3.20 decreased linearly until the minimum value was reached. The decrease in the COR is due to an increase in the material time dependence due to the exponential term adding less to the long term shear modulus at each time step which gives the shear modulus a lower value. In figure 3.23, the contact time vs. the decay constant is plotted for models 1, 2, and 3. At the minimum value, the contact time is such that the exponential term has decayed at the very end of the impact. The contact times were observed to be constant for small values of the decay constant. The sudden increase in the contact time in figure 3.23 corresponds to the COR minimum value in figure 3.20.

Following the minimum value, the COR again approached an elastic collision with increasing β. From this point on, the exponential term goes to zero before the end of the collision, causing the COR to increase with the increase in time dependent behavior. The relaxation modulus in figure 3.22 is equal to the long term shear modulus for the large values of the decay constant. The contact time was observed to increase in this range of decay constant values due to the ball becoming softer.

The dynamic compression vs. the decay constant was observed to decrease with increasing decay constant values. For low values of the decay constant, the dynamic compression values were a maximum thus forming the flat linear region of the curve. As the decay constant increased, a sharp linear decrease in the dynamic compression was observed. At high values of the decay constant the dynamic compression leveled off at a minimum.

The shape of the dynamic compression curve can be attributed to the exponential term in eq. 3.1. For small values of the decay constant, the exponential term in eq. 3.1 does not die out very quickly and therefore, the long and short term shear moduli contribute to the overall stiffness of the ball during the collision, causing the dynamic compression to be large. For high values of the decay constant, the exponential term of eq. 3.1 dies out quickly reducing the time dependent shear modulus to a constant (G_∞), accounting for the level and minimum values of the dynamic compression. At decay constant values between these two extremes, a linear decrease in the dynamic compression was observed due to an increasingly smaller contribution of the exponential term to the time dependent relaxation modulus. The positioning of the curve was also dependent on the value of the short term shear modulus. In general, a vertical offset in the curve was observed due to an increase in the short term shear modulus. Therefore, the dynamic compression appears to be proportional to the shear modulus.

The COR and dynamic compression vs. bulk modulus k curves for models 1, 2, and 3 are shown in figures 3.24 and 3.25. The COR only varied by 0.1 and the dynamic compression varied by less than 600 lbs. In comparison to figures 3.12 to 3.21, these changes are small. Also, small values of the bulk modulus could not be evaluated due to negative Poisson's ratio. The values of the bulk modulus were varied to provide the largest allowable range in the Poisson's ratio. Small and large values of the bulk modulus resulted in Poisson's ratio values

approaching zero and one half, respectively. It is suggested that the bulk modulus be used for fine tuning the values of the COR and dynamic compression.

3.3.4 Rate Dependence

A model is needed that can accurately describe the COR and dynamic compression of the viscoelastic softball over a range of pitch speeds. The rate dependence of the models described in table 3.3 was investigated by varying the incoming speed of the ball. The speeds were increased from 60 mph to 110 mph in 10 mph increments.

A plot of the COR vs. pitch speed is shown in figures 3.26 and 3.27 for the models in table 3.5 and for experimental data. Models 1-5 are plotted in figure 3.26 and models 6-10 are plotted in figure 3.27 to allow a better view of the data. The experimental data is the average of one dozen 44/375 balls fired at 60, 90, and 110 mph.

The general trend of the COR decreasing linearly with increasing pitch speed was observed for models 1-10. However, the finite element results appear to have a flatter slope compared to that of the experimental data which implies that the rate dependence has not been accurately characterized. Table 3.6 lists the slopes of the straight lines for the COR vs. pitch speed (the y-intercept was not of interest as it is trivial to adjust the parameter values to obtain a vertical offset). For the standard mesh density, model 1 provided the closest fit to the experimental COR data while model 8 provided the worst fit. The fine mesh density revealed that model 6 had the best fit with experimental data. It is apparent that the slope of the COR vs. pitch speed of the softball can be varied depending on the parameter values of eq. 3.1, however, none of the finite element models investigated can match the dynamic characteristics of a typical softball.

Table 3.6: The slopes of the COR and dynamic compression vs. pitch speed for each model and experimental data. Data for the fine and the standard mesh densities are shown. The COR slopes have been multiplied by 10,000 to allow easier comparison.

	Standard Mesh		Fine Mesh	
Model	COR Slopes (x 10,000) (1/mph)	Dyn. Comp. Slopes (lb/mph)	COR Slopes (x 10,000) (1/mph)	Dyn. Comp. Slopes (lb/mph)
1	-10.489	69.99	-11.54	67.945
2	-10.04	75.068	-12.46	79.93
3	-9.51	63.457	-12.3300	69.233
4	-8.55	88.61		
5	-8	65.162		
6	-9.76	56.947	-13.0200	54.386
7	-9.24	55.816	-12.7000	58.94
8	-6	82.343		
9	-9.34	70.71		
10	-8.03	95.029		
Experimental	-15.12	43.508	-15.12	43.508

The dynamic compression vs. pitch speed is shown in figures 3.28 and 3.29 for the models in table 3.5 and for experimental data. Again, models 1-5 are plotted in figure 3.28 and models 6-10 are plotted in figure 3.29 to allow a better view of the finite element results. The experimental data is the average of one dozen 44/375 balls fired at 60, 90, and 110 mph. The curves of dynamic compression vs. pitch speed appear to be linear with a positive slope. While the finite element slopes of the COR vs. pitch speed were too shallow, the dynamic compression curves were generally found to be too steep. Table 3.6 gives the slopes of the straight lines for each model. It was found that models 6 and 7 produced the best fit with experimental data for both the standard and the fine mesh density.

The best overall model of the softball rate dependence must agree well with both COR and dynamic compression experimental data. Table 3.6 suggests that model 6 provides the best fit with the COR and dynamic compression values, especially for the fine mesh density. Model 7 was also observed to correlate well with experimental data. It is recommended that either of these two models be used for bat impact studies where rate dependence is important. It is interesting to note that models 6 and 7 have the lowest values of the long term shear modulus of

any of the models investigated. This trend was further investigated for a long term shear modulus value of 100 psi. However, the COR was observed to increase with increasing pitch speed for this model, which disagrees with experimental results.

The experimental and numerical force versus time curves are shown in figures 3.30 through 3.32 for speeds of 60, 90, and 110 mph. The results are shown for model 7 and a 44/375 ball from manufacturer A. The unfiltered experimental force-time data from the piezoelectric load cell appears to be smoother than the numerical results. This result was observed to be model dependent. The contact time of the experimental and numerical results were observed to vary by less than 0.4%. The experimental curves were observed to increase and decrease uniformly while the numerical curves had a fast compression response and a slower expansion response. This result may be related to the high Poisson's ratio of the numerical model.

3.3.5 Cylindrical Impact Surface

The finite element model of the softball will be used in the bat-ball collision model, where the cylindrical surface of the bat is different from that of the flat wall used for the COR test. It was found experimentally in section 2.6 that the softball COR and dynamic compression were affected by the cylindrical impact surface. The experimental COR and dynamic compression were observed to decrease by 6.5% and 7.8%, respectively. The finite element model of the cylindrical surface softball COR test should be consistent with experimental data.

The experimental setup described in section 2.6 was modeled in LS-DYNA. The 2 ¼" diameter half cylinder with 1296 eight node solid elements is shown in figure 3.7. The half cylinder was constrained in all directions and the ball was given an initial velocity prior to impact. The COR, dynamic compression, impulse COR, and contact time were measured at speeds of 60, 90, and 110 mph for ball models 1, 2, and 3 of table 3.3.

The cylindrical surface COR and dynamic compression vs. pitch speed for models 1, 2, and 3 are shown in figures 3.33 and 3.34. The flat and cylindrical surface and experimental COR and dynamic compression values are shown for comparison in each figure. The finite element COR vs. pitch speed for the cylindrical surface was observed to increase by approximately 11%, which does not agree with experimental data that was observed to decrease. Increasing the mesh density did not significantly affect the cylindrical COR data.

The dynamic compression was observed to decrease by approximately 15%, which follows the same trend as experimental data. The experimental data, however, only decreased by 7.8% when compared to the flat plate. The contact time was observed to increase by 11.2% from the flat plate to the cylindrical surface for the standard mesh density and 15.7% for the fine mesh density. The experimental data showed a 7.5% increase in contact time for 90 mph impacts. The COR measured from the impulse of the impact was seen to decrease by 2.2% from the flat to the cylindrical impact surfaces. It appears therefore, that the decrease in the dynamic compression had a larger effect than the increase in the contact time.

The cylindrical impact surface effectively reduces the contact area of the ball at impact. The reduced area results in greater local deformation, which should cause a decrease in the COR, as observed in the experimental data. The finite element COR results are in disagreement possibly due to the model having a Poisson's ratio that is too high. The Poisson's ratio of this model is nearly 0.5, while that of the actual ball is approximately 0.1. The difference in the compression due to this large discrepancy may explain why the COR of the cylindrical impact surface is too high. The reduction in dynamic compression is associated with the increased local ball deformation due to the reduced contact area, as evidenced by the increase in the contact duration.

3.4 Prony Series Model

3.4.1 Introduction

Viscoelastic materials are characterized as having a time dependent response. For example, the gradual deformation of a viscoelastic material when subjected to a constant stress (creep behavior) and stress relaxation behavior when the material is subjected to a constant strain. Several constitutive laws have been proposed that describe the stress-strain relationship in terms of the creep compliance, relaxation modulus, and the storage and loss modulus [3.7]. Several of these models have used mechanical elements such as springs and dashpots to model the viscoelastic behavior. The Prony series model, for example, consists of a sequence of N spring and dashpot units in parallel (Voigt elements), as shown in figure 3.32. The Prony series relaxation function $G(t)$ is given by

$$G(t) = \sum_{i=1}^{N} g_i e^{-\beta_i t}, \tag{3.4}$$

where g_i and β_i are the shear moduli and the decay constants, respectively. The β_i have a physical interpretation as the time required for the i^{th} spring to reach its equilibrium position [3.7]. A viscoelastic foam such as the polyurethane core of the softball can have many time constants, ranging from a fraction of a second to many days. Rate effects are taken into account through linear viscoelasticity using the convolution integral of the form

$$\sigma_{ij} = 2\int_0^t G_{ijkl}(t-\tau)\frac{\partial \varepsilon_{kl}}{\partial \tau} d\tau, \tag{3.5}$$

where $G_{ijkl}(t-\tau)$ is the relaxation functions for the different stress measures. Equation 3.5 computes the overall stress and strain state, in comparison to eq. 3.2, which accounts for the deviatoric stress and strain components.

The storage and the loss moduli, E' and E'', can also be written in terms of the Prony series such that

$$E'(\omega) = \sum_{i=1}^{N} \frac{g_i \omega^2}{\frac{1}{\beta_i^2} + \omega^2} \tag{3.5}$$

and

$$E''(\omega) = \sum_{i=1}^{N} \frac{\frac{g_i}{\beta_i}\omega}{\frac{1}{\beta_i^2} + \omega^2}, \tag{3.6}$$

where ω is the frequency (Hz) [3.8]. The Prony series can be used to fit experimentally determined material property curves such as the relaxation modulus, storage modulus, and loss modulus. The Prony series constants are determined from experimental data using numerical techniques such as a least squares fit.

3.4.2 Relaxation Curve Development

Dynamic mechanical analysis was used to obtain the relaxation curve of the polyurethane foam core of the softball. DMA test coupons were machined from the core of a 44/375 ball from manufacturer A. The rectangular coupons, with dimensions of 20 x 6.4 mm with a 2.72 mm thickness, were machined using a circular saw and a milling machine. Stress relaxation testing was performed using a three point bending flexure setup, as shown in figure 3.36. In stress relaxation, a constant strain is applied to the coupon and the resulting stress decrease is measured over time [3.9]. The stress relaxation test gives insight into how a polymer relaxes. Stress relaxation tests were performed at temperatures ranging from $-60^{\circ}C$ to $10^{\circ}C$. The raw stress relaxation data vs. time is shown in figure 3.37.

The time temperature superposition principle (TTSP) states that the effect of changing the temperature on the relaxation modulus is the same as the effect of a corresponding change in the time scale [10]. Testing over a wide temperature span allows the properties of the viscoelastic material to be determined at high strain rates such as those observed in a softball COR test.

A popular method of applying the TTSP is via the WLF equation (eq. 1.34). In this work, the WLF equation was used to shift the relaxation vs. time data horizontally to account for the temperature differences. The data was shifted to a reference temperature of $72^{\circ}F$ ($22^{\circ}C$). The material dependent constants c_1 and c_2 of the WLF equation were found to be -2.584 and -112.486, respectively. The TTSP has been shown to be valid at temperatures below the glass transition temperature T_g for short term test data. However, due to physical aging (a slow loss of free volume in the polymer) the TTSP is not valid for long term test data when evaluated at temperatures below the T_g [10]. Table 3.7 gives the shift factor constants associated with each temperature. The resulting master curve is shown in figure 3.35. The data in figure 3.38 is the measured stress from three point bending, which gives the Young's modulus E (Psi). The shear modulus is related to Young's elastic modulus by the equation

$$G = \frac{E}{2(1+\nu)}, \tag{3.7}$$

where ν is the Poisson's ratio.

Table 3.7: Shift factors associated with each temperature in the WLF equation. The shift factor values are on a logarithmic scale.

Temperature °C	-62	-47.5	-33	-20	-4	10
Shift Factor a(t)	-12.7259	-9.70115	-7.05584	-5.04093	-3.05585	-1.77455

3.4.3 General Viscoelastic Finite Element Model

Having performed the DMA and obtained the master relaxation curve for the 44/375 ball from manufacturer A, impact simulations were carried out using LS-Dyna. The parameters of

interest were the COR and dynamic compression. These values were obtained as described in section 3.2. The standard mesh density flat wall COR and dynamic compression tests were modeled as described in section 3.3. The ball contained 2096 eight node solid elements and was assigned the general viscoelastic material model (mat_general_viscoelastic #76) within LS-Dyna which uses the Prony series of eq. 3.4 to define the viscoelastic deviatoric behavior [3.6]. The Prony constants can either be manually entered or can be found internally in LS-Dyna if the relaxation curve is input. LS-Dyna allows up to six terms in the Prony series to be used in the simulation.

In this work, the Prony series coefficients were found using MathCad (Version 2001 Professional, MathSoft Inc.). The coefficients were also obtained from the LS-Dyna curve fit as well as by a 3rd party. A summary of the coefficient values is given in table 3.8. The values shown are for the elastic relaxation modulus, and therefore the symbol E_i was used instead of g_i.

The purpose of curve fitting the elastic relaxation curve was to examine the effectiveness of each curve fitting technique so that one method could be chosen and then adhered to for subsequent testing. LS-Dyna's internal curve fit resulted in a poor fit to the experimental data and the 3rd party had negative values that do not have a physical interpretation. Further, the 3rd party curve did not follow the same trend as the master curve. It was found that the MathCad curve fit produced the most accurate results. The MathCad program required an initial guess value for each coefficient and when these values were chosen carefully, the resulting curve was an excellent fit. Six terms were used in order to have a fit as close as possible to experimental data. The MathCad program has been included in appendix two.

Table 3.8: Prony Series coefficients obtained by different software. The MathCad results were found to be the closest fit to the experimental master curve data.

	MathCad	LS-Dyna	3rd Party
E_1	10890	229	1937500
β_1	5834000	0	0.00000
E_2	6679	43289	-2225300
β_2	70610	0	0.00118
E_3	10960	1689	299560
β_3	204200000	2	0.10001
E_4	6997		8184
β_4	0.00413		1258
E_5	4259		25263
β_5	5.64300		31571000
E_6	4767		
β_6	767		

As discussed above, the Poisson's ratio must be known to obtain the shear relaxation modulus, which is required for the general viscoelastic material model. Since the Poison's ratio is unknown for the polyurethane foam core of the softball, three values of the Poisson's ratio were chosen to examine the effectiveness of the master curve in characterizing the softball. Values of $\nu = 0$, 0.25, and 0.5 were used to plot the master curve in terms of the shear modulus G(t). The three resulting master curves are shown in figure 3.39. The Prony series coefficients of eq. 3.4 were fit to the resulting master curves using MathCad and are listed in table 3.9. A representative curve fit is shown in figure 3.40 for a Poisson's ratio of 0.0.

The coefficients listed in table 3.9 were input into LS-Dyna and each model was simulated on the flat plate COR test at 60 mph. For direct comparison, the bulk modulus was kept constant at an arbitrary value of 200,000 psi. The COR of the three models remained constant at 0.877. The dynamic compression was observed to decrease with increasing Poisson's ratio. For Poisson's ratio values of 0.0, 0.25, and 0.5, the dynamic compression was 5,703 lb, 5,200 lb, and 4,840 lb, respectively. This trend could be expected since the ball is becoming

softer as the shear modulus decreases. From these results, it appears that the COR is not affected by the vertical offset in the master curve due to varying the Poisson's ratio.

The results of the three models do not agree well with experimental data. The COR value obtained numerically is nearly two times that of the experimental 0.44 value. The experimental dynamic compression for a 44/375 ball at 60 mph was found to be approximately 3,000 lb and the numerical results were 50% higher than this.

Mase [11] suggested that a horizontal shift in the master curve could improve the accuracy of the COR results. The data was shifted to a reference temperature of $10^{\circ}C$, which had the effect of moving the master curve to the right, as shown in figure 3.41. It was hypothesized that this shift would result in higher dynamic compression since the values of the shear relaxation modulus were increased. Also, it was shown experimentally in figure 2.43 that a temperature reduction causes the hardness and COR to increase. The horizontal shift to $T_{ref} = 10^{\circ}C$ resulted in a 14.5% increase in the dynamic compression value and a 2.5% reduction in the COR when compared to $T_{ref} = 22^{\circ}C$. It appears, therefore, that the COR and dynamic compression are moving away from each other and it may be difficult to match experimental data for more than one property at a time.

The COR and dynamic compression rate dependence was also examined for the general viscoelastic material. It was found that the COR increased with increasing pitch speeds, which is contrary to experimental and numerical results presented in previous sections. A 2.5% increase was observed in the COR from 60 mph to 110 mph. The dynamic compression was observed to increase by nearly 5,000 lbs over the same range.

While the general viscoelastic material presented a new way to characterize the softball, the results do not appear to support experimental data. Due to the lack of correlation with

experimental data, a more in depth analysis was not undertaken. Several possibilities exist as to the reasons why the model was not successful. A large horizontal shift in the master curve may be able to describe the rate dependence of the softball. When the master curve has been shifted sufficiently, the numerical results should correlate with the experimental data at several speeds. However, shifting of the data defeats the purpose of using DMA. If this method worked, experimental calibration would not be needed. Further, it is feasible that the DMA stress relaxation curves are not accurate and that a different type of DMA test could provide better data. Also, Mase [11] suggested another viscoelastic material model within LS-Dyna (mat_hyperelastic #77) that uses the Prony series as well as force-displacement data to characterize a material. Mase has had success using this model for the golf ball core. It is recommended that future work examine this model.

Table 3.9: Prony series coefficients used to curve fit the three different master curves from three values of Poison's ratio. Six terms Prony series coefficients were used for each master curve.

Prony Constants	MathCad Prony Constants		
	PR=0.0	PR=0.25	PR=0.50
g_1 (psi)	4.807×10^3	3.846×10^3	3.2×10^3
β_1 (1/s)	1.794×10^9	1.435×10^9	1.196×10^9
g_2 (psi)	3.0255×10^3	2.42×10^3	2.017×10^3
β_2 (1/s)	15.52×10^6	12.42×10^6	10.35×10^6
g_3 (psi)	6.16×10^3	4.928×10^3	4.107×10^3
β_3 (1/s)	167.2×10^9	133.8×10^9	111.5×10^9
g_4 (psi)	3.442×10^3	2.754×10^3	2.295×10^3
β_4 (1/s)	0.343×10^0	0.2748×10^0	0.229×10^0
g_5 (psi)	2.068×10^3	1.654×10^3	1.379×10^3
β_5 (1/s)	0.4813×10^3	0.385×10^3	0.3208×10^3
g_6 (psi)	2.364×10^3	1.891×10^3	1.576×10^3
β_6 (1/s)	124.4×10^3	99.51×10^3	82.93×10^3

3.5 Comparison of Models

Direct comparison of the Power law and the Prony series viscoelastic models is possible. Inspection of eq. 3.4 reveals that for $N = 2$ (with $\beta_1 = 0$), the Prony series model becomes the

Power law model. The Power law coefficients G_∞, $(G_0 - G_\infty)$, and β of model 7 corresponded to G_1, G_2 and β_2 in the two coefficient Prony series model. This comparison is important since the Power law uses the deviatoric part of the stress and strain, whereas the Prony series model uses the complete stress and strain state. The effects of this difference may be responsible for the inability of the Power law model to accurately describe the ball response to the cylindrical impact surface.

The two coefficient Prony series and the Power law models were compared at 60, 90, and 110 mph against a rigid flat plate. The two coefficient Prony series model was observed to agree with experimental data, however, the speed dependence of the COR and dynamic compression were 3.0% lower and 7.6% higher, respectively, when compared to the Power law model. Similar results were observed on the cylindrical surface.

The cylindrical impact surface was also modeled using the relaxation curve, which was fit to a six coefficient Prony series (using a Poisson's ratio of 0.5). The COR and dynamic compression of the six coefficient Prony series model were observed to decrease from the flat plate to the cylindrical impact surface. The decrease in the COR and dynamic compression show that the Prony series model is capable of describing the ball response on the cylindrical impact surface. However, the speed dependence of the COR remained opposite to experimental data.

3.6 Summary

In this research, a three parameter Power law and a more general Prony series viscoelastic model were studied using finite element analysis . The COR, dynamic compression, contact time, and impulse COR were compared to experimental data for each viscoelastic model. Also, the rate dependence was examined for each model. A parameter study was performed on

the Power law model to understand how each parameter affects the COR and dynamic compression.

The four parameters investigated in the parameter study were the long term shear modulus, short term shear modulus, the decay constant, and the elastic bulk modulus. Three of the four parameters were held constant while a fourth was varied over several decades. Three different sets of initial parameters were examined. The COR and dynamic compression were recorded for each model variation.

The COR and dynamic compression were observed to increase proportionally to the long term shear modulus. The behavior of the COR and dynamic compression vs. the short term shear modulus was seen to be dependent on the value of the decay constant. For small values of the decay constant, the COR curve had a minimum and the dynamic compression increased linearly. For large values of the decay constant, the COR decreased and reached a constant value and the dynamic compression remained approximately constant. Varying the decay constant caused the COR to have a minimum value and the dynamic compression to decrease. The bulk modulus was observed to have a very small effect on the COR and dynamic compression, and should be used for fine tuning a model.

While performing the parameter study of the Power law model, ten parameter combinations were found that fit experimental COR and dynamic compression data for a 60 mph impact. Each of these models were tested at several speeds to determine the ability of the model to describe the rate dependent behavior of the softball. It was found that two of these models were in good agreement with experimental rate dependent data for the flat impact surface. However, none of the models investigated were able to fit the experimental cylindrical impact surface COR data.

DMA of the polymeric core of the softball was used to obtain a master relaxation curve of the shear modulus vs. time. The Prony series was used to fit this experimental master curve, and the resulting Prony coefficients were used in LS-Dyna to model the softball. This technique presented an opportunity to use absolute material properties to model the softball. However, the results of this model did not agree well with experimental results. The COR and dynamic compression were observed to be 100% and 50% higher than experimental results.

The ability of each viscoelastic finite element model to capture the rate dependence of the COR and dynamic compression was examined. The Power law model was found to have good correlation with experimental data while the Prony series model was deviant. The cylindrical impact surface was modeled in the Power law viscoelastic model. It was found that the dynamic compression and contact time had good correlation with experimental data, while the COR did not. The Prony series model appeared to effectively describe the reduction in the COR and dynamic compression due to the cylindrical impact surface. The speed dependence of the COR, however, did not agree with experimental results.

The Power law material model appears to have much better correlation with experimental data than does the Prony series model. However, the Power law model was not able to simulate the results of the cylindrical impact test. It is recommended, therefore, that the ball model be calibrated on a cylindrical impact surface prior to use in a bat-ball model.

REFERENCES

[3.1] Nicholls, R.L. *Private communication*. October, 2004.

[3.2] Sandmeyer, B.J. *Simulation of bat/ball impacts using finite element analysis*. Masters thesis, Oregon State University. 1994.

[3.3] Shenoy, M.M. *Numerical simulation of baseball bat performance*. Masters thesis. Washington State University, 2000.

[3.4] Smith, L.V. *Private communication*. November, 2004.

[3.5] Cook, R.D., Malkus, D.S., Plesha, M.E., Witt, R.J. *Concepts and applications of finite element analysis*. John Wiley and Sons, New York. 2002.

[3.6] LS-DYNA Keyword Users Manual. Livermore Software Technology Corporation. April, 2003. Version 970.

[3.7] Singh, R., Davies, P., Bajaj, A.K. Estimation of the dynamical properties of a polyurethane foam through use of a Prony series. J. Sound and Vibration. 264, p. 1005-1043. 2003.

[3.8] Fisher, F.T., Eitan, A., Andrews, R., Schadler, L.S., Brinson, L.C. *Spectral response and effective viscoelastic properties of MWNT reinforced polycarbonates*. Advanced Composites Letters. 2004.

[3.9] Menard, K.P. *Dynamic mechanical analysis-a practical guide*. CRC Press, New York. 1999.

[3.10] Gibson, R.F. *Principles of composite material mechanics*. McGraw-Hill, New York. 1994.

[3.11] Mase, T. *Private communication*. November, 2004.

[3.12] Flugge, W. *Viscoelasticity*. New York, Springer-Verlag, 2nd edition. 1975.

Figures (modeling)

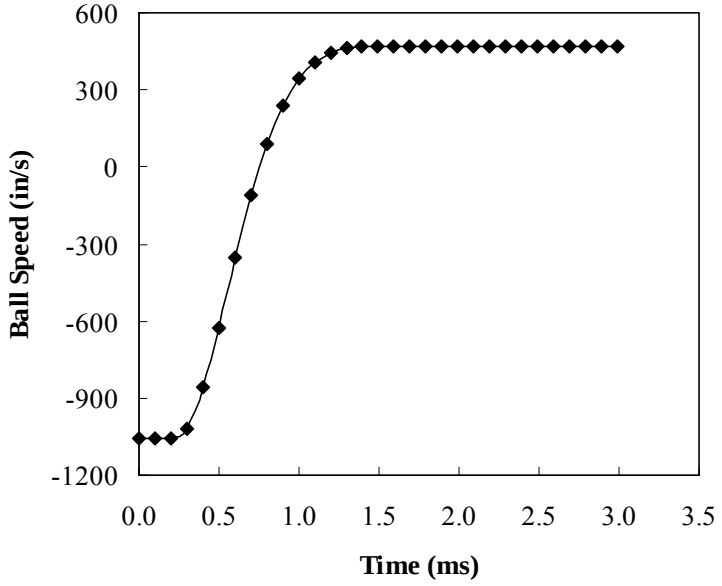

Figure 3.1: A plot of the finite element results of ball speed vs. time for model 1 impacting a flat rigid plate. The pitch speed is negative while the rebound speed is positive. The plot shown is a 60 mph (1056 in/s) pitch with a rebound of 26.6 mph (468 in/s) which yields a COR of 0.4431.

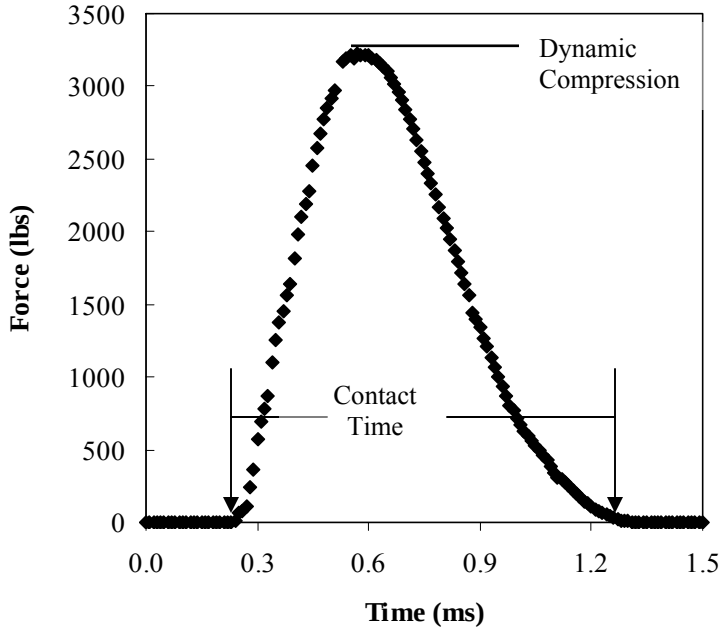

Figure 3.2: A plot of the finite element results of force vs. time for model 4 at 60 mph (1056 in/s). The peak impact force is recorded as the dynamic compression and the contact time is the time that the force data is nonzero.

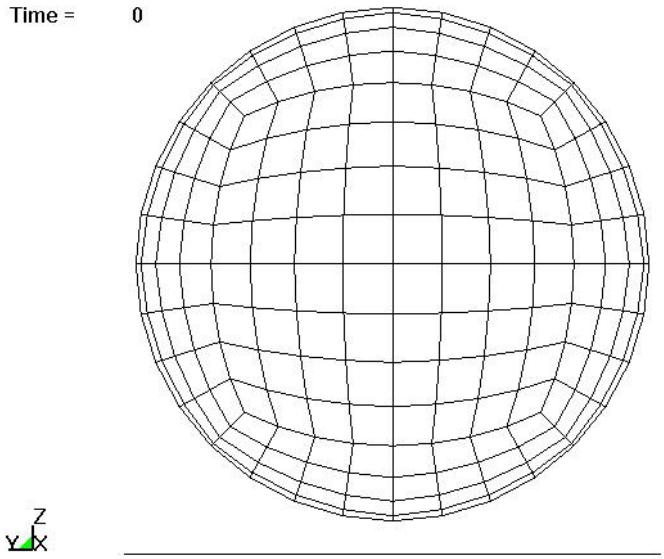

Figure 3.3: Side view of standard ball mesh density containing 2816 elements impacting a flat, rigid wall.

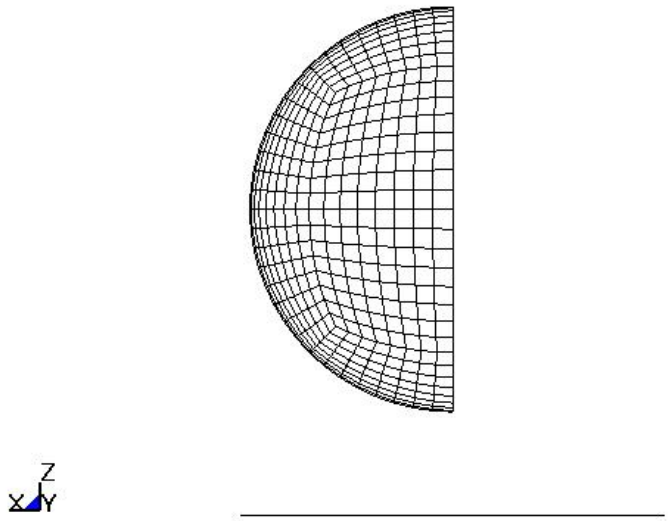

Figure 3.4: Side view of fine ball mesh density containing 4096 elements impacting a flat, rigid wall. The model shown utilized symmetry with ¼ of the ball being modeled.

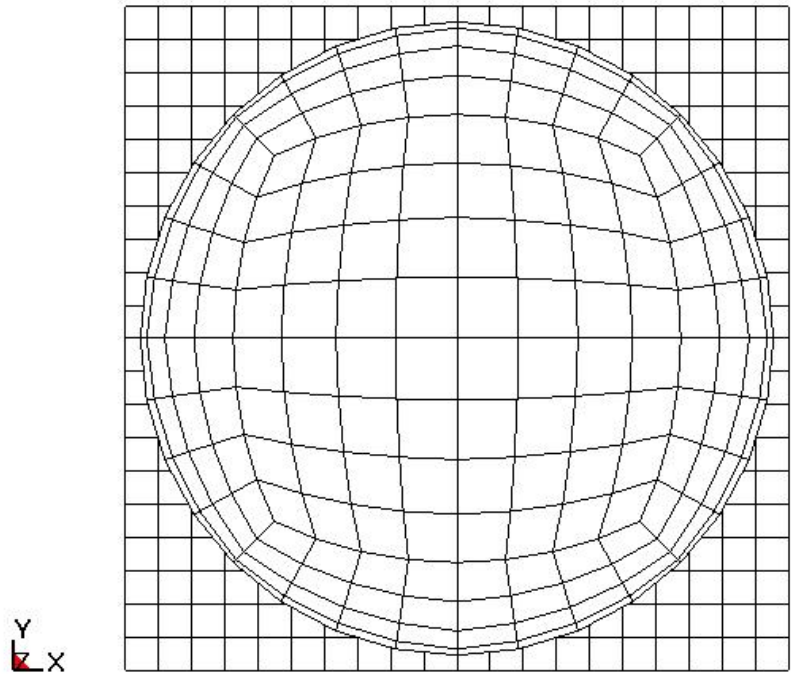

Figure 3.5: Top view of standard mesh density containing 2816 and 400 elements in the ball and flat plate, respectively.

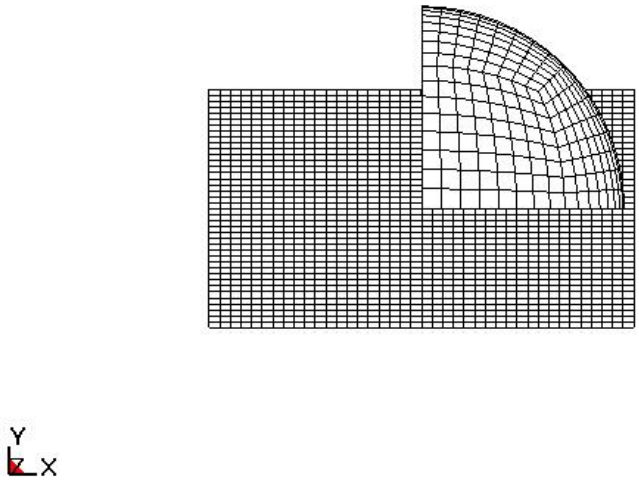

Figure 3.6: Top view of fine mesh density. The ball has 4096 elements and the flat plate has 1600 elements.

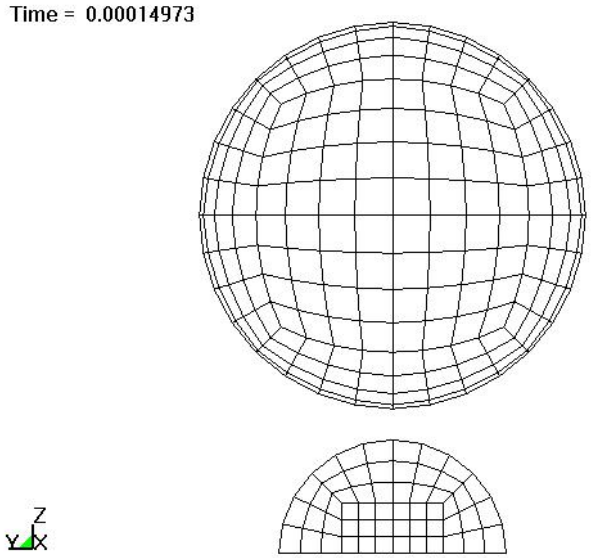

Figure 3.7: Standard mesh density of cylindrical impact surface model.

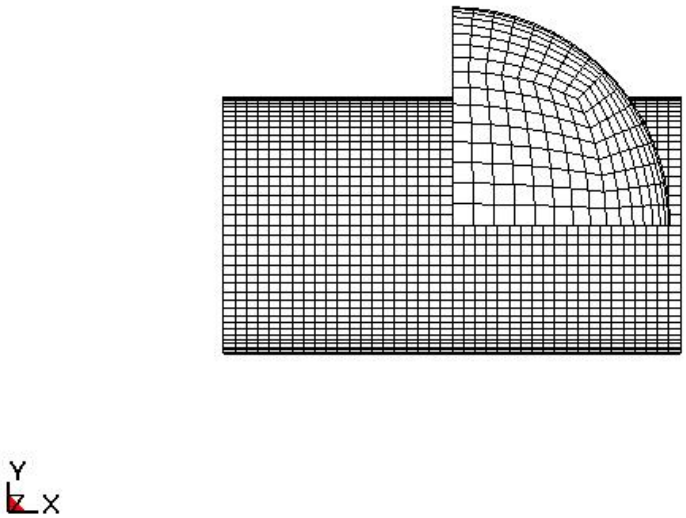

Figure 3.8: Top view of fine mesh density of cylindrical impact surface and softball model.

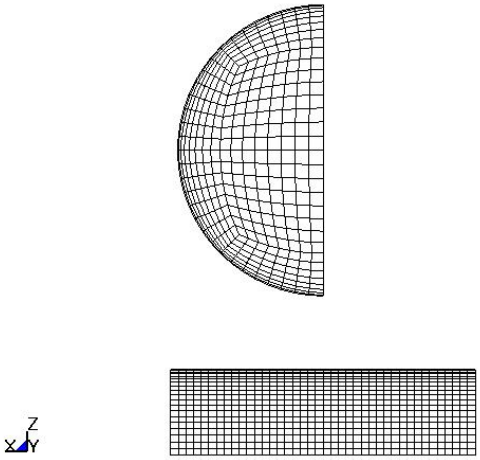

Figure 3.9: Side view of fine mesh density of the cylindrical impact surface and softball.

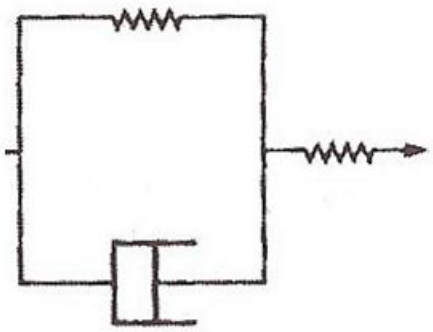

Figure 3.10: Spring in parallel with a spring and damper (three parameter solid).

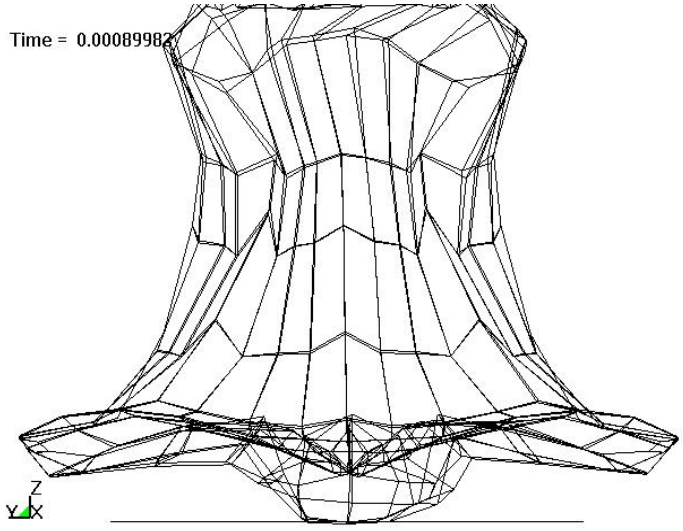

Figure 3.11: Picture of an unstable model.

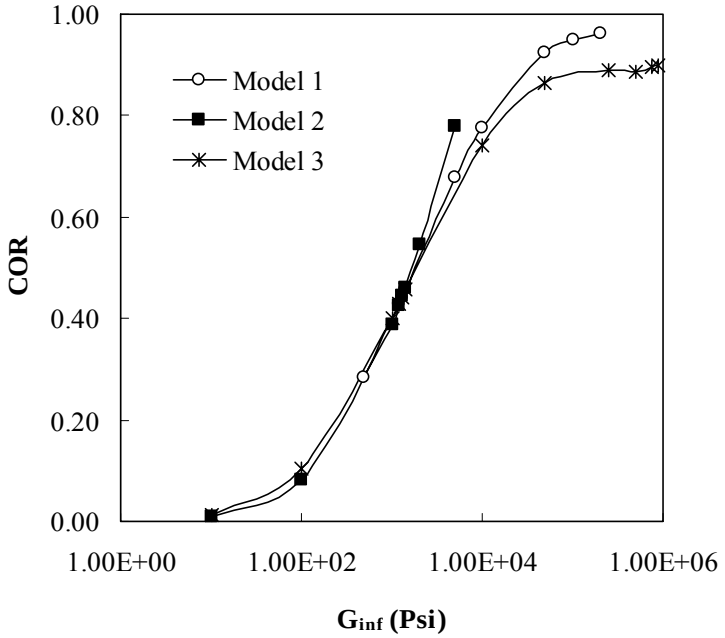

Figure 3.12: COR vs. G_∞ (logarithmic scale) with all other parameters from each model held constant.

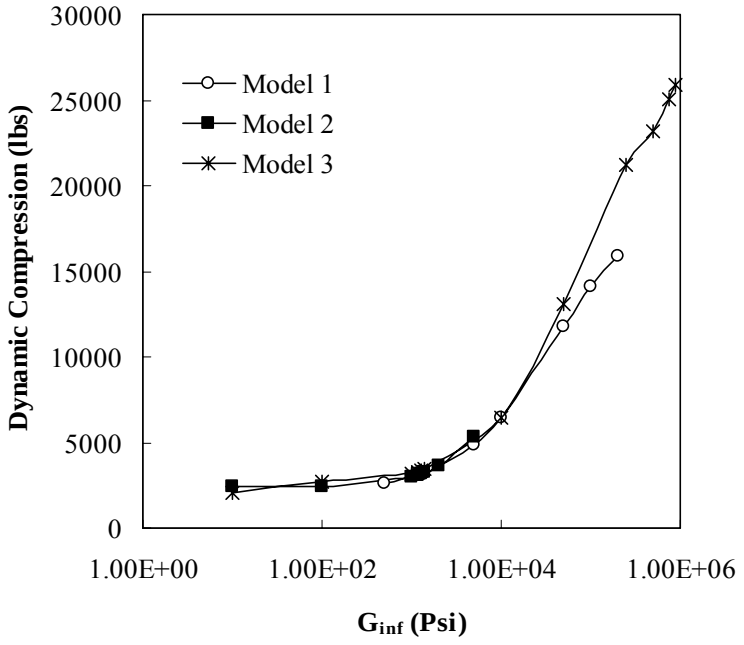

Figure 3.13: Dynamic compression vs. G_∞ (logarithmic scale) with all other parameters from each model held constant.

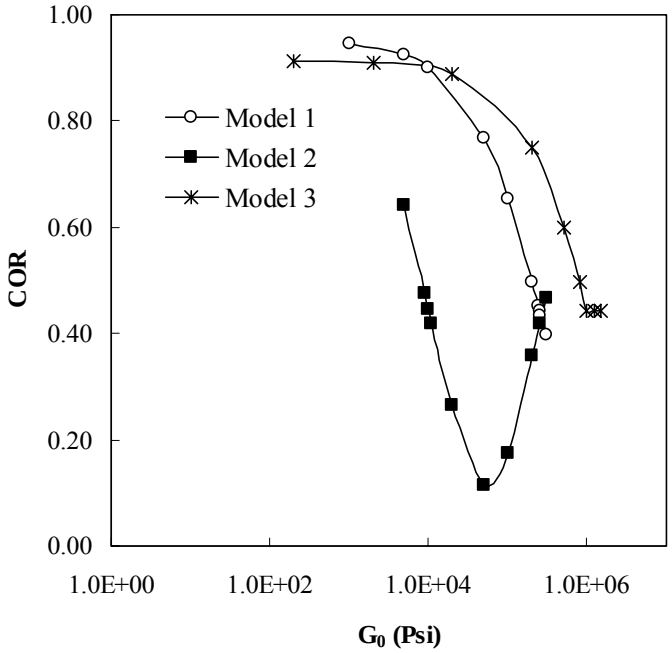

Figure 3.14: COR vs. G_0 (logarithmic scale) with all other parameters from each model held constant.

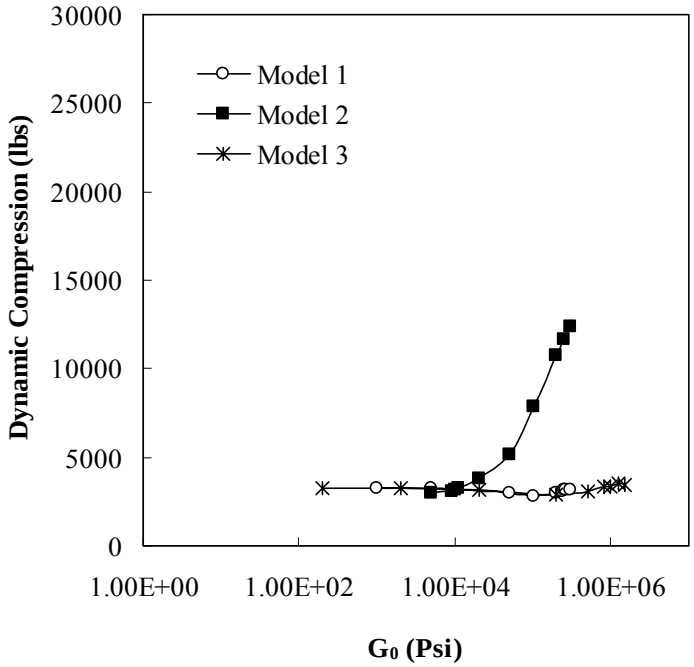

Figure 3.15: Dynamic compression vs. G_0 (logarithmic scale) with all other parameters from each model held constant.

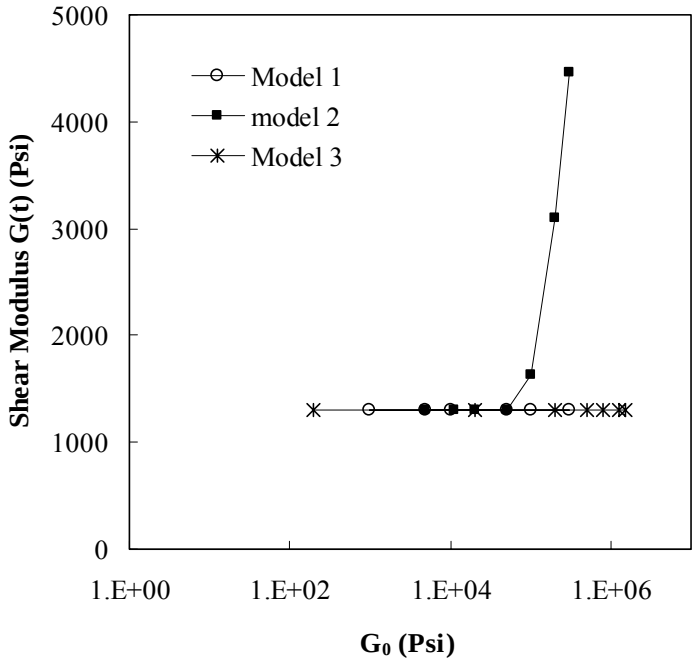

Figure 3.16: Shear modulus vs. the short term shear modulus G_0 for models 1, 2, and 3 with all other parameters from each model held constant. The shear modulus was evaluated at half of the contact time $t = 0.5t_c$.

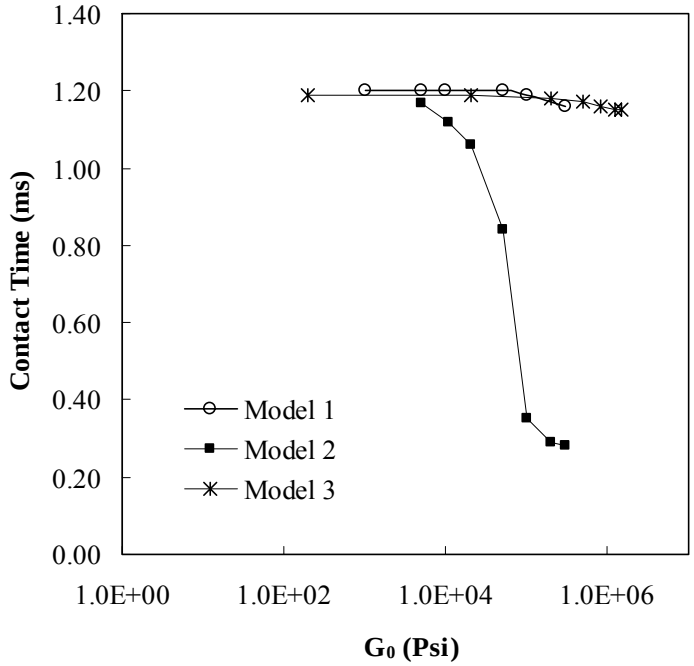

Figure 3.17: Contact time vs. the short term shear modulus G_0 for models 1, 2, and 3 with all other parameters from each model held constant.

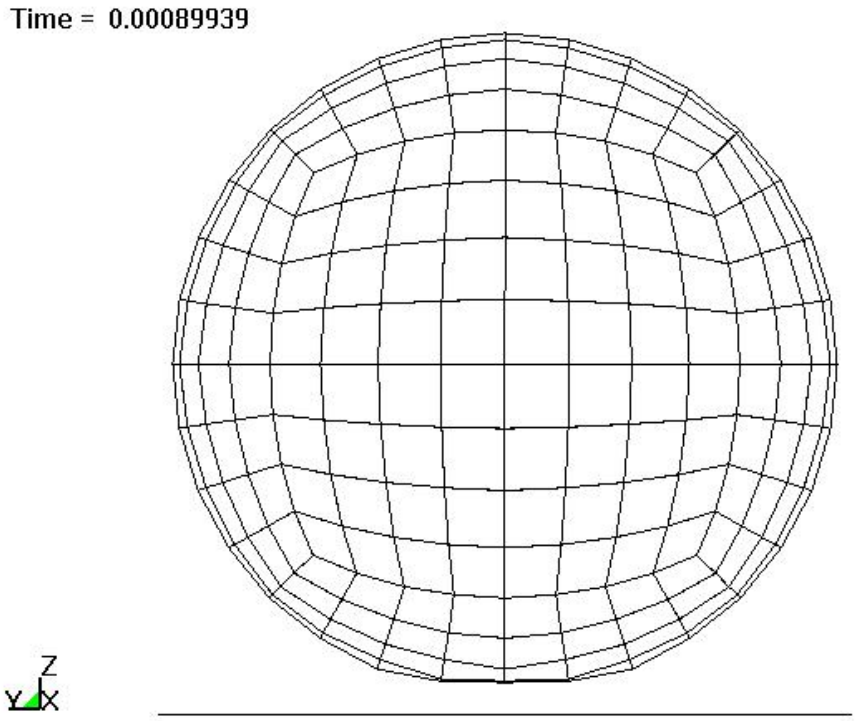

Figure 3.18: Model 2 with $G_0 = 300{,}000$ psi. The contact surface of the ball remains flat after impact.

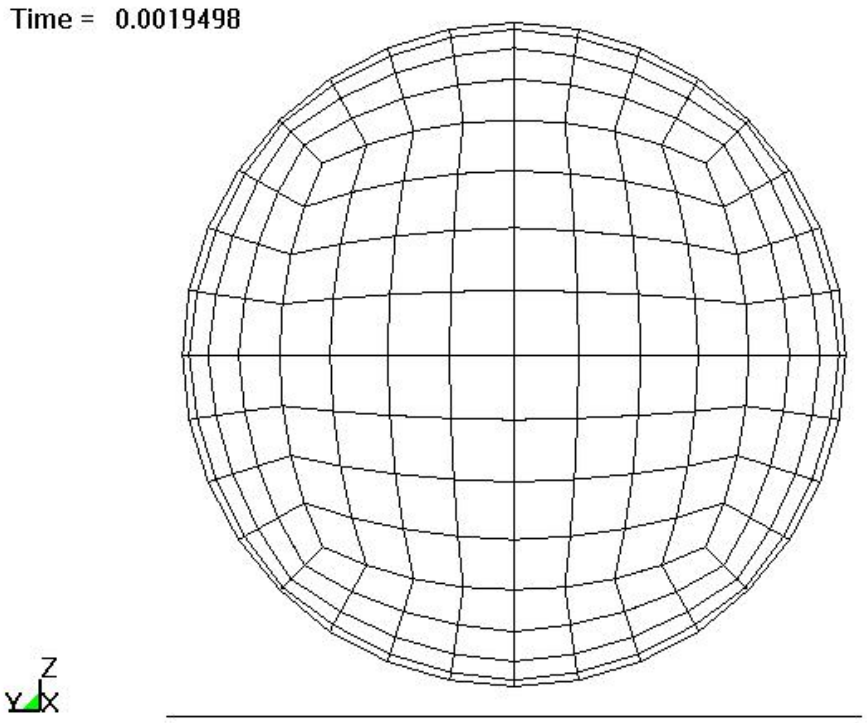

Figure 3.19: Contact surface of typical ball that returns to round after impact.

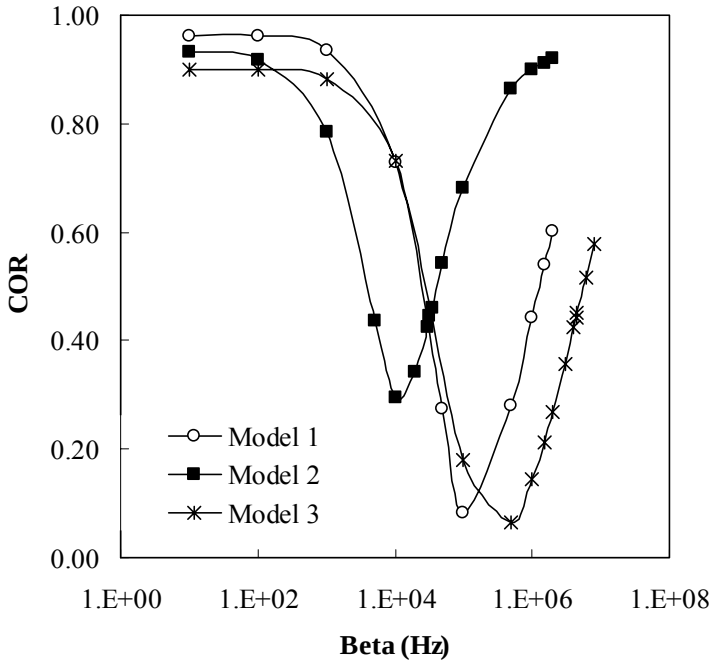

Figure 3.20: COR vs. decay constant β (logarithmic scale) with all other parameters from each model held constant.

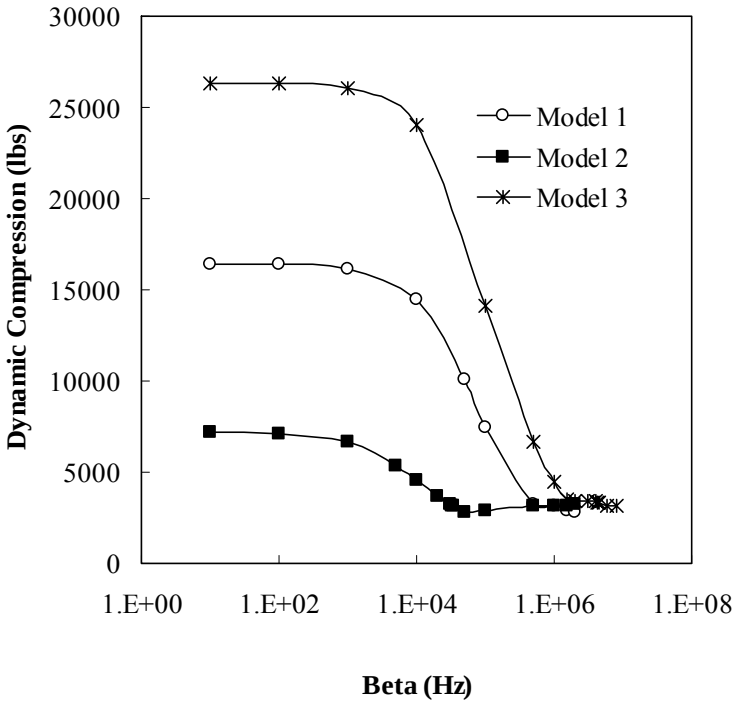

Figure 3.21: Dynamic compression vs. decay constant β (logarithmic scale) with all other parameters from each model held constant.

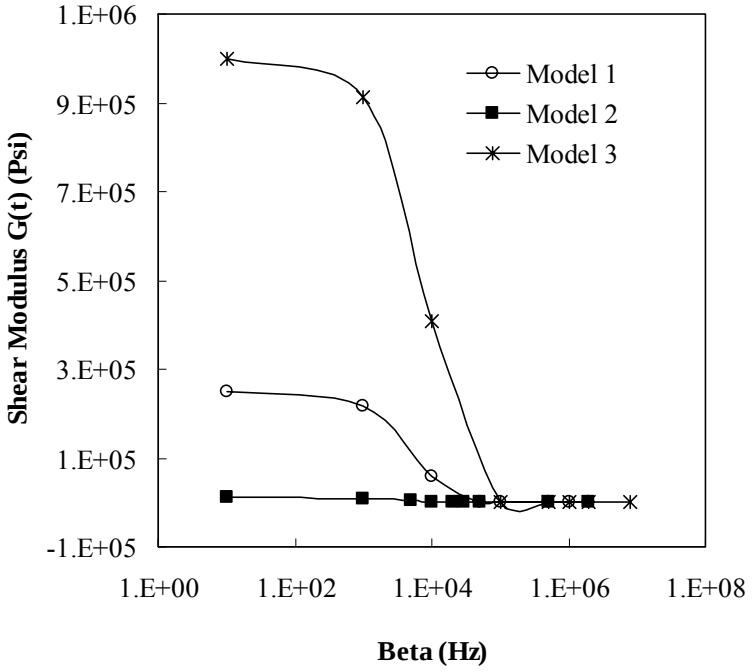

Figure 3.22: Shear modulus vs. the decay constant β (logarithmic scale) for models 1, 2, and 3. The remaining parameters from each model were held constant. The shear modulus was evaluated at half of the contact time $t = 0.5t_c$.

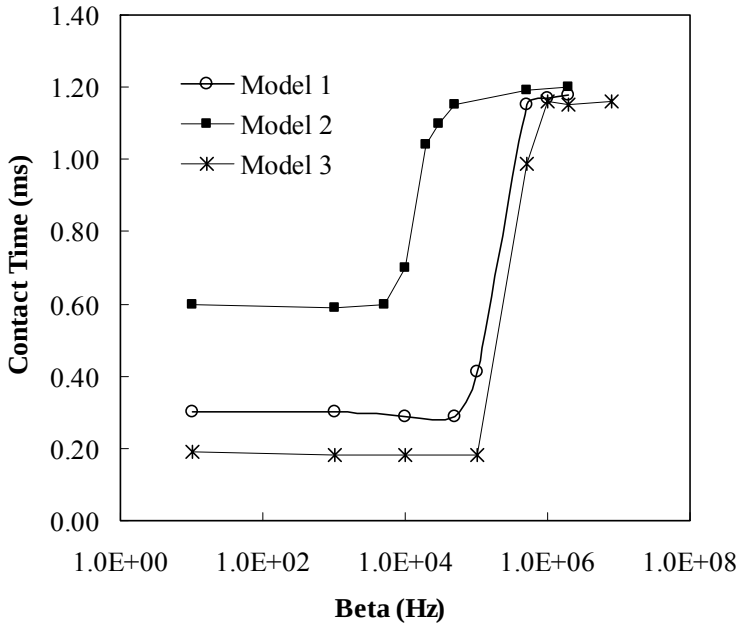

Figure 3.23: Contact time vs. the decay constant β (logarithmic scale) for models 1, 2, and 3. The remaining parameters from each model were held constant.

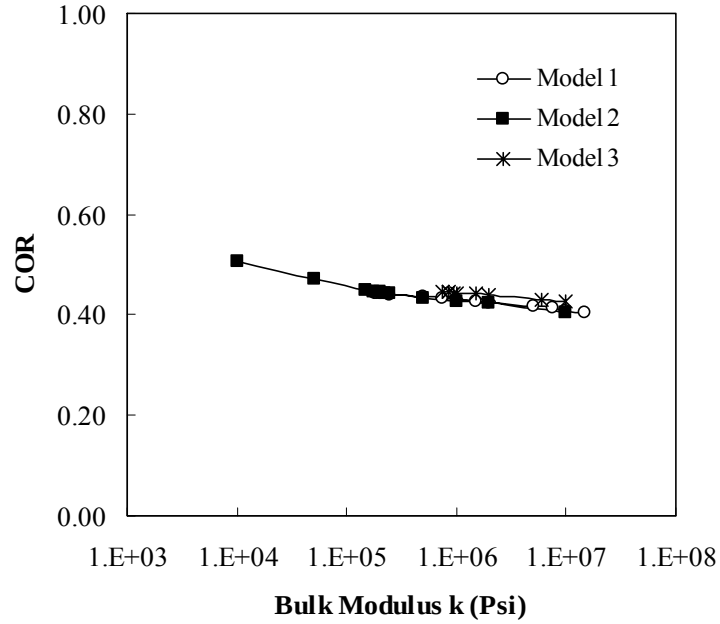

Figure 3.24: COR vs. bulk modulus k (logarithmic scale) with all other parameters from each model held constant.

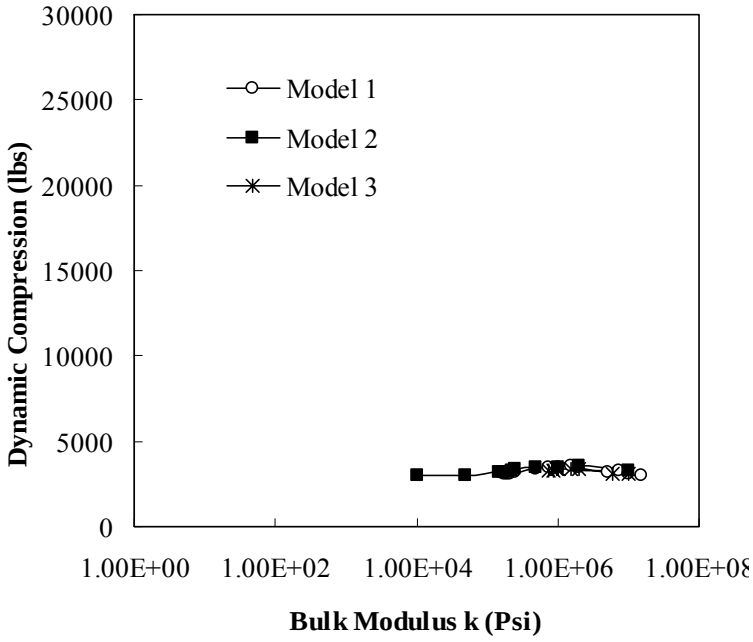

Figure 3.25: Dynamic compression vs. bulk modulus k (logarithmic scale) with all other parameters from each model held constant.

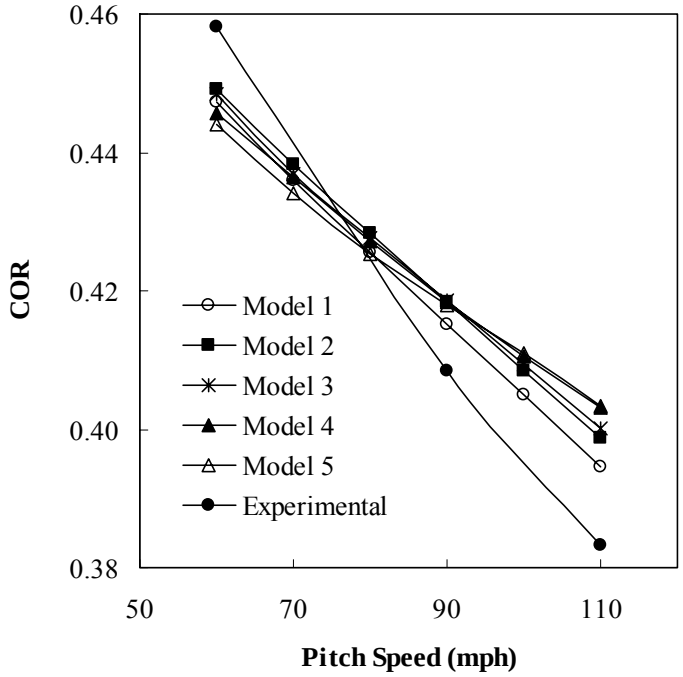

Figure 3.26: COR vs. pitch speed for finite element models 1-5 and experimental data of one dozen 44/375 balls.

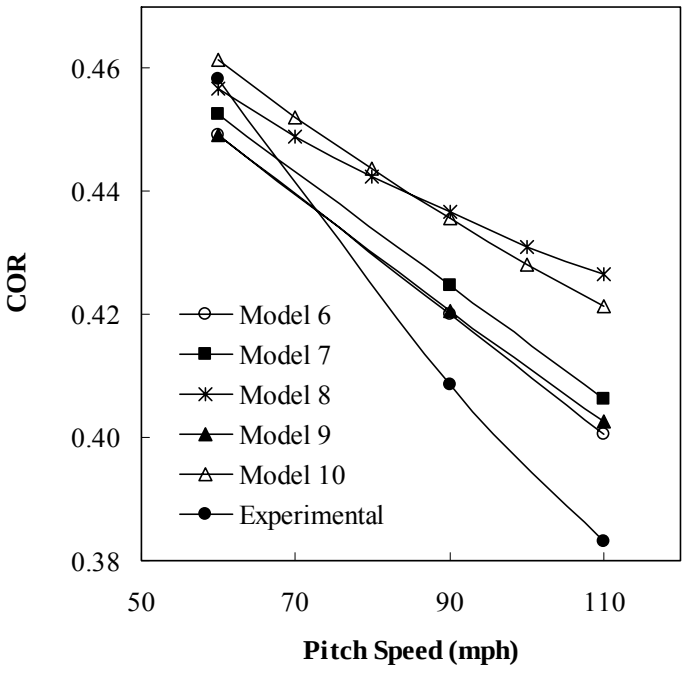

Figure 3.27: COR vs. pitch speed for finite element models 6-10 and experimental data of one dozen 44/375 balls.

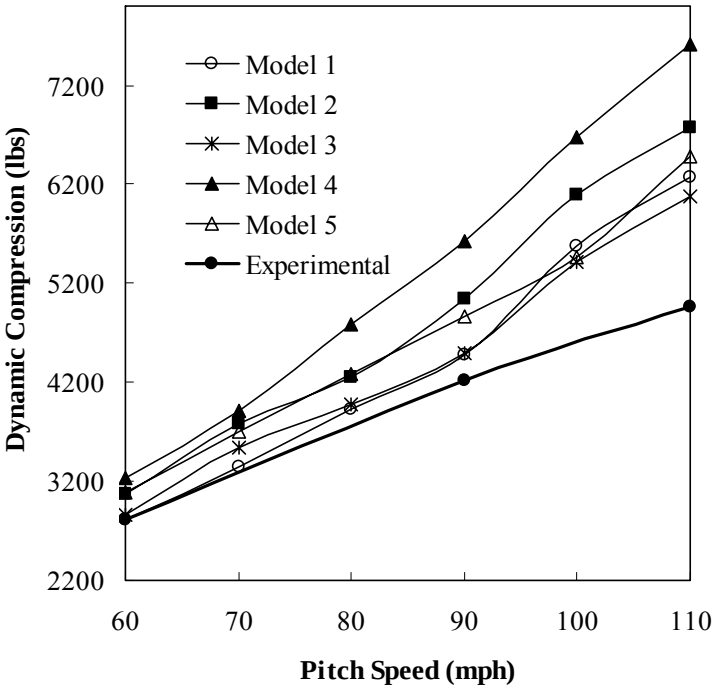

Figure 3.28: Dynamic compression vs. pitch speed for finite element models 1-5 and experimental data of one dozen 44/375 balls.

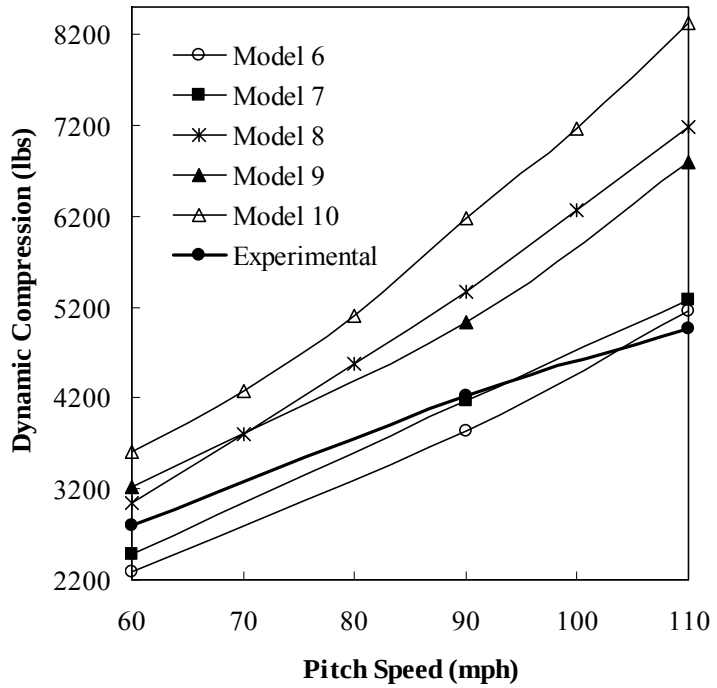

Figure 3.29: Dynamic compression vs. pitch speed for finite element models 6-10 and experimental data of one dozen 44/375 balls.

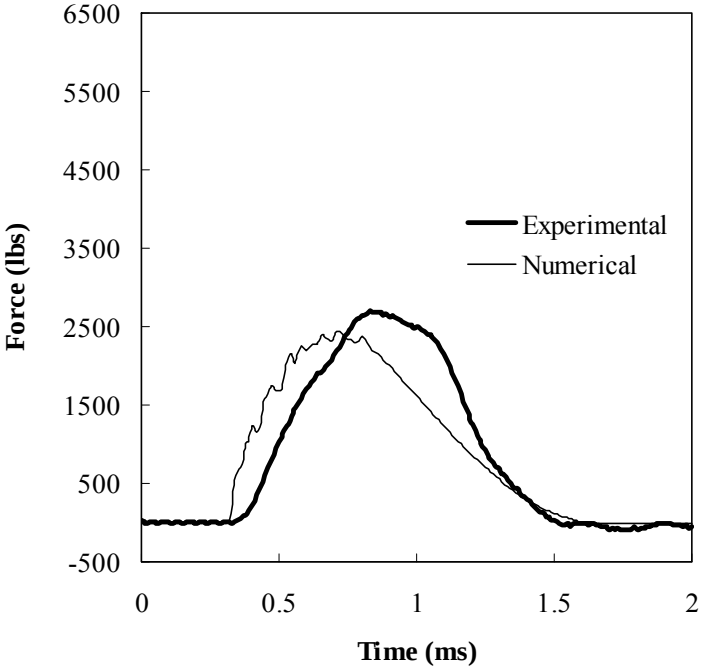

Figure 3.30: Force vs. time for experimental and numerical data for a 60 mph pitch speed against a rigid flat plate.

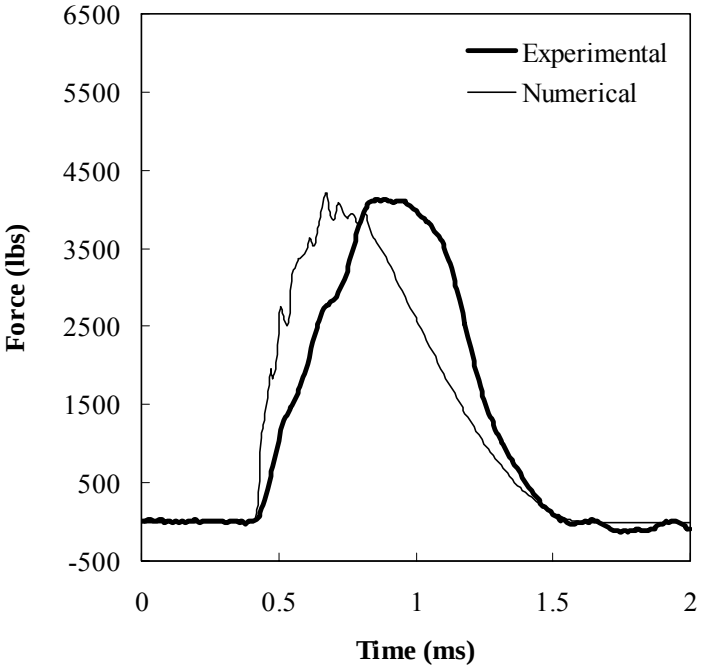

Figure 3.31: Force vs. time for experimental and numerical data for a 90 mph pitch speed against a rigid flat plate.

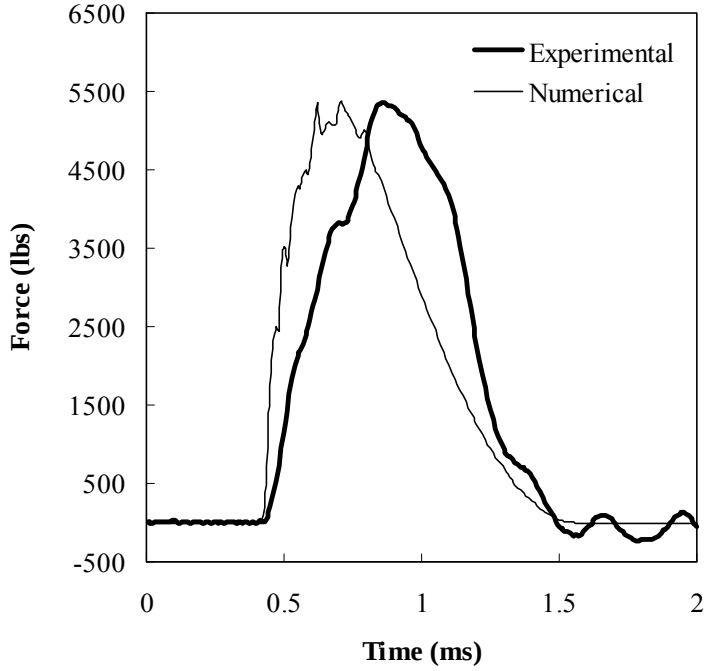

3.32: Force vs. time for experimental and numerical data for a 110 mph pitch speed against a rigid flat plate.

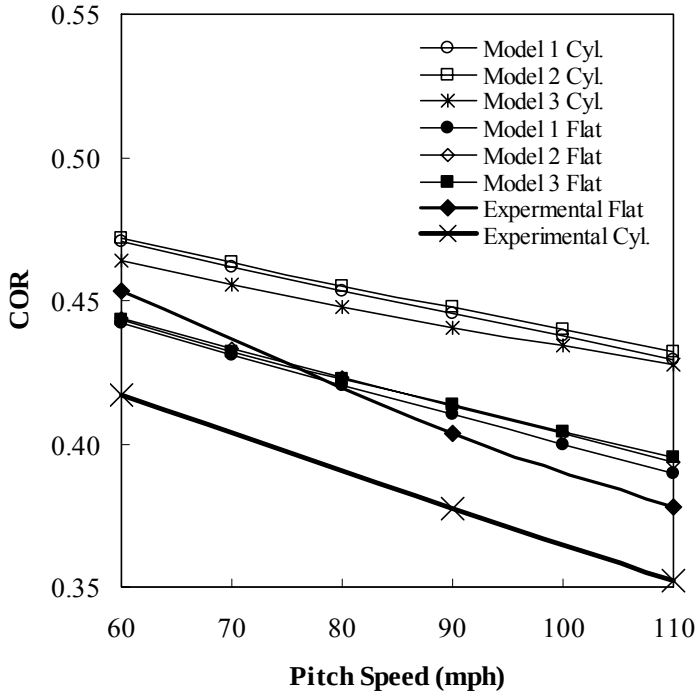

Figure 3.33: COR vs. pitch speed for softball models 1,2, and 3 impacting a cylindrical and flat impact surface. The experimental data is shown for comparison.

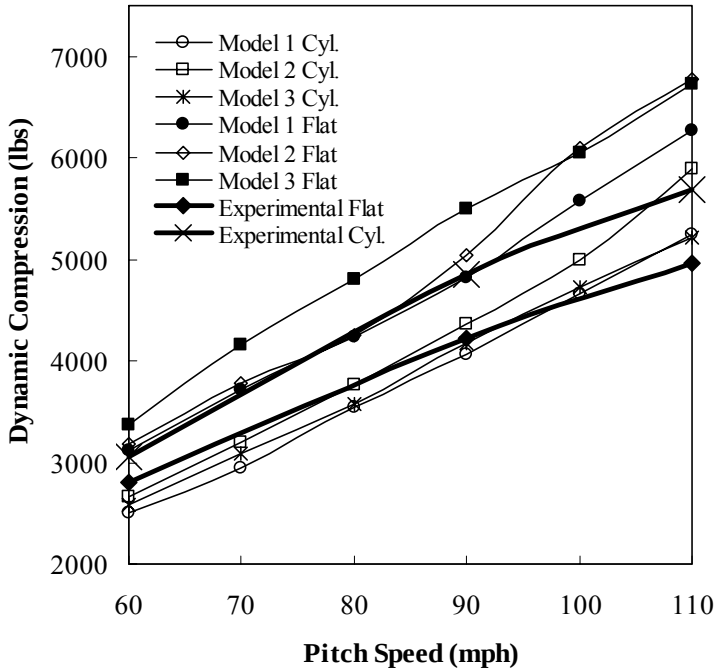

Figure 3.34: Dynamic compression vs. pitch speed for softball models 1,2, and 3 impacting a cylindrical and flat impact surface. The experimental data is shown for comparison.

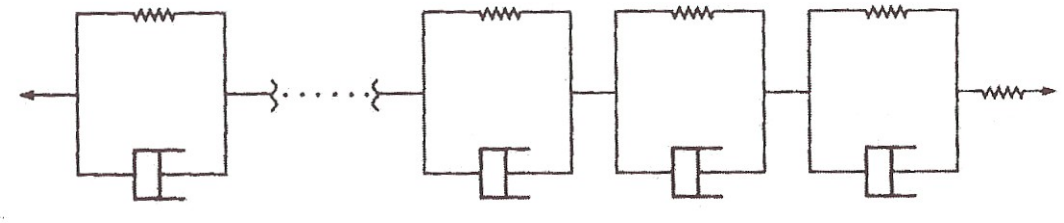

Figure 3.35: Diagram of the Maxwell elements in a Prony series.

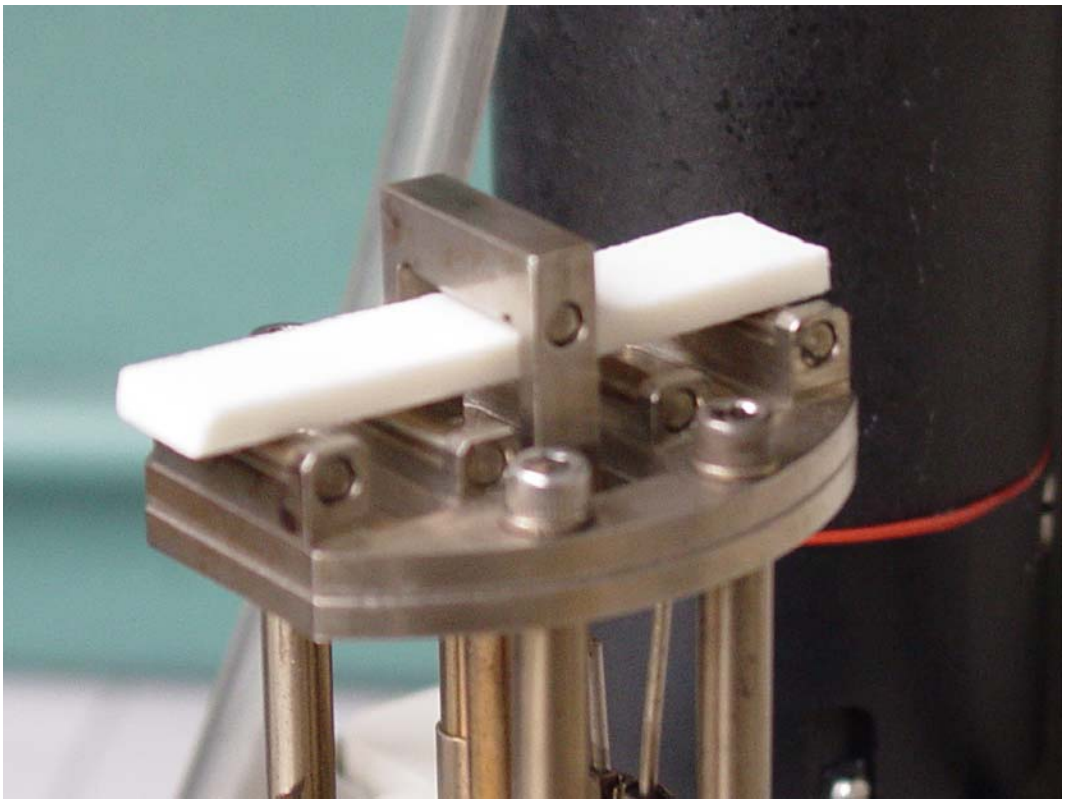

Figure 3.36: Picture of the three point bending fixture with the softball core specimen.

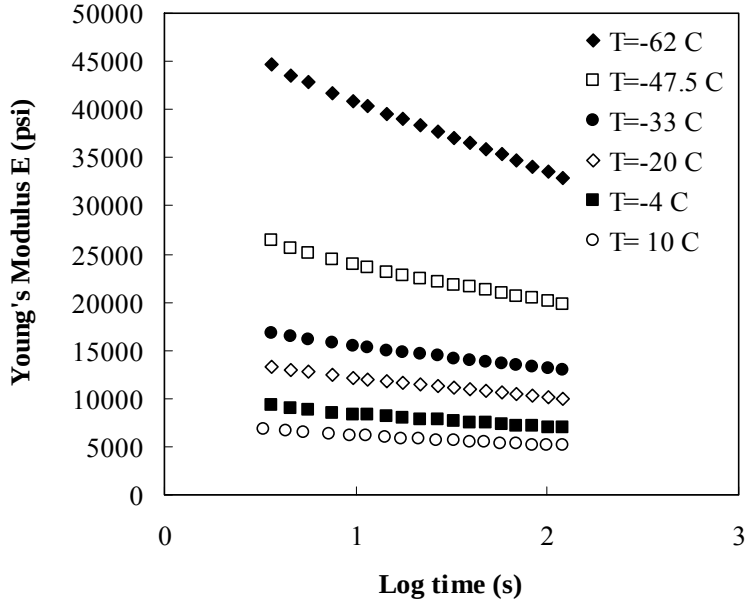

Figure 3.37: Unshifted stress relaxation data for various temperatures.

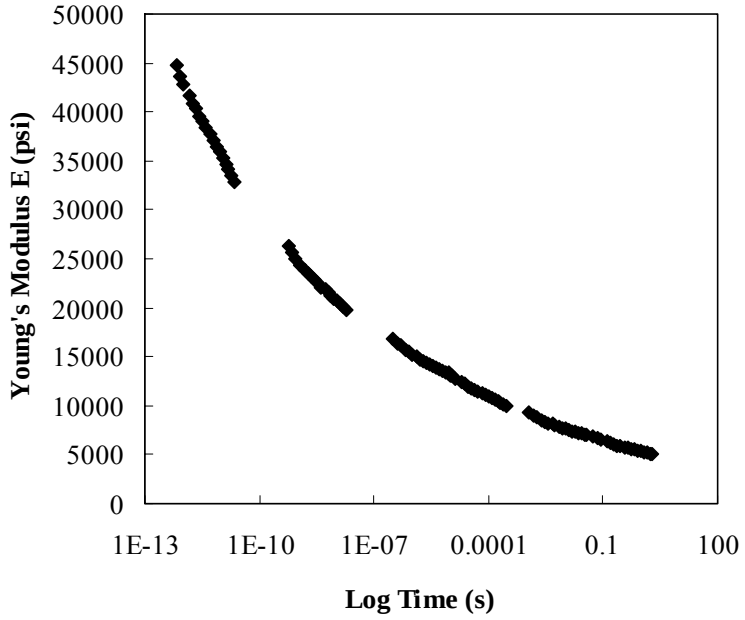

Figure 3.38: Master curve of stress relaxation data shifted according to the WLF equation.

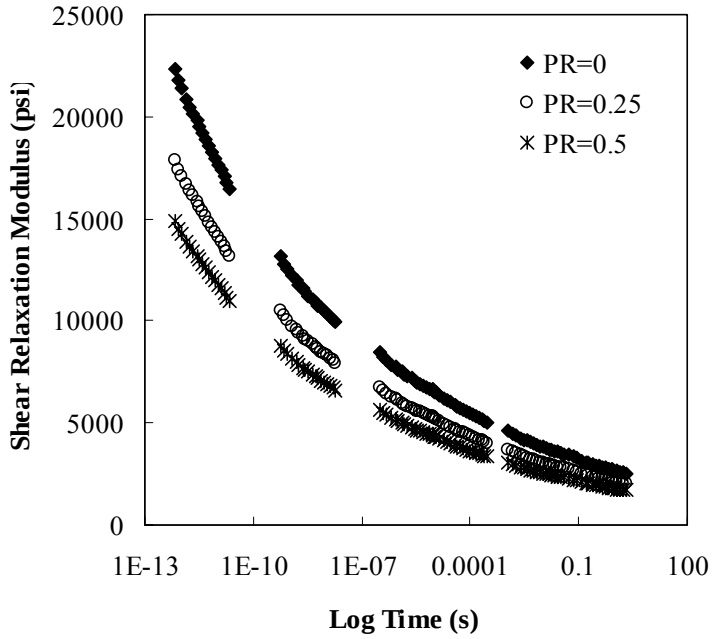

Figure 3.39: Shear relaxation modulus vs. time (logarithmic scale) for three values of the Poison's ratio.

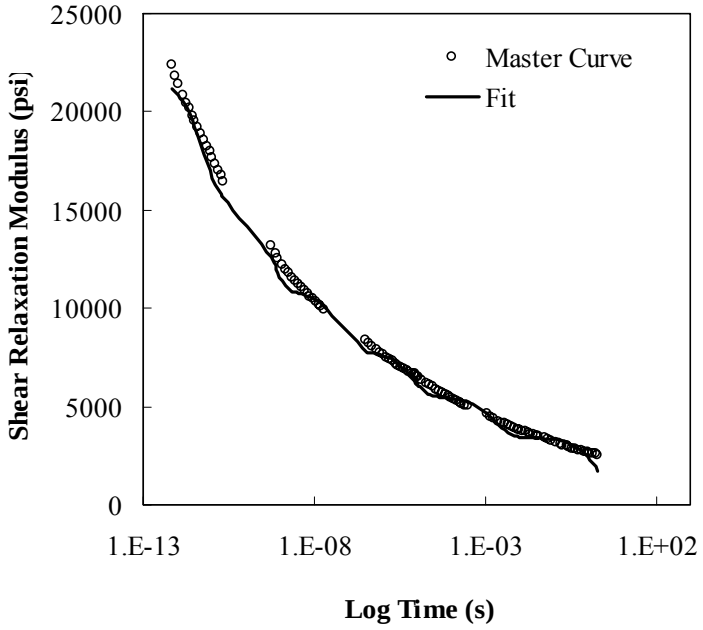

Figure 3.40: Typical MathCad curve fit for master curve data. The master curve is for a Poisson's ratio of 0.0.

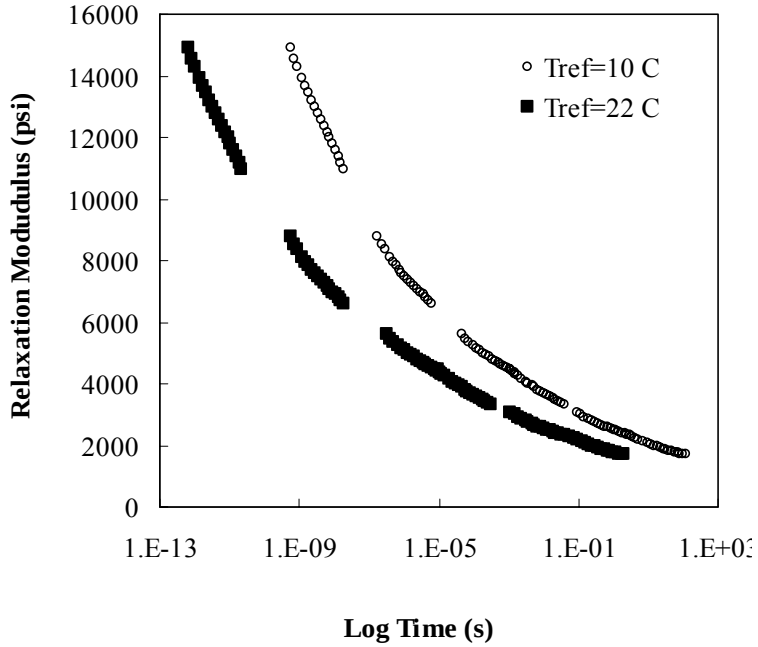

Figure 3.41: Shear relaxation modulus vs. time (logarithmic scale) for two different reference temperatures. A Poisson's ratio of ½ was assumed as it appeared to give the best results.

CHAPTER FOUR

SUMMARY AND FUTURE WORK

4.1 Summary

4.1.1 Experimental Results

The softball can have a large effect on bat performance. Performance limits have been placed on the softball bats by regulating agencies. There is a need, therefore, to characterize the properties of the softball as accurately as possible. The two properties currently used to characterize a softball are the COR and static compression. There is concern that these methods may not adequately describe the viscoelastic softball.

A cannon was built that is capable of firing softballs accurately and without spin at speeds ranging from 0-150 mph. The pitch and rebound speeds were measured using three light curtains. The cannon was used in this work to measure the COR and dynamic compression as a function of speed, geometry, time, and environment.

A dynamic hardness test was developed that used load cells to measure the impact force versus time. A strain gage load cell was initially investigated, but due to electrical noise and vibrational effects, a piezoelectric load cell was used. Dynamic compression was taken as the peak force in the force vs. time curve. Simultaneous measurements of the dynamic compression and COR were shown to be feasible, and the compliance of the load cell was shown to have a negligible effect on the COR measurements.

A nearly linear correlation was observed between static and dynamic ball hardness. This correlation only appears to be valid for balls of similar design and static hardness. It is not appropriate, for example, to estimate the dynamic hardness of a 44/525 ball from the results of a

44/375 ball. Also, an offset in the correlation was observed that is associated with the ball momentum. The dynamic compression appeared to increase proportionally with increasing pitch speed. The momentum change measured from the impulse of the impact was in good agreement with that from the light curtains.

The COR was observed to decrease proportionally with speed. The decrease in the COR is attributed to increased deformation of the ball at higher speeds. Since the ball COR is only measured at one speed, the slope of the COR vs. pitch speed can be manipulated by the ball manufacturers. Having COR requirements at more than one speed would eliminate this opportunity. It appears that the ball momentum change in a 60 mph rigid wall impact is significantly less than occurs in a 110 mph bat-ball impact. An increased COR pitch speed of 75 mph is recommended to reconcile this difference.

A multi layer ball has recently been introduced that shows the necessity of updating the current ball testing procedures. This multi layered ball conforms to current ASTM softball COR and static compression requirements, but was observed to increase the BBS by 6.5 mph. The dynamic compression of this ball was observed to be 13.9% higher than that of a traditional ball. Also, a ½" static compression test was able to better characterize the hardness of the multi layer ball than the typical ¼" test.

A cylindrical impact surface was shown to reduce the COR and dynamic compression and increase the contact time. The reduction in the COR and dynamic compression is associated with increased local deformation in the ball due to the reduced contact area. The cylindrical impact surface reduced the slope of the COR vs. pitch speed. Equating the momentum change for a 110 mph bat-ball impact with that of the cylindrical impact surface results in an 80 mph pitch speed.

The softball COR and dynamic compression were observed to decrease due to test induced heating. A maximum testing frequency of 10 impacts per hour is recommended to minimize this effect. A recoverable viscoelastic effect was apparent when the first impact of a balls surface was compared to subsequent impacts of that surface. The static compression was observed to depend on the moisture content as well as temperature. The COR and dynamic compression did not appear to be affected by the moisture content of the ball. This suggests that the rate effects of softballs may be dependent on their moisture content.

It was determined that the cover of the softball had a measurable effect on the COR and dynamic compression. The COR was observed to increase by 4.2% and the dynamic compression was observed to decrease by 16.6% when the cover was removed. These changes are primarily due to the weight of the cover and stitches, which account for 21% of the ball's mass.

Bat performance measures are currently normalized for ball weight and COR to account for differences from one ball to the next. A normalizing study showed that the current COR normalizing procedure is not valid. However, the study did reveal that normalizing for ball weight is appropriate. It was also found that increasing ball hardness has the effect of increasing bat performance, especially for high performing bats. Ball hardness cannot be normalized due to its dependence on bat performance level.

4.1.2 Numerical Results

While many baseballs models have been developed in the past, the softball has received very little attention. In this research, a Power law model and a more general Prony series viscoelastic model of the softball were studied using finite element analysis. The COR and dynamic compression rate dependence were examined for each viscoelastic model. Also, the

parameters of the Power Law model were investigated to determine the effect of each parameter on the COR and dynamic compression.

The four parameters of interest in the parameter study were the long term shear modulus, the short term shear modulus, the decay constant, and the bulk modulus. Three of the four parameters were held constant while a fourth was varied over several decades. The COR and dynamic compression were recorded for each model variation. The results of this parameter study can be generalized to any viscoelastic impact situation.

The COR and dynamic compression were observed to increase proportionally to the long term shear modulus. The behavior of the COR and dynamic compression vs. short term shear modulus was observed to be dependent on the value of the decay constant. Small values of the decay constant caused the COR vs. short term shear modulus to have a minimum value while the dynamic compression was observed to increase linearly. Large values of the decay constant caused the COR to decrease until a constant value was reached and the dynamic compression remained approximately constant. Varying the decay constant caused the COR to have a local minimum value and the dynamic compression to decrease. The bulk modulus was seen to have a very small effect on the COR and dynamic compression, and should therefore be used for fine tuning a model.

While performing the parameter study of the Power law model, ten parameter combinations were found that fit experimental COR and dynamic compression data for a 60 mph impact. Each of these models were tested at several speeds to determine the ability of the model to describe the rate dependent behavior of the softball. It was found that two of these models were in good agreement with experimental rate dependent data for the flat impact surface.

However, none of the models investigated were able to fit the experimental cylindrical impact surface COR data.

DMA of the polymeric core of the softball was used to obtain a master relaxation curve of the shear modulus vs. time. The Prony series was used to fit this experimental master curve, and the resulting Prony coefficients were used in LS-Dyna to model the softball. This technique presented an opportunity to use absolute material properties to model the softball. However, the results of this model did not agree well with experimental results. The COR and dynamic compression were observed to be 100% and 50% higher than experimental results.

The Power law viscoelastic material model appears to have much better correlation with experimental data than the Prony series model. However, the Power law model was unable to describe the cylindrical impact surface. It is recommended, therefore, that the Power law model of the ball be calibrated on a cylindrical impact surface prior to use in a bat-ball collision model.

4.2 Future Work

4.2.1 Experimental

It was shown that current methods of softball testing are not adequate. For changes to be implemented, additional dynamic compression and COR data at several speeds is needed. The effect of the cylindrical impact surface must also be further explored.

The normalizing study showed that the current method of normalizing for softball COR is not valid. A new method to account for differences in the COR is needed. This new method must be experimentally verified using a similar study as described in section 2.10.

4.2.2 Numerical

Although the Power law model was able to describe the softball against a flat plate, its inability to fit experimental cylindrical data suggests that the ball has not been adequately

modeled. It is hypothesized that the Power law model is not capable of describing the ball response when impacting a cylindrical impact surface. Therefore, a different material model needs to be investigated.

It is possible that the stress relaxation curve developed from DMA data is not accurate and that a different type of DMA test could provide better data. Testing from a secondary source is therefore advised, so that the existing relaxation curve can be compared to other data. Also, the master relaxation curve can be shifted along the time axis. It is possible that this technique could result in a better fit to experimental data.

A hyperelastic material model may be able to better characterize the rate dependent softball. This material model requires a relaxation curve as well as a force displacement curve to describe a material. The Prony series is used to fit the relaxation curve. Several foam models exist within LS-Dyna that may be able to describe the response of the softball more accurately.

APPENDIX ONE

Parameter Study Variations

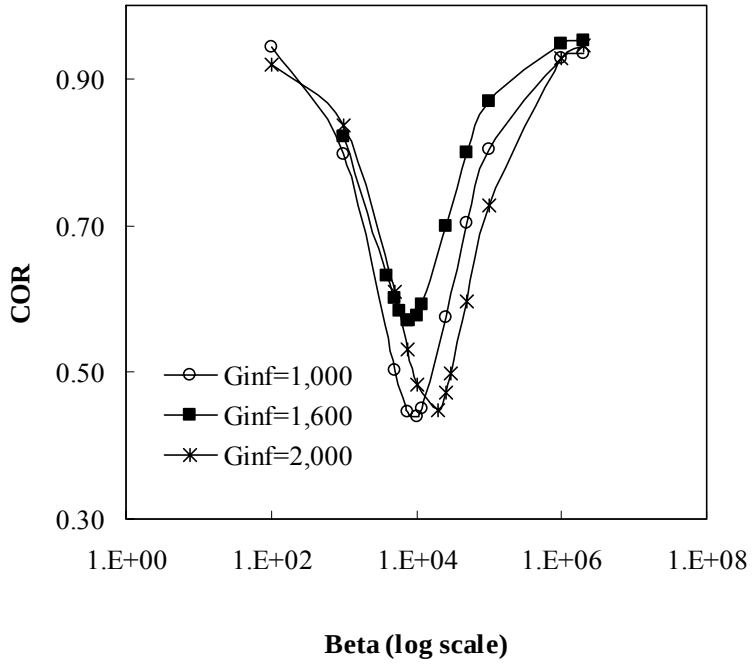

Figure A1.1: Bulk modulus k=10,000 and short term shear modulus G_0=5,000. COR vs. decay constant β for varying G_∞.

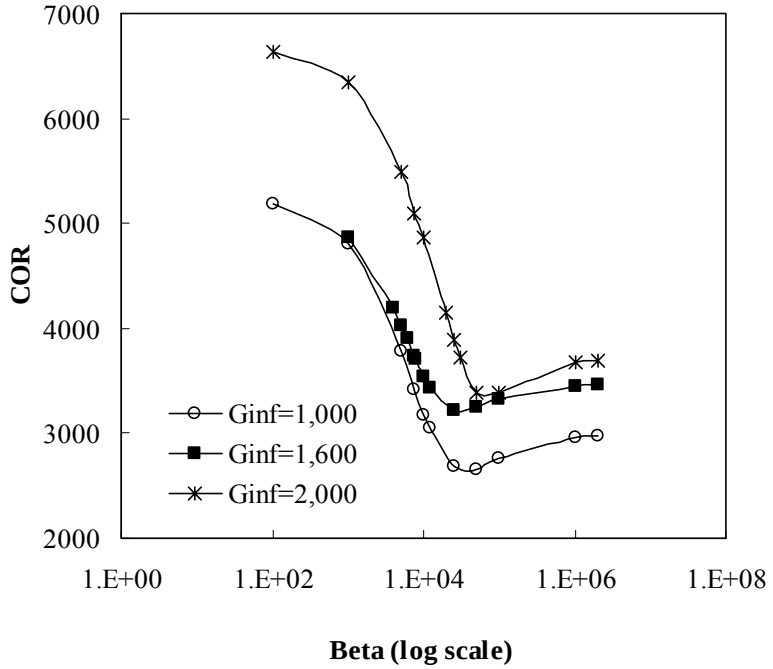

Figure A1.2: Bulk modulus k=10,000 and short term shear modulus G_0=5,000. Dynamic compression vs. decay constant β for varying G_∞.

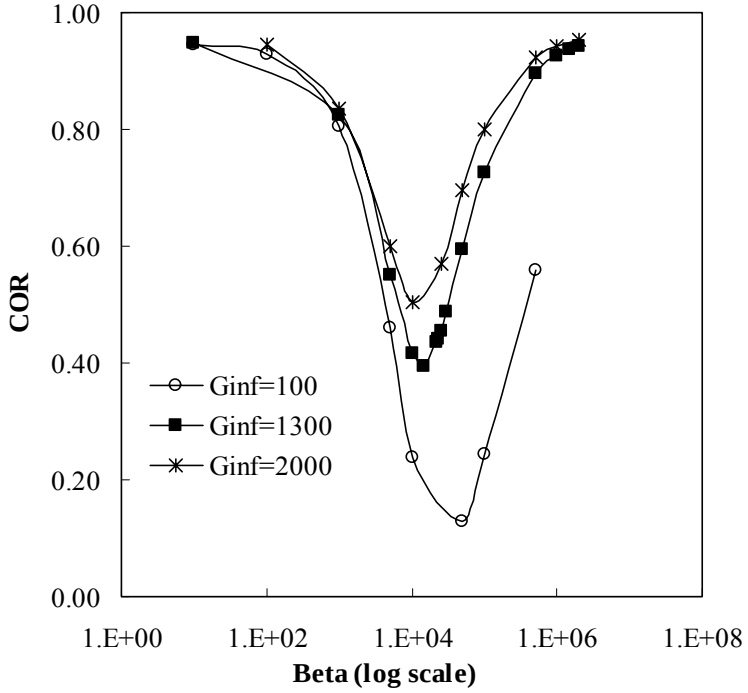

Figure A1.3: Bulk modulus k=10,000 and short term shear modulus G_0=10,000. COR vs. the decay constant β for varying G_∞.

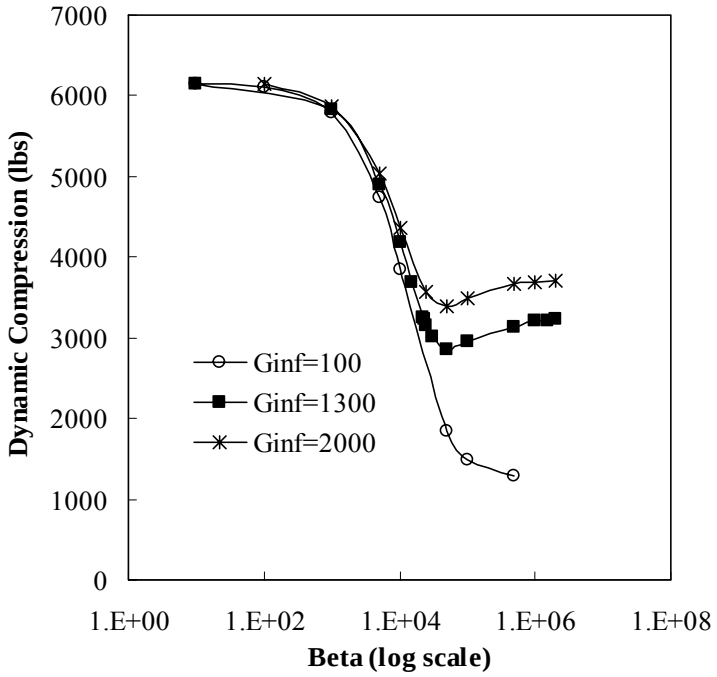

Figure A1.4: Bulk modulus k=10,000 and short term shear modulus G_0=10,000. Dynamic compression vs. the decay constant β for varying G_∞.

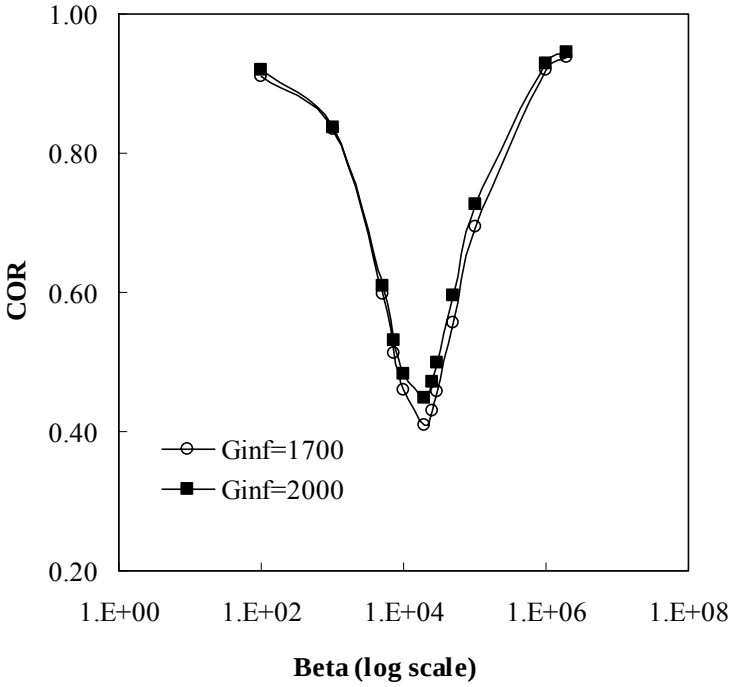

Figure A1.5: Bulk modulus k=10,000 and short term shear modulus G_0=15,000. COR vs. the decay constant β for varying G_∞.

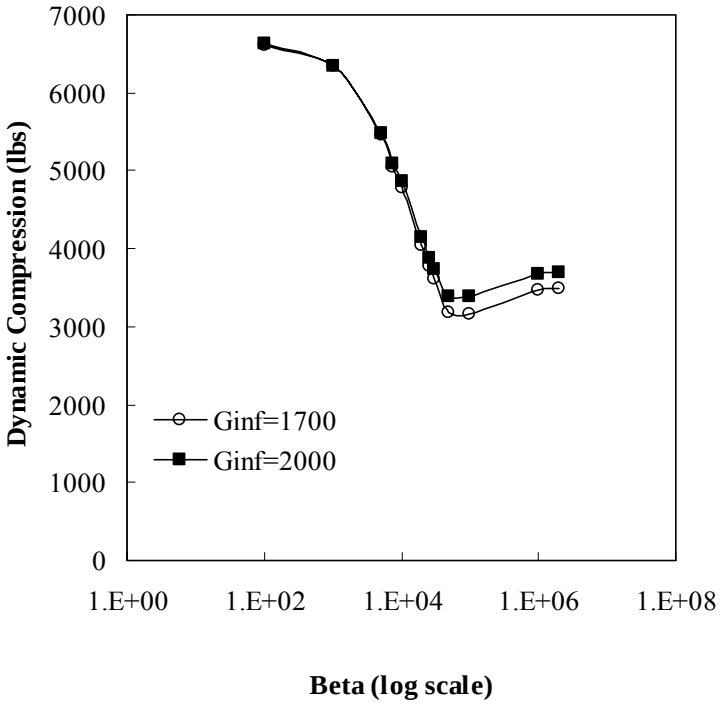

Figure A1.6: Bulk modulus k=10,000 and short term shear modulus G_0=15,000. Dynamic compression vs. the decay constant β for varying G_∞.

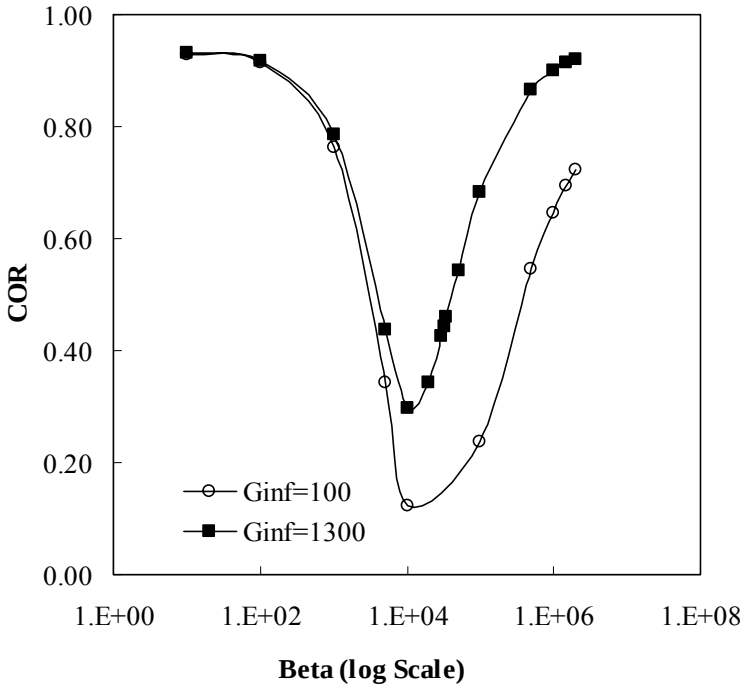

Figure A1.7: Bulk modulus k=200,000 and short term shear modulus G_0=10,000. COR vs. the decay constant β for varying G_∞.

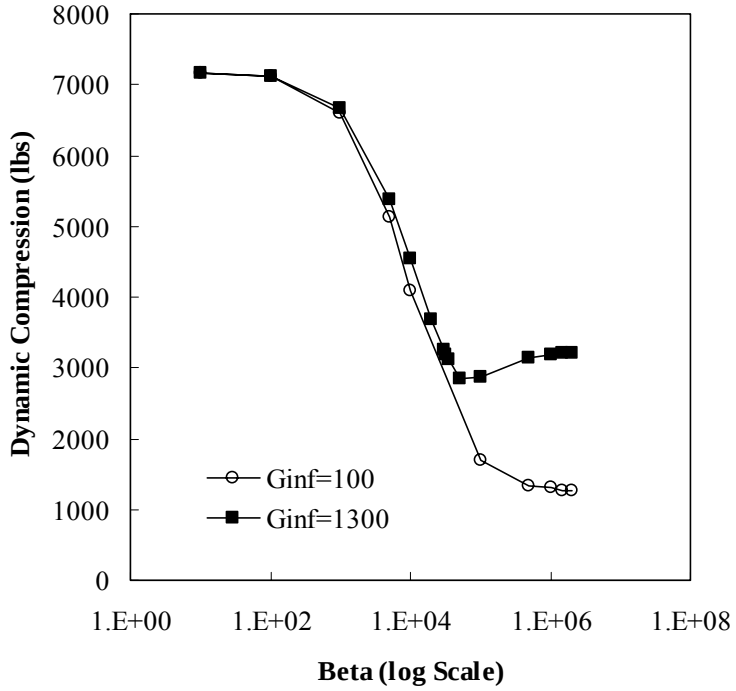

Figure A1.8: Bulk modulus k=200,000 and short term shear modulus G_0=10,000. Dynamic compression vs. the decay constant β for varying G_∞.

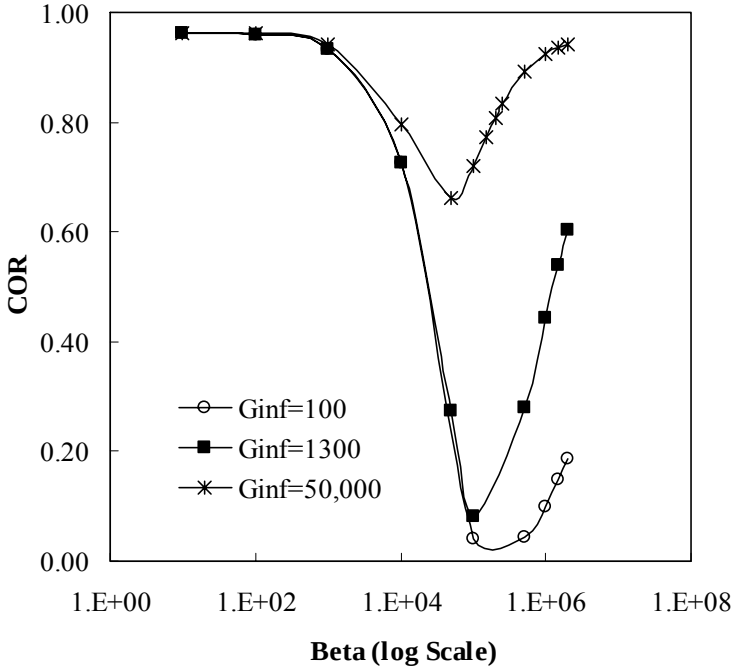

Figure A1.9: Bulk modulus k=200,000 and short term shear modulus G_0=250,000. COR vs. the decay constant β for varying G_∞.

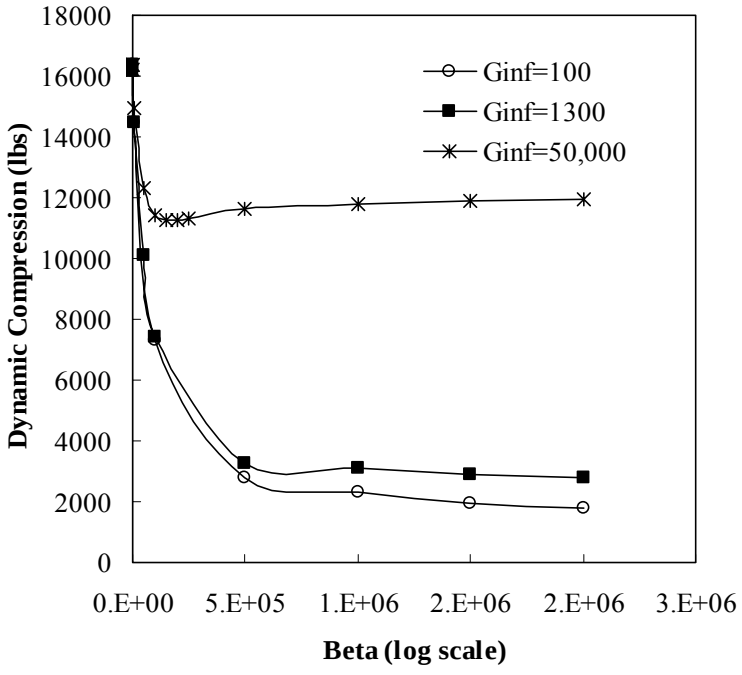

Figure A1.10: Bulk modulus k=200,000 and short term shear modulus G_0=250,000. Dynamic compression vs. the decay constant β for varying G_∞.

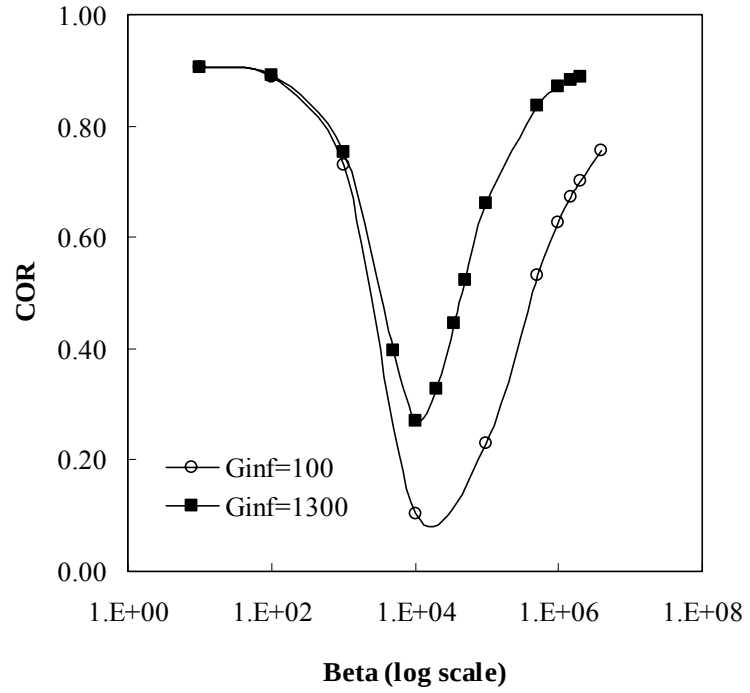

Figure A1.11: Bulk modulus k=1,000,000 and short term shear modulus G_0=10,000. COR vs. the decay constant β for varying G_∞.

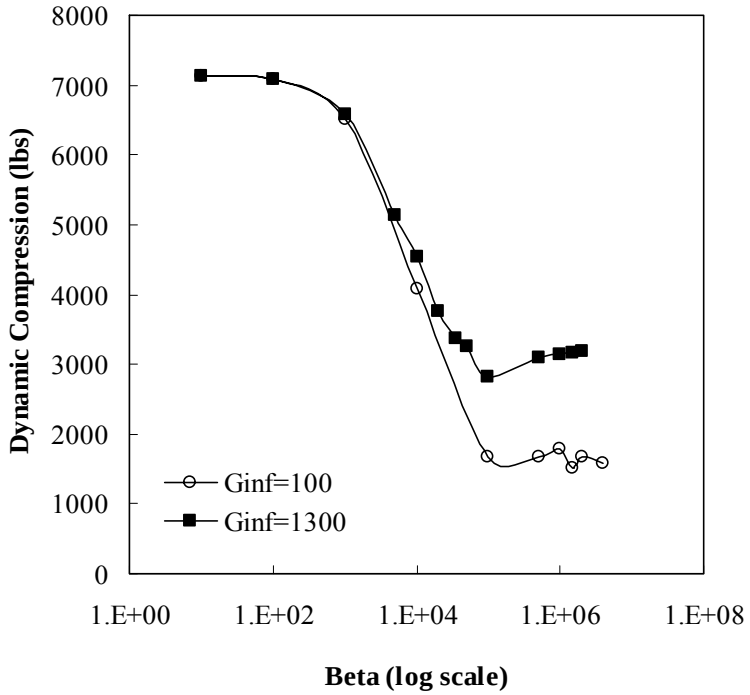

Figure A1.12: Bulk modulus k=1,000,000 and short term shear modulus G_0=10,000. Dynamic compression vs. the decay constant β for varying G_∞.

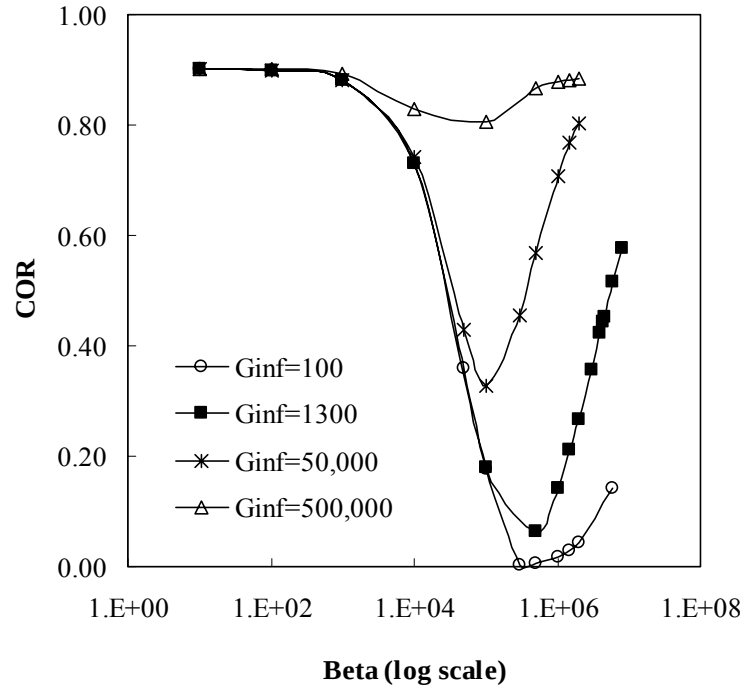

Figure A1.13: Bulk modulus k=1,000,000 and short term shear modulus G_0=1,000,000. COR vs. the decay constant β for varying G_∞.

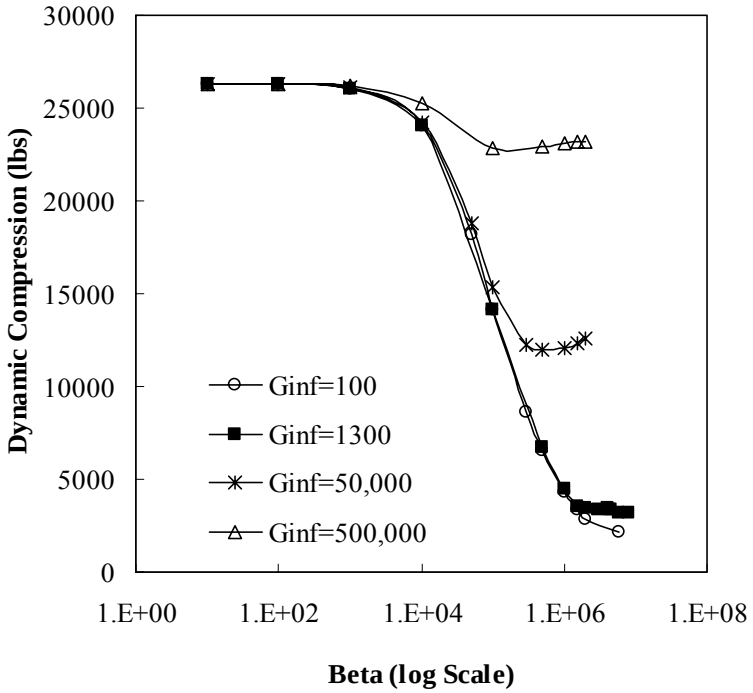

Figure A1.14: Bulk modulus k=1,000,000 and short term shear modulus G_0=1,000,000. Dynamic compression vs. the decay constant β for varying G_∞.

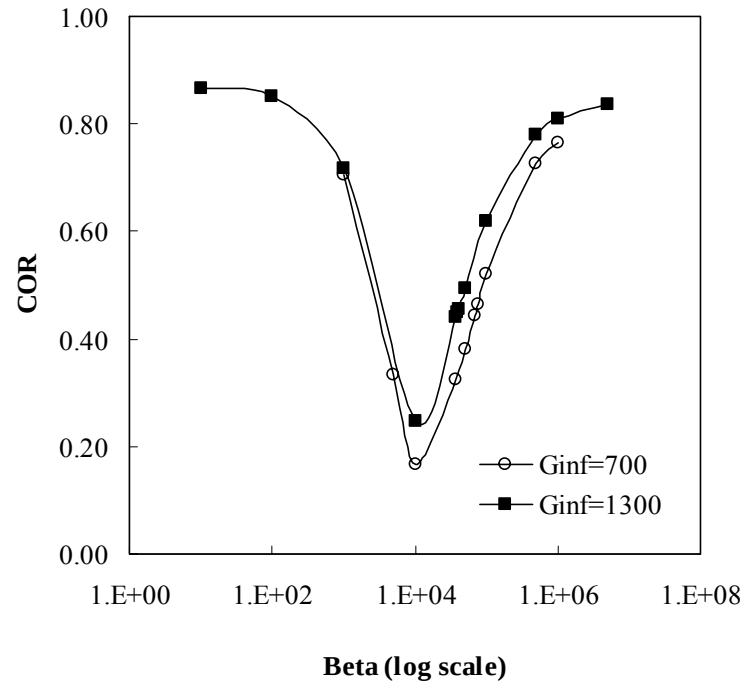

Figure A1.15: Bulk modulus k=10,000,000 and short term shear modulus G_0=10,000. COR vs. the decay constant β for varying G_∞.

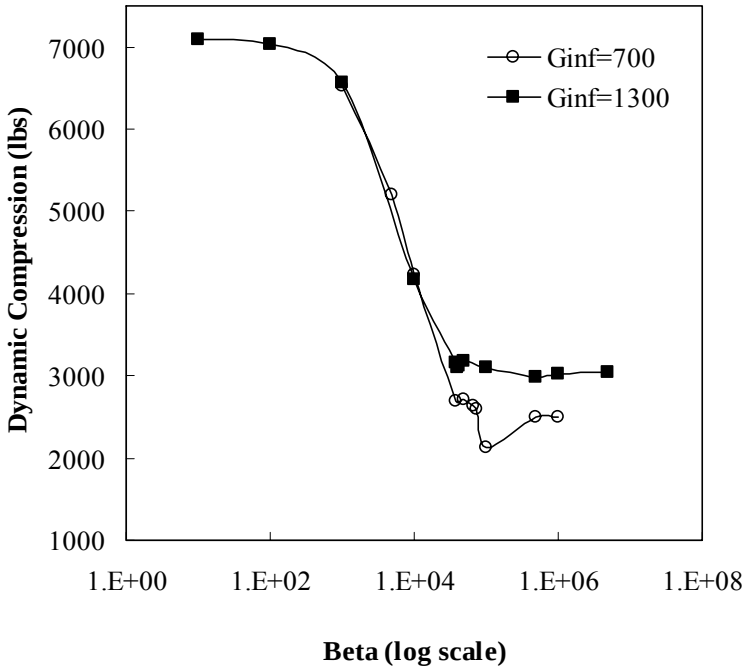

Figure A1.16: Bulk modulus k=10,000,000 and short term shear modulus G_0=10,000. Dynamic compression vs. the decay constant β for varying G_∞.

APPENDIX TWO

MathCad Program to Find Prony Series Coefficients

Governing Equation

$$G(g,\beta,t) := \left[\sum_{i=1}^{6} \left[g_i \cdot e^{(-\beta_i \cdot t)} \right] \right]$$

Guess Values for Parameters defined in following manner

$$vg := \begin{pmatrix} 1 \\ 1 \\ 1 \\ 1 \\ 1 \\ 1 \\ 1 \\ 1 \\ 1 \\ 1 \\ 1 \\ 1 \end{pmatrix} \quad \text{Corresponding to} \quad \begin{pmatrix} g_1 \\ \beta_1 \\ g_2 \\ \beta_2 \\ g_3 \\ \beta_3 \\ g_4 \\ \beta_4 \\ g_5 \\ \beta_5 \\ g_6 \\ \beta_6 \end{pmatrix}$$

vx is a vector of x values from the experimental data
vy is a vector of y values from the experimental data

$$vx := \begin{pmatrix} 1 \\ 2 \\ 3 \\ 4 \\ 5 \\ 6 \\ 7 \\ 8 \\ 9 \\ 10 \\ 11 \\ 12 \\ 13 \\ 14 \end{pmatrix} \qquad vy := \begin{pmatrix} 1 \\ 2 \\ 3 \\ 4 \\ 5 \\ 6 \\ 7 \\ 8 \\ 9 \\ 10 \\ 11 \\ 12 \\ 13 \\ 14 \end{pmatrix}$$

Vector containing governing equation and its partial derivatives for i=6 terms in Prony Series:

$$F(t,G) := \begin{bmatrix} G_0 \cdot e^{(-G_1 \cdot t)} + G_2 \cdot e^{(-G_3 \cdot t)} + G_4 \cdot e^{(-G_5 \cdot t)} + G_6 \cdot e^{(-G_7 \cdot t)} + G_8 \cdot e^{(-G_9 \cdot t)} + G_{10} \cdot e^{(-G_{11} \cdot t)} \\ e^{(-G_1 \cdot t)} \\ -t \cdot G_0 \cdot e^{(-t \cdot G_1)} \\ e^{(-G_3 \cdot t)} \\ -t \cdot G_2 \cdot e^{(-t \cdot G_3)} \\ e^{(-G_5 \cdot t)} \\ -t \cdot G_4 \cdot e^{(-t \cdot G_5)} \\ e^{(-G_7 \cdot t)} \\ -t \cdot G_6 \cdot e^{(-t \cdot G_7)} \\ e^{(-G_9 \cdot t)} \\ -t \cdot G_8 \cdot e^{(-t \cdot G_9)} \\ e^{(-G_{11} \cdot t)} \\ -t \cdot G_{10} \cdot e^{(-t \cdot G_{11})} \end{bmatrix} *$$

Defining the General Fit built in function which fits arbitrary functions to data

$$Pls := genfit(vx, vy, vg, F)$$

Plotting function for the curve fit

$$f(t) := F(t, Pls)_0$$

Parameter Values Calculated by MathCad which correlate with the guess values

$$Pls = \begin{bmatrix} 0.436 \\ -0.125 \\ 0.436 \\ -0.125 \\ 0.436 \\ -0.125 \\ 0.436 \\ -0.125 \\ 0.436 \\ -0.125 \\ 0.436 \\ -0.125 \end{bmatrix}$$

Plot of raw (vy and vx) and curve fit (f(x) and x) data.